14

THE KINETICS OF THE BIOLEACHING OF A REFRACTORY GOLD-BEARING PYRITE CONCENTRATE

by

MARIANNA DROSSOU
BSc Eng (Athens University) 1982

Submitted to the University of Cape Town in fulfillment of the requirements for the degree of Master of Science in Engineering

September 1986

ACKNOWLEDGEMENTS

I would like to express my thanks to:

The Council for Scientific and Industrial Research (CSIR) for their financial support.

The Council for Mineral Technology (MINTEK) for their invaluable technical assistance.

Professor G.S. Hansford of the Department of Chemical Engineering for his supervision.

Mr R. Dunne, Dr I. Corrans, Dr W. te Riele and Dr P. Miller for their assistance and interest in this work.

Mrs D. Moody and Mrs K. Clarke for their support, help and technical advice.

Mr K. Wheeler, Mr A. Barker and Mr R. Senekal for the construction and maintenance of equipment.

Mr P. Ellis for his assistance with the SEM.

Mr G. de la Cruz and Mr J. Maart for their patience and help throughout the duration of this work.

The Department of Microbiology at U.C.T. for letting us use their equipment

My friends L. Barker, J. Chapman, P. Norman, Dr E. Barros and S. Bocken for their invaluable help and encouragement.

All the staff of the Chemical Engineering Department and all the postgraduate students for their assistance on various occasions.

And George Vouzas for his understanding and enthusiastic help throughout this work.

ABSTRACT

The growing interest in the bioleaching of gold-bearing sulphide ores as the pre-oxidation step has created the need for extensive research work in this field. A review of the pertinent literature has shown the necessity for the derivation of kinetic models, which can be used to derive performance equations for a bioleach reactor.

The present work is a study of the kinetics of the bioleaching of a refractory gold-bearing pyrite concentrate. This work includes the derivation of kinetic models, their testing against experimental data as well as the establishment of a relationship between sulphur oxidation and corresponding gold liberation.

Four narrow size fractions of the pyrite concentrate were subjected to batch bacterial leaching using a pure culture of the bacterium Thiobacillus ferrooxidans ATCC 33020. Time profile data of the sulphur oxidation and gold liberation were obtained for each size fraction.

Gold liberation was found to be much higher than sulphur oxidation. For example 90% gold liberation typically corresponded to 30% sulphur oxidation, thus suggesting that the bacteria preferentially attack the gold-rich regions in the pyrite grains.

The leaching process was modelled according to two mechanisms; a shrinking-particle and a propagating-pore mechanism. The two models were tested against the experimental data. The shrinking-particle model did not give a good fit to the experimental data. On the other hand the propagating-pore model fitted the data well. Furthermore, scanning electron micrographs of the leached residues showed a highly leached particle surface as well as pore development. Thus both the curve fitting and the

micrographs complemented each other in supporting the propagating-pore mechanism.

A new parameter, the surface oxidation rate (kg m^{-2} day^{-1}) was introduced and used in both models in lieu of the volumetric oxidation rate (kg m^{-3} day^{-1}), as the surface oxidation rate could characterise bioleaching systems better. The surface oxidation rate calculated in this study of $3,5x10^{-4}$ kg (sulphur) m^{-2} day^{-1} was compared to values calculated from data in the literature.

The free bacterial concentration was found to reach its maximum value of approximately $2,8x10^{9}$ cells/ml about 10 days after the start of leaching. Thereafter the cell concentration remained close to this value.

From this work it can be concluded that bacterial leaching of pyrite occurs according to the propagating-pore mechanism. A mathematical model based on this mechanism was found to fit the experimental data. The surface oxidation rate is a useful parameter for characterising the leach kinetics and may form the basis for the derivation of performance equations for continuous bioleach reactors.

TABLE OF CONTENTS

CHAPTER 4
APPARATUS AND EXPERIMENTAL PROCEDURE

CHAPTER 5
RESULTS AND DISCUSSION

CHAPTER 6
CONCLUSIONS AND RECOMMENDATIONS

APPENDICES

LIST OF ILLUSTRATIONS

LIST OF TABLES

LIST OF FIGURES

NOMENCLATURE

r_v	volumetric oxidation rate, [kg m^{-3} day^{-1}]
r_{v0}	initial volumetric oxidation rate, [kg m^{-3} day^{-1}]
r_a	surface oxidation rate, [kg m^{-2} day^{-1}]
r_{a0}	initial surface oxidation rate, [kg m^{-2} day^{-1}]
n	number of particles per unit volume of solution, [m^{-3}]
a_p	particle surface area, [m^{-2}]
ρ	density, [kg m^{-3}]
ρ_p	pyrite density, [kg m^{-3}]
ρ_s	sulphur density in the pyrite concentrate, [kg m^{-3}]
d	particle diameter, [m]
d_0	initial particle diameter, [m]
c_t	solids concentration at time t, [kg m^{-3}]
c_0	initial solids concentration, [kg m^{-3}]
n_a	number of active pores per unit surface area, [m^{-2}]
n_{a0}	initial number of active pores per unit surface area, [m^{-2}]
b	area of pore base, [m^2]
r_p	oxidation rate at the pore base, [kg m^{-2} day^{-1}]
v_p	rate of pore propagation, [m day^{-1}]
L	pore length, [m]
L_i	minimum pore length, [m]
L_e	maximum pore length, [m]
t	time, [day]
T_i	time at which pore deactivation starts, [day]
T_e	time at which all pores have become inactive, [day]

CHAPTER 1

INTRODUCTION

Bioleaching has been used for the extraction of base metals from low-grade ores or from waste ore dumps in crude operations, such as dump or heap leaching. About 10 to 15% of the copper production in the U.S.A. is carried out by bacterial leaching of low-grade ores and waste dumps (Lundgren and Malouf, 1983). Dump bacterial leaching has been used in Bulgaria for the extraction of copper from low-grade sulphides (Groudev *et al.*, 1978). A study on the intended *in-situ* leaching of a complex sulphide ore containing chalcopyrite, sphalerite, galena and pyrite has been reported by Burton *et al.* (1983)

In recent years the interest in bacterial leaching has shifted from the recovery of base metals to the recovery of precious metals from refractory sulphide ores. This came as a result of the depletion of high grade gold- and silver-bearing ores and the need for alternative methods for the exploitation of low-grade ores or for the reprocessing of mine dumps. Furthermore, the search for alternative methods for the treatment of high-grade gold bearing ores (such as those from Barberton), which contain arsenic and antimony and which interfere with cyanidation, also contributed to the increasing interest in bacterial leaching.

Refractory gold ores are those in which the major proportion of gold remains unrecovered after a conventional cyanidation treatment. Alternative pretreatment methods for gold recovery from such sulphide ores are:

- roasting (Chant, 1975; Penman, 1985)
- pressure leaching (Chant, 1975)
- bacterial leaching (Chant, 1975)

Roasting is a well established method and has been used for a long time in gold extraction. However the gas scrubbing

facilities needed to prevent atmospheric pollution add substantially to its operating cost. Pressure leaching is generally an expensive method of processing materials as high temperatures and oxygen pressures are often applied. Bacterial leaching is conducted at atmospheric pressure and ambient temperature. However, there is little experience on the technical problems of bioleaching processes to assess their advantages and disadvantages, since no large-scale bioleach reactor has been operated yet.

In contrast to the bioleaching of base metal ores, where the process is economical only when a natural reactor system is employed (Renner et al., 1984), recent studies claim that gold recovery by bioleaching in continuous reactors can be competitive to the alternative methods mentioned above (Livesey-Goldblatt et al., 1983; Renner et al., 1984; Lawrence and Gunn, 1985). However, in none of these studies is there any indication that the results have been interpreted in terms of a quantitative kinetic model. Scale-up appears to have been done on an empirical basis.

Therefore the general objective of this work was to investigate the kinetics of a refractory gold-bearing pyrite concentrate in terms of mathematical models, with a view to providing a quantitative basis for the design of a bioleach reactor. This was achieved by:

1. obtaining time profile data for the batch bioleaching of four narrow size fractions.
2. deriving mathematical models which could be tested against the data.
3. examining the relationship between gold liberation and pyrite oxidation.
4. an electron microscope examination of the leach residues in order to elucidate possible leach mechanisms.

This thesis contains:

- a survey of the literature on the relevant aspects of bacterial leaching followed by a review of those aspects which are directly related to this work,

- a theoretical presentation and derivation of the models,
- a description of the experimental materials and methods involved,
- a presentation and discussion of the pyrite batch leach data and the testing of the models against this data. The gold liberation data as well as the scanning electron micrographs are also presented and discussed.
- In conclusion, the major findings of this work are summarised, the limitations discussed and recommendations for future work are presented.

CHAPTER 2

LITERATURE SURVEY

2.1 Introduction

In this chapter a literature survey of the relevant aspects of the bacterial leaching of minerals is presented. The general background on the bacterium *Thiobacillus ferrooxidans* and the basic principles of the bacterial leaching of minerals are briefly mentioned. Aspects that are directly related to this work such as evidence of bacterial attachment to the solids, the role of particle size and surface area concentration on leaching, existing kinetic models, the gold occurrence in the sulphide ores, as well as previous studies on gold recovery by means of bacterial leaching, are presented in more detail.

2.2 General Background on the Bacterium *Thiobacillus ferrooxidans* and the Bacterial Leaching of Minerals

Since the first isolation of the bacterium *Thiobacillus ferrooxidans* (Colmer and Hincle, 1947) a number of studies on its morphology, physiology, and metabolic mechanisms have been presented. This work has been reviewed by Silverman and Ehrlich (1964), Tuovinen and Kelly (1972), Karaivko *et al.* (1977), Torma (1977), Brierley (1978) and Kelly *et al.* (1979).

From the abovementioned reviews the main features of the bacteria *Thiobacillus ferrooxidans* and their use in the bacterial leaching of minerals can be summarised as follows: *Thiobacillus ferrooxidans* is a motile, Gram-negative, rod-shaped bacterium, typically 0,1 micron in diameter and 1,5 micron in length. They occur singly or occasionally in pairs.

In a batch culture the growing cells go through lag, logarithmic, stationary and death phases.

Thiobacillus ferrooxidans derives energy for its activities from the oxidation of ferrous iron, as well as from inorganic substances, such as reduced sulphur compounds and is, therefore, described as a chemolithotrophic organism. Specifically in the process of obtaining energy the organism oxidises:
- ferrous iron, Fe^{++}, to ferric iron, Fe^{+++}, and
- sulphur in various forms to sulphate ion, SO_4^{--}. The oxidisable sulphur can be in the form of elemental sulphur, soluble or insoluble sulphides, thiosulphate ion, $S_2O_3^{--}$, or tetrathionate ion, $S_4O_6^{--}$.

The organism is also described as autotrophic, as it uses carbon for the synthesis of cellular components from carbon dioxide in the atmosphere.

Important nutrients have been found to be ammonium nitrogen, phosphorus, sulphate and magnesium (Tuovinen et al., 1971; Lenisov et al., 1980; Rawlings, 1981). The organism is characterised as acidophilic and moderately thermophilic, growing in very acidic environments, between a pH of 1.5 and 3.0, the optimum pH value being about 2,5 and in a temperature range between 20°C and 35°C. Its natural habitats are hot springs, volcanic fissures and sulphide ore deposits whose environments ensure high sulphuric acid concentration (Brierley, 1982).

Other thiobacilli which are recognised as having potential in the bacterial leaching of minerals are:
- Thiobacillus thiooxidans (Karaivko et al., 1977), which grows on elemental sulphur and some soluble sulphur compounds, is important, especially when used in mixed cultures with Thiobacillus ferrooxidans (Wakao et al., 1982). These mixed cultures are more effective in leaching certain minerals than either organism is alone (Brierley, 1982).
- Leptospirillum ferrooxidans are also important thiobacilli in minerals processing (Groudev, 1982; Brierley, 1982).

- Sulpholobus are extremely thermophilic and acidophilic bacteria. As they are tolerant of high metal concentrations they are potentially capable of leaching minerals resistant to other microorganisms (Brock et al. 1972; Brierley, 1977; Brierley, 1982; Norris and Parrott, 1985).

The manner in which the mineral is oxidised by bacteria has been studied by many investigators (Razzell and Trussell, 1963; Silverman, 1967; Lau et al., 1970; Duncan et al., 1967; Corrans et al 1972; Le Roux et al., 1973; Imai, 1978). Two mechanisms have been suggested and are referred to as the indirect and direct mechanisms.

- The indirect mechanism proposes that the mineral is chemically oxidised by ferric ions which are then regenerated in solution by the bacterial oxidation of ferrous ions.
- The direct mechanism proposes that the bacteria associated with the mineral surface bring about the mineral oxidation.

The relative importance of those two mechanisms is still uncertain. It is realised however, that certain factors, such as the type of the mineral, the state of the bacteria (to what extent they are adapted to a specific mineral) and physical conditions such as pH, temperature, agitation and the concentration of certain metal ions might have an effect on the mechanisms.

Mineral sulphides that can be oxidised by Thiobacillus ferrooxidans are:

- iron sulphides, such as pyrite, FeS_2, (Silverman, 1967; Atkins, 1978), pyrrhotite, FeS, marcasite, FeS_2, (Silverman et al., 1961)
- copper sulphides, such as chalcopyrite, $CuFeS_2$, (Bruynesteyn and Duncan, 1974; Rangachari et al., 1978; Mc Elroy and Bruynesteyn, 1978;), covellite, CuS and chalcocite, Cu_2S, (Corrans et al., 1972; Sakaguchi et al., 1976)
- arsenic sulphides, such as arsenopyrite, FeAsS, (Pinches, 1972) and orpiment, As_2S_3, (Ehrlich, 1963)
- zinc sulphide, sphalerite, ZnS, (Torma et al., 1970; Gormely et al., 1975)
- nickel sulphide, pentlandite, $(Ni,Fe)_9S_8$, (Corrans, 1974)

- lead sulphide, galena, PbS (Torma and Subramanian, 1974; Torma, 1978)

Other sulphide minerals that have also been found to be oxidised by bacteria are molybdenite, MoS_2, antimonite, Sb_2S_3, enargite, Cu_3AsS_4, stibnite, Sb_2S_3, tetrahedrite, $(Cu, Fe)_{12}Sb_4S_{13}$, etc. (Torma, 1977).

A further application of bacterial leaching is in uranium production, where the bacteria oxidise the ferrous ions to ferric ions, which in turn leach the uranium minerals (Miller et al., 1963; Fisher, 1966; Harrison et al., 1966; Guay et al., 1976; Dispirito and Tuovinen, 1982). Furthermore the bacteria Thiobacillus ferrooxidans are capable of oxidising inorganic sulphur in coal. Studies on bacterial coal desulphurisation have been reported (Silverman et al., 1961; Dugan and Apel, 1978; Kargi and Weissman, 1984; Myerson and Kline, 1984)

The basic reactions in bacterial leaching systems have been summarised by Torma (1977) and Karaivko et al. (1977). In the South African context the bacterial oxidation of gold-bearing pyrite and arsenopyrite ores is of great interest. Irrespective of the oxidation mechanism applying, the oxidation of pyrite in bacterial leaching can be represented by the following overall reaction:

$$4\ FeS_2 + 15\ O_2 + 2\ H_2O \longrightarrow 2\ Fe_2(SO_4)_3 + 2\ H_2SO_4 \qquad 2.1$$

This is the result of a number of intermediate reactions, where ferrous sulphate, $FeSO_4$, and elemental sulphur are the intermediate products. These are in turn oxidised by the bacteria to ferric sulphate, $Fe_2(SO_4)_3$ and sulphuric acid, H_2SO_4, Karaivko et al. (1977):

$$2\ FeS_2 + 7\ O_2 + 2\ H_2O \longrightarrow 2\ FeSO_4 + 2\ H_2SO_4 \qquad 2.2$$

$$4\ FeSO_4 + O_2 + 2\ H_2SO_4 \longrightarrow 2\ Fe_2(SO_4)_3 + 2\ H_2O \qquad 2.3$$

$$FeS_2 + Fe_2(SO_4)_3 \longrightarrow 3\ FeSO_4 + 2\ S \qquad 2.4$$

$$2\ S + 2\ H_2O + 3\ O_2 \longrightarrow 2\ H_2SO_4 \qquad 2.5$$

The bacteria can accelerate the oxidation of ferrous iron to ferric by a factor of $1x10^6$ and the oxidation of pyrite by a factor of $1x10^3$ (Karaivko et al., 1977).

Depending on the pH of the system, secondary reactions can take place , mainly iron hydrolysis reactions. The possible insoluble products are basic ferric sulphate, ferric hydroxide, or jarosite according to the reactions (Torma, 1977; Ivarson, 1973):

$$Fe_2(SO_4)_3 + 2\ H_2O \longrightarrow 2\ Fe(OH)SO_4 + H_2SO_4 \qquad 2.6$$

$$Fe_2(SO_4)_3 + 6\ H_2O \longrightarrow 2\ Fe(OH)_3 + 3\ H_2SO_4 \qquad 2.7$$

$$3\ Fe_2(SO_4)_3 + 12\ H_2O \longrightarrow 2\ H[Fe(SO_4)_2\ 2\ Fe(OH)_3] + 5\ H_2SO_4 \qquad 2.8$$

The H^+ in the jarosite can be substituted by $NH4^+$, Na^+ or K^+ ions (ammonio-, natro-, potassiojarosite). It has been suggested that precipitation of jarosite inhibits further oxidation of the sulphide by inhibiting the intimate contact between the sulphide particles and the bacteria and, that the reaction is then controlled by the diffusion phenomena (Ivarson, 1973; Torma, 1977).

In the leaching of arsenopyrite the corresponding overall reaction is (Torma, 1977):

$$2\ FeAsS + 7\ O_2 + 2\ H_2O \longrightarrow 2\ FeAsO_4 + 2\ H_2SO_4 \qquad 2.9$$

This is the result of the following intermediate reactions (Polkin et al., 1970):

$$4\ FeAsS + 13\ O_2 + 6\ H_2O \longrightarrow 4\ H_3AsO_4 + 4\ FeSO_4 \qquad 2.10$$

$$4\ FeSO_4 + 2\ H_2SO_4 + O_2 \longrightarrow 2\ Fe_2(SO_4)_3 + 2\ H_2O \qquad 2.11$$

$$2FeAsS + Fe_2(SO_4)_3 + 4H_2O + 6O_2 \longrightarrow 2H_3AsO_4 + 4FeSO_4 + H_2SO_4 \qquad 2.12$$

Arsenous acid can react with ferric sulphate to precipitate as iron arsenate:

$$2\ H_3AsO_4 + Fe_2(SO_4)_3 \longrightarrow 2\ FeAsO_4 + 3\ H_2SO_4 \qquad 2.13$$

The bacterial leaching operations used on an industrial scale have been described by Corrans et al. (1972), Brierley (1978), Brierley (1982) and Lundgren and Malouf (1983). The predominant commercial bacterial leaching operations are dump and heap leaching.

Dump leaching is used when treating low-grade, run-of-mine ores or waste ore dumps, which naturally contain Thiobacilli. The leach solution is introduced at the top, percolates through the rock and the pregnant solution is collected at the base of the dump. This is an uncontrolled process, where mass transport limitations, precipitation of iron compounds, high temperatures and high metal concentrations might inhibit metal extraction rates.

When ores have a higher metal concentration, they are subjected to heap leaching. Heaps are generally smaller than dumps. They are often provided with an aeration system. The ore is also crushed to provide better mass transport. Dump and heap leaching have been used in copper extraction from low-grade sulphide ores or from mine dumps in the U.S.A. It has also been used in low-grade uranium ores (Brierley 1978).

Bacterial leaching can also be applied in-situ to low-grade ores when conventional mining is uneconomical, or to abandoned previously exploited ore bodies (Burton et al., 1983). Deposits are exploited by drilling holes into the ore

body and/or by blasting the ore so that the leach solution can percolate through.

Finally, in the case of high-grade concentrates stirred-tank leaching can be applied. This involves the leaching of finely ground concentrates under controlled conditions in a stirred reactor. This process may be economical when high-grade sulphide concentrates (Bruynesteyn and Duncan, 1971; Duncan et al., 1966) or precious metal-containing sulphides are considered (Renner et al., 1984).

2.3 Review of the Relevant Research Literature

In considering the objectives of this work, viz. the derivation of mathematical models for the bioleaching of pyrite and the examination of the relationship between pyrite oxidation and gold liberation, aspects that need to be taken into account are:

- the bacterial attachment to the solids, which is closely related to the mechanism of oxidation.
- the effect of particle size and surface area on the kinetics of leaching.
- previously developed bacterial leaching models.
- the occurrence of gold in the sulphide ores, as this knowledge can be used to interpret the relationship between pyrite oxidation and gold liberation.
- the published work on gold recovery using bioleaching as the pre-oxidation step.

2.3.1 Bacterial Attachment

The mode and characteristics of bacterial attachment to solids have been examined for various Thiobacilli in a number of studies (Vogler and Umbreit, 1941; Schaeffer et al., 1963; Weiss, 1973; Baldensperger et al., 1974; Murr and Berry, 1976).

Duncan and Drummond (1973) used the scanning electron microscope to examine the surface of pyrite grains leached by Thiobacillus ferrooxidans, as well as those leached with ferric sulphate solutions in the absence of bacteria. The bacterially leached pyrite grains presented a rough and irregular surface etched with many pits and grooves, while this was not the case in the chemically leached samples. Based on these observations the authors suggested that this was evidence of direct microbial attack. However, the authors did not observe preferential attack along crystallographic axes.

Berry and Murr (1978) studied the attachment of the bacteria Thiobacillus ferrooxidans and Sulpholobus to thin sections of a low-grade chalcopyrite waste ore by examining the leached samples in the scanning electron microscope. Bacteria were observed to be preferentially attached to the energy providing sulphide regions, pyrite and chalcopyrite. The authors suggested that this indicates the ability of bacteria to select optimum attachment sites.

Bennett and Tributsch (1978) used the scanning electron microscope to examine the surface of pyrite crystals that had been leached with Thiobacillus ferrooxidans for a lengthy time period. Attached bacteria and corrosion pits were observed. In many cases bacterial corrosion chains were observed to intersect each other approximately at right angles. Since it is known that dislocations in pyrite crystals are often parallel to the crystallographic axes and, therefore, perpendicular to each other the above distribution of the corrosion patterns seemed to reflect crystal imperfections in the pyrite crystal lattice. In view of the fact that these dislocations represent weaknesses in the crystal lattice the authors suggested that the microorganisms are able to select optimum sites of attachment.

In addition to the direct observation of bacterial attachment using the scanning electron microscope or the transmission electron microscope various methods of

enumerating bacteria (total number of bacteria and free bacteria, the difference being the number of attached bacteria) prove that bacterial attachment does occur. Furthermore these methods give quantitative information about the relative numbers of attached and free bacteria.

The growth of Thiobacillus ferrooxidans on various solid substrates was studied by McGoran et al. (1969). The authors used a variation of the micro-Kjeldahl technique for bacterial count and found that 98% of the bacteria were attached to the solid particles when grown on chalcopyrite, and 76% were attached when grown on sulphur. It was also observed that the bacteria hold tenaciously to the solids' surface, a capability that enables them to grow under conditions of violent agitation.

Gormely and Duncan (1974) modified the micro-Kjeldahl technique for bacterial nitrogen determination, to account for the nitrogen in the precipitate formed during the oxidation of iron-bearing sulphides. The authors estimated bacterial numbers growing on various sulphides. When a zinc sulphide concentrate was used the bacterial population was estimated to be $1,9x10^{10}$ cells/ml and 65% of the cells were attached to the solids. When chalcopyrite was used the cell concentration was $8,9x10^{9}$ cells/ml with approximately 95% of the bacteria on the solids.

Bacterial numbers were also measured by Le Roux et al. (1973) and Groudev (1979) during the bioleaching of pyrite. In both studies most of the bacteria were found associated with the solids.

From the findings presented above it appears that the majority of the bacteria in a leaching system are attached to the surface of the sulphide particles. There is evidence to suggest that this attachment is not random but occurs selectively in regions of weaker crystal structure, where it is easier for the bacteria to obtain energy through oxidation of the mineral.

2.3.2 Role of Particle Size and Surface Area on Leach Rates

An important factor which has to be taken into account in a kinetic model for the bacterial leaching of minerals is the size of the mineral particles. The early studies on the subject showed that decreasing the particle size increased the leach rate significantly

By reducing the particle size of molybdenite from +30-10 mesh (-1,68+0,5 mm) to 60 mesh (250 micron) an increase in the oxidation rate of the smaller size fraction was observed (Bryner and Anderson, 1957). Malouf and Prater (1961) observed that the highest rate of pyrite dissolution in column experiments was obtained with the finest size fraction of -325 mesh (about -48 micron). Silverman et al. (1961) studied the bacterial leaching of four different sulphuritic materials. At a particle size of 65 mesh (about 230 micron) only one of them showed an appreciable oxygen uptake in the presence of the test organism. By decreasing the particle size the oxidation rate in all samples was markedly improved. The rate of copper release from chalcopyrite increased with decreasing particle size down to sizes below 400 mesh (38 micron), (Duncan et al., 1966). Reducing the particle size of synthetic copper sulphide from +125-177 micron to less than 62 micron almost doubled the rate of bacterial oxidation (Ehrlich and Fox, 1967). All the above studies on the effect of particle size in leaching kinetics showed that decreasing the particle size increased the leach rate significantly.

In addition to particle size, two other physical parameters were found to be critical regardless of the scale and type of equipment involved. These are the solids concentration (pulp density), expressed as the mass of concentrate per unit volume of liquid (kg m^{-3}, w/v%) and, the specific surface area, expressed as the surface area of concentrate per unit mass of concentrate (m^2 kg^{-1}), which is closely related to particle size. In a number of studies it was found that the rate of metal extraction by Thiobacillus

ferrooxidans was first order with solids concentration over a range of values, after which the curve started levelling off (Torma *et al.*, 1970; Torma *et al.*, 1972; Torma and Subramanian, 1974; Pinches, 1972; Pinches *et al.*, 1976). The solids concentration for which maximum extraction rate was achieved, was dependent on the particle size or the specific surface area employed for any particular sulphide. Thus for a single solids concentration, extraction rate increased as the particle size was reduced (or the specific surface area was increased). This indicates that the true rate limiting factor is the surface area available for the bacteria to attack or the *surface area concentration*, expressed as the surface area of solids available for oxidation per unit volume of liquid ($m^2\ m^{-3}$).

In the abovementioned studies the effect of surface area concentration on the volumetric metal leach rates was examined by varying:
- particle size at constant solids concentration and,
- solids concentration at constant particle size.

It was found that the data for both sets of experiments coincided at least for the region of low surface area concentrations, thus suggesting that the true rate limiting factor associated with the substrate is the surface area concentration. It was also found that the volumetric leach rate was linearly dependent on surface area concentration over a region of surface area concentrations, after which the curve started levelling off.

Despite the above observations no attempt was made to correlate the linear relationship described above with a physical parameter of the minerals. This physical parameter can be obtained from the slope of the linear part of the curve leach rate versus surface area concentration ($kg\ m^{-3}\ day^{-1} / m^2\ m^{-3}$), and represents the surface leach rate of the metal or the mineral ($kg\ m^{-2}\ day^{-1}$). Thus the abovementioned findings provide evidence which supports the assumption that, the surface oxidation rate is independent of particle size or surface area concentration at least over a range of surface

area concentrations. This will be further discussed and analysed in the Results and Discussion section.

2.3.3 Kinetic Models for Bacterial Leaching

In bacterial leaching processes the substrate used is usually a solid insoluble sulphide mineral. While bacterial growth kinetics on a soluble substrate has classically been described by Monod growth kinetics (Monod, 1949; Herbert *et al.*, 1956) this does not necessarily apply to the case of a solid substrate. Therefore a number of models have been developed for bacterial leaching systems. They can be categorized as:

- those models which predict bacterial growth in the system and,
- those models which predict the leach rate of a metal of the ore or concentrate used.

Because both bacterial growth and leach rates are of interest and because these are closely interlinked (Pinches, 1972; Gormely, 1973; Lawrence, 1974), a mathematical model would ideally describe and relate both these variables. However most attempts at modelling reported in the literature have focused either on bacterial growth or metal leaching.

Gormely (1973) derived a model for the kinetics of bioleaching of an insoluble non-ferrous sulphide mineral, zinc sulphide, in a continuous stirred tank reactor (CSTR). The model was based on a growth model in a medium with two liquid phases proposed by Erickson *et al.* (1970). Gormely's basic assumptions were that growth was only limited by the solid substrate, and that the attached bacteria were growing at their maximum specific growth rate. The free bacteria were assumed not to grow. He also assumed a dynamic equilibrium between free and attached bacteria and that attachment and release followed first order kinetics. The model predicts the steady state cell concentration as a function of dilution rate and surface area concentration of the solids. Testing of the model against the experimental

data generally verified the prediction of the model, viz., that unlike Monod kinetics, when a solid substrate is used the specific growth rate of the bacteria is not a unique function of the substrate concentration or the surface area concentration. However deviations between experimental results and predicted values were observed and this was attributed to non-ideal mixing in the reactor as well as the method of surface area measurement used, (BET), which usually overestimates the oxidisable surface area.

Sanmugasunderam et al. (1985) verified and extended the model proposed by Gormely to apply to two CSTRs in series with and without recycle. The assumptions used were the same as in Gormely's work and the model was tested for the continuous leaching of a pure zinc sulphide concentrate in two CSTRs in series. The authors were careful to overcome the drawbacks in Gormely's work by verifying the ideal mixing in their reactors and by using an air permeability technique to measure surface area. The predicted values show good agreement with the experimental data. However the values for the model parameters, specific growth rate and area occupied per cell, differ from the values given elsewhere in the literature (Chang and Myerson, 1982; Myerson and Kline, 1984) and this was attributed by the authors to the different conditions employed in their study.

A limitation in the model derived by Gormely is that it does not account for bacterial growth in solution. Therefore it cannot be used in the case of an iron-containing sulphide, where bacterial ferrous ion oxidation in solution may occur. Chang and Myerson (1982) have extended Gormely's model to account for growth both of those bacteria in solution as well as those attached to the solid substrate, taking into consideration the effect of soluble substrate concentration. They developed and tested the model on the bioleaching of pyrite in a CSTR. They proposed that the specific growth rate on the solids is not necessarily equal to the specific growth rate in solution. They also introduced two dilution rates, one for the solid phase and another for the liquid phase,

which they could vary independently. The authors also derived an equation for the relationship between free and attached bacteria, as well as for pyrite leach rates. In testing their model against experimental data the authors verified its qualitative predictions, viz. 1) that the pyrite leach rate increases with pyrite surface area, dilution rate and inlet ferrous iron concentration and 2) that the specific growth rate of the attached bacteria increases with increasing solid dilution rate and decreases with increasing pyrite surface area and soluble substrate concentration.

In attempting to model the leaching of concentrates Blancarte-Zurita et al. (1985) made use of the shrinking-particle model, which is a special case of the unreacted-core or shrinking-core model described by Levenspiel (1972). In the shrinking-core model there is a reaction zone surrounding a constantly decreasing unreacted core. In the shrinking-particle model the leaching occurs on a sharp front at the interface between the reactant solid and the reactant liquid. Any reaction products formed either flake off the main particle, or are formed as liquid products and mix with the bulk liquid, resulting in a constant decrease in particle size.

A shrinking-particle model might be applied to bacterial leaching in the case where the substrate consists of a pure sulphide, and where the bacterial oxidation takes place uniformly on the outer surface of the particle. On the other hand a shrinking-core model might be applied in a case where the particles contain a large amount of inert material, which maintains the basic particle structure and size during leaching and forms a zone of unreacted solids through which the leaching liquor and bacteria have to diffuse.

In applying the shrinking-particle model to a batch bioleach system, Blancarte-Zurita et al. (1985) derived an expression which predicts the mean particle diameter as a function of leach time. This expression incorporates the

metal leach rate which depends on particle size and leach time. In testing the model the dependence of the metal extraction rate on leach time and particle size needs to be found from experimental data. The authors tested the model against the batch leach data of two concentrates, a chalcopyrite and a sphalerite concentrate:
- for the chalcopyrite concentrate the dependence of the copper extraction rate on time and particle size was found by fitting a curve to the time profile copper extraction data for various particle size fractions. The predictions of the model did not show good agreement with the experimental data. If indeed a shrinking-particle model did apply in this case, the deviation from the model might be due to the low extent of leaching of this concentrate, which resulted only in small particle diameter changes inadequate to test the model.
- for the sphalerite concentrate the time profile data of zinc extraction for various size fractions were used. All these curves had a linear section assumed to represent a constant metal extraction rate. A relationship between these constant rates and the particle diameters was found and used in the mathematical model. The predicted values of particle diameter versus time were in good agreement with the experimental data.

It has been observed that the shrinking-particle model is not adequate to describe the leaching mechanism in bacterial systems where there has been evidence of preferential bacterial attack on the solids. The surface of leach residue particles are often very rough and irregular compared with the surfaces of the feed material particles. Bruynesteyn and Duncan (1974) observed preferential oxidation of a particular metal in an ore and suggested that this cannot be satisfactorily explained by a shrinking-particle mechanism.

Southwood and Southwood (1985) observed that cylindrical pores develop in pyrite particles undergoing leaching by Thiobacillus ferrooxidans. Studying polished sections of leached residues, the authors found that the pores are preferentially orientated parallel to the three

crystallographic axes of the cubic pyrite lattice and they occur mainly in structurally disturbed regions of the pyrite crystal. This is consistent with earlier work suggesting that bacterial attachment is selective in regions of imperfections in the sulphide lattice (Berry and Murr, 1978; Bennett and Tributsch, 1978). By measuring the diameters of several pores in two leached concentrates, an essentially pure pyrite and a mixed pyrite-arsenopyrite, they found that the mean pore diameters were 4,5 and 8,0 micron respectively. The authors also observed that the diameter of the pore was essentially constant along the pore length and independent of the pore depth, suggesting that leaching was restricted to the leading face of the pore while the pore walls remained inactive. This mechanism of oxidation, which takes preferential bacterial attack into account, is very different from the shrinking-particle mechanism. The authors did not derive a mathematical model based on their observations but they emphasized the fact that these observations may be of great importance in the bacterial leaching of gold-bearing sulphide ores, as described below.

2.3.4 Mode of Gold Occurrence in Sulphide Ores and its Implications for Gold Recovery by Bacterial Leaching

Pyrite is frequently associated with all South African gold ore deposits, whereas arsenopyrite is only commonly found in the non-Witwatersrand ores. The association of sulphides with gold ore deposits is a very common phenomenon. In an investigation of 115 gold deposits, mostly in North America, it was found that gold was associated with pyrite in 48 cases and arsenopyrite in 45 cases (Schwartz, 1944).

The nature of gold occurrence in sulphide ores can vary considerably from one deposit to another. Gold can occur in the microscopic or submicroscopic range. Submicroscopic gold is considered to be that gold which cannot be detected in a statistically sufficient number of polished sections under vertically reflected light, i.e. with dimensions less than 1

micron. Using the scanning electron microscope this limit can be lowered to grains with dimensions of 0,01 micron (Southwood, 1985).

There is evidence that sulphides can contain a significant amount of submicroscopic gold (Henley, 1975). In many cases this submicroscopic gold is refractory, i.e. it responds poorly to conventional recovery methods.

The submicroscopic gold can either be accommodated in the pyrite crystal lattice of certain sulphides in a solid solution form or may occur as fine discrete inclusions within the sulphide grain. Many investigations have been carried out on the above subject and are reviewed by Henley (1975), Boyle (1979) and Southwood (1985). Summarising the conclusions from the third review it can be said that:
- the relative proportion of coarse (microscopic) and submicroscopic (colloidal and in solid solution) gold varies significantly from one deposit to another.
- the mode of occurrence of submicroscopic gold in sulphide minerals, solid solution or discrete inclusions, can also vary from one deposit to another.
- irrespective of the primary occurrence of gold in the host-sulphide ore, the gold may, either during the cooling of the host ore or later under conditions of elevated temperature and pressure (metamorphism), exsolve or remobilise respectively, and migrate to low energy sites, such as fractures, grain boundaries and lattice dislocations.
- a positive correlation between the arsenic and submicroscopic gold content has been found in many auriferous sulphides (Sorokin and Lomakin, 1971; and Mironov et al., 1981, cited in Southwood, 1985).

The fact that gold may often occur as discrete inclusions in structurally disturbed regions of the pyrite grain is of great importance in gold recovery by means of bacterial leaching. In light of Southwood and Southwoods' (1985) observations, it is expected that high gold recovery can be achieved with only low sulphide breakdown, since the bacteria

will preferentially attack the structurally disturbed regions of the pyrite where the gold is located.

2.3.5 Previous Work on the Bacterial Leaching of Gold-Bearing Sulphides.

To date papers on gold recovery by means of bacterial leaching have dealt either with studies on the economic viability of the process or with studies on the amenability of refractory gold-bearing ores to bacterial leaching.

In considering alternative routes for gold recovery from a pyrite-arsenopyrite ore, Livesey-Goldblatt et al. (1983) have looked at the cost of recovering gold from:
- the bacterial leaching-cyanidation of a run-of-mine ore,
- the bacterial leaching-cyanidation of the flotation concentrate and
- the conventional roasting-cyanidation of the concentrate.

They found that gold recoveries from both bacterial leaches, 92,7% and 97,8% respectively, were higher than the flotation-roasting process, 86%. They concluded that an economically viable process is not possible for the-run-of mine ore (at the given gold head value, 9,75 g/t), while it is possible for the bacterial leach of the flotation concentrate.

A number of refractory precious metal sulphide concentrates with varying mineralogical composition were subjected to bacterial leaching so as their amenability to biological pre-oxidation treatment could be determined (Bruynesteyn, 1984). Apart from the conclusion that gold and silver extractions were significantly improved by the bioleach process no information on the kinetics of the process is presented in this work.

A study on a continuous bioleaching process for gold and silver recovery using refractory Porgera concentrate from New Guinea was presented by Lawrence and Gunn (1985). The average degree of pyrite oxidation was about 88% obtained at

a rate of 0,688 g pyrite/l/hr (16,53 kg pyrite m^{-3} day^{-1}). This was achieved at a solids concentration of 16% with a retention time of 121 hrs. Gold and silver extractions after cyanidation of the residue were 92,1% and 73,6% respectively. Part of the gold and silver (4,9% and 18,3%) was found dissolved in the bioleach solution. The authors report that it was possible to recover the metals from the solution and thus the overall gold recoveries came to 97% and 91,9% respectively. Although the process proved successful for this particular ore, no attempt was made to interpret the results in terms of a bioleach model.

Marchant (1985) studied the effect of batch bacterial leaching on a refractory gold and silver-containing flotation tailing of pyrite-arsenopyrite. Marchant found that bacterial pretreatment proved to be successful as gold and silver recoveries increased significantly. The gold recovery appeared to be independent of pyrite oxidation and it lay between 65% and 78% for 6% to 65% iron extraction. On the other hand, the silver recovery was highly dependent on iron extraction and increased from 27% for 6% iron extraction to 60% for 60% iron extraction respectively. Another interesting finding was that arsenic dissolution was preferential, and essentially complete, after only 30% of the total pyrite had been oxidised. From the batch leach tests Marchant proceeded to continuous bench scale and pilot plant tests. However, the basis on which this scale-up was done was empirical by simply using the data obtained in the batch leach tests. Although this empirical procedure gives indications of the required residence times, rates of mineral oxidation and gold liberation, it does not provide any indication of a general method for bioleach reactor design.

2.3.6 Summary of the Literature Survey

In summary, a review of the literature shows that bacterial leaching has a potential role in the extraction of refractory gold from sulphide ores.

The principal microorganism involved, Thiobacillus ferrooxidans, has been extensively studied and the conditions optimising its growth are well defined. While there is evidence for its attachment to the surface of solid substrates, there is still uncertainty as to how this attachment is effected and at what sites of the mineral it occurs. It seems to be accepted however that attachment is not random.

The role of particle size and surface area has been investigated in the leaching of many ores. However no attempt was made to correlate these results with the surface oxidation rate of metals, minerals or ores.

There have been a large number of studies on bacterial leaching but many of these have been qualitative in nature, insofar as that they have not attempted to relate either bacterial growth or mineral leaching to any kinetic expression. A few models have been described in the literature. These have been based on bacterial growth (Gormely, 1973; Chang and Myerson, 1982; Sanmugasunderam et al., 1985;) or on metal leach rates (Blancarte-Zurita et al., 1985). Microscopic examination of leach residues has indicated that bacterial action occurs along pores orientated along crystallographic axes and microfractures within the crystal, where gold is likely to be included. The incorporation of this phenomenon into a kinetic model will be attempted in this study.

Bioleaching of gold bearing ores has been studied by several authors (Livesey-Goldblatt et al., 1983; Renner et al., 1984; Lawrence and Gunn, 1985; Lawrence and Bruynesteyn, 1983; Marchant, 1985) but interpretation of results has not

been done in terms of any leaching mechanism or any kinetic model.

From the literature survey presented above it has been concluded that there is still considerable scope for the development of sound kinetic expressions for bacterial leaching as well as for substantiation of these in experimental studies.

CHAPTER 3

THEORY: MODEL DERIVATION

3.1 Introduction.

For the design of a bioleach reactor mass balance and rate expressions need to be derived. These expressions can be obtained from a kinetic model, which describes the manner in which mineral oxidation takes place during bacterial leaching. Two models, the shrinking-particle model and the propagating-pore model, and their predictions for the kinetics of a batch leach system are presented and discussed in this chapter.

The classical shrinking-particle model (Levenspiel, 1972), which has previously been used to describe batch bacterial leaching (Blancarte-Zurita *et al.*, 1985), assumes that the leaching due to bacterial action takes place uniformly over the external surface area of the particle. This leads to a decrease in the size and surface area of the particle while its shape does not significantly change. On the other hand, the propagating-pore model is based on the observations of Southwood and Southwood (1985) who reported the development of pores in bacterially leached sulphide minerals. They concluded that leaching takes place by bacterial action within the pores and as a result the external shape and size of the particle do not change significantly as leaching progresses.

The following system has been assumed for the derivation of both models: a pure pyrite concentrate with density ρ_p and initial particle diameter d_0, is leached with bacteria in a batch system with initial solids concentration c_0. Although a particular mineral was assumed the models can be applied to any sulphide mineral undergoing bacterial leaching.

3.2 Shrinking-Particle Model.

3.2.1 Assumptions.

For the derivation of the shrinking-particle model the following assumptions have been made:

1. The mineral particles are considered to be spheres.
2. The particles consist of a single mineral.
3. Bacterial saturation on the solids takes place rapidly.
4. The rate of mineral dissolution per unit solids surface area, r_a, is constant throughout the leaching process.
5. The number of particles per unit volume of solution, n, does not change during the course of leaching.
6. Mass transfer of nutrients, oxygen and carbon dioxide to the bacteria and the solids surface and of reaction products away from the solids surface is not rate-limiting.
7. The reaction products do not inhibit the growth of bacteria nor the rate of mineral leaching.
8. None of the soluble nutrients become rate-limiting.

3.2.2 Derivation of the Equations.

For the derivation of the kinetic expressions the pyrite oxidation rate was expressed in two ways:

- As volumetric pyrite oxidation rate, r_v, which expresses the mass of pyrite oxidised per unit volume of solution per unit time, ($kg\ m^{-3}\ day^{-1}$).
- As surface pyrite oxidation rate, r_a, which expresses the mass of pyrite oxidised per unit solids surface area per unit time, ($kg\ m^{-2}\ day^{-1}$).

The volumetric pyrite oxidation rate, r_v, can be expressed in terms of the surface pyrite oxidation rate, r_s, as follows:

r_v = (surface pyrite oxidation rate) x (particle surface area) x (number of particles per unit volume of solution)

$$= r_s \, a_p \, n \qquad 3.1$$

$$= r_s \, \pi \, d^2 \, n \qquad 3.2$$

where a_p and d are the particle surface and particle diameter respectively, and the number of particles per unit volume of solution, n, calculated at initial solids concentration, c_0, is:

$$n = \frac{\text{mass of solids per unit volume of solution}}{\text{mass per particle}}$$

$$= \frac{\text{mass of solids per unit volume of solution}}{\text{(pyrite density) x (volume per particle)}}$$

$$= \frac{c_0}{\rho_p \, \frac{4}{3} \, \pi \, \frac{d_0^3}{2^3}}$$

$$= \frac{6 \, c_0}{\rho_p \, \pi \, d_0^3} \qquad 3.3$$

where ρ_p is the pyrite density and d_0 the initial particle diameter.

From Equations 3.2 and 3.3 r_v is given as:

$$r_v = 6 \, r_s \, \frac{c_0}{\rho_p} \, \frac{d^2}{d_0^3} \qquad 3.4$$

The volumetric pyrite oxidation rate, r_v, can also be expressed as the mass loss due to oxidation per unit volume of solution per unit time, i.e:

r_v = mass loss per unit volume per unit time
= (mass loss per particle per unit time) x (number of particles per unit volume)
= (pyrite density) x (volume loss per particle per unit time) x (number of particles per unit volume)

$$= \rho_p \left(-\frac{dv}{dt}\right) n$$

$$= \rho_p \frac{d}{dt}\left(-\frac{\pi d^3}{6}\right) n \qquad 3.5$$

Combining Equations 3.3 and 3.5 gives:

$$r_v = -\rho_p \frac{d}{dt}\left(\frac{\pi d^3}{6}\right) \frac{6 c_o}{\rho_p \pi d_o^3}$$

$$= -3 c_o \frac{d^2}{d_o^3} \frac{d}{dt}(d) \qquad 3.6$$

Equating Equations 3.6 and 3.4 produces:

$$-3 c_o \frac{d^2}{d_o^3} \frac{d}{dt}(d) = 6 r_a \frac{c_o}{\rho_p} \frac{d^2}{d_o^3} \quad \text{or}$$

$$\frac{d}{dt}(d) = -2 \frac{r_a}{\rho_p} \qquad 3.7$$

Integrating Equation 3.7 (from assumption 4, r_a is constant), from the initial condition of $d = d_o$ at $t = 0$ to $d = d$ at $t = t$ gives:

$$d = d_o - 2 \frac{r_a}{\rho_p} t \qquad 3.8$$

Substituting the value of d from Equation 3.8 into Equation 3.4 and rearranging yields:

$$r_v = 6\, r_a \frac{c_0}{\rho_p\, d_0} \left(1 - 2 \frac{r_a}{\rho_p\, d_0}\, t\right)^2 \qquad 3.9$$

This rate expression can be used as a basis for the derivation of a performance equation of a continuous bioleach reactor.

In batch leaching the kinetics can be related to the fraction of pyrite oxidised with time. An expression for the predicted fraction of pyrite oxidised as a function of time can be derived from the rate expression in Equation 3.9 as follows: the fraction of pyrite oxidised at any time t, F(t), is:

$$F(t) = \frac{\text{mass of pyrite oxidised at time t}}{\text{initial mass of pyrite}}$$

$$F(t) = \frac{c_0 - c_t}{c_0} \qquad 3.10$$

where c_0 is the mass of pyrite per unit volume of solution at the start of the leach and c_t is the mass of unreacted pyrite per unit volume of solution at time t. The mass of pyrite oxidised per unit volume of solution at time t is given by:

$$c_0 - c_t = {}_0\int^t r_v\, dt \qquad 3.11$$

Substituting the value of $c_0 - c_t$ from Equation 3.11 into Equation 3.10 and combining with Equation 3.9 for the initial condition of F(t) = 0 at t = 0 gives:

$$F(t) = \frac{{}_0\int^t r_v\, dt}{c_0}$$

$$= \frac{{}_0\int^t 6\, r_a \frac{c_0}{\rho_p\, d_0} \left(1 - 2 \frac{r_a}{\rho_p\, d_0}\, t\right)^2}{c_0}$$

$$= 6 \frac{r_a}{\rho_p \, d_o} \left(t - \frac{2 \, r_a}{\rho_p \, d_o} t^2 + \frac{4 \, r_a^2}{3 \, \rho_p^2 \, d_o^2} t^3 \right)$$

$$= 6 \frac{r_a}{\rho_p \, d_o} t - 12 \frac{r_a^2}{\rho_p^2 \, d_o^2} t^2 + 8 \frac{r_a^3}{\rho_p^3 \, d_o^3} t^3 \qquad 3.12$$

Since the term $\frac{r_a}{\rho_p \, d_o}$ is a constant, Equation 3.12 can be simplified by substituting $R = \frac{r_a}{\rho_p \, d_o}$:

$$F(t) = 6 \, R \, t - 12 \, R^2 \, t^2 + 8 \, R^3 \, t^3 \qquad 3.13$$

which shows that the fraction of pyrite oxidised is a third-order polynomial in time with parameters ρ_p, d_o and r_a.

3.2.3 Discussion

As has been shown, when a shrinking-particle mechanism applies the leaching kinetics can be described by means of Equations 3.8 and 3.12. Therefore, for a given mineral of density ρ and particle diameter d_o if the surface mineral oxidation rate, r_a, is known then the change in particle diameter with time, as well as the fraction of the mineral oxidised with time can be predicted from those two equations. The surface pyrite oxidation rate, r_a, can be estimated experimentally as follows: for the initial stage of the leaching process during which the change in particle diameter can be considered negligible ($d = d_o$), Equation 3.4 becomes:

$$r_{vo} = 6 \, r_a \frac{c_o}{\rho_p} \frac{1}{d_o} \qquad \text{or} \qquad 3.14$$

$$r_a = \frac{r_{vo}}{6} \frac{\rho_p}{c_o} d_o \qquad 3.15$$

where $r_{v,o}$ is the initial volumetric oxidation rate. This can be calculated from the initial slope of the experimental curve F(t) versus t multiplied by the solids concentration, c_o. Generally the volumetric oxidation rate at any time can be calculated by the experimental F(t) versus t curve:

$$r_v = \frac{dF(t)}{dt} c_o \qquad 3.16$$

Blancarte-Zurita et al. (1985) have also considered a shrinking-particle model and have derived a kinetic expression similar to Equation 3.6. For the integration of this equation it is necessary to know how r_v varies with respect to particle size and time. For this purpose the above researchers carried out a series of experiments, in which metal extraction versus time was recorded for various size fractions. From these results the dependence of the volumetric oxidation rate, r_v, on particle size and time could be found and used for the integration of Equation 3.6. However a more fundamental parameter than the volumetric leach rate, the surface leach rate, r_s, was introduced in the derivation of the shrinking-particle model in the present study. It has been assumed that this parameter remains constant throughout the leaching process (assumption 4), thus enabling the integration of Equation 3.7. It seems reasonable, although as yet unproved, that this assumption is valid when a shrinking-particle mechanism applies. On the other hand this assumption may not be valid in the case of a shrinking-core mechanism, where reactions are expected to be diffusion controlled along the reaction zone and therefore the surface oxidation rate may change during the course of leaching.

The effect of particle size on the shrinking-particle model is shown in Figure 3.1. The F(t) versus t curve was obtained using Equation 3.12 at the four particle diameters 90,5, 64,0, 45,5 and 31,5 micron (see Table B1). The pyrite density was set equal to ρ_p = 5000 kg m^{-3} and the $r_s = 7 \times 10^{-4}$ kg m^{-2} day^{-1}. This r_s value is approximately equal to the surface pyrite oxidation rate estimated in the present study.

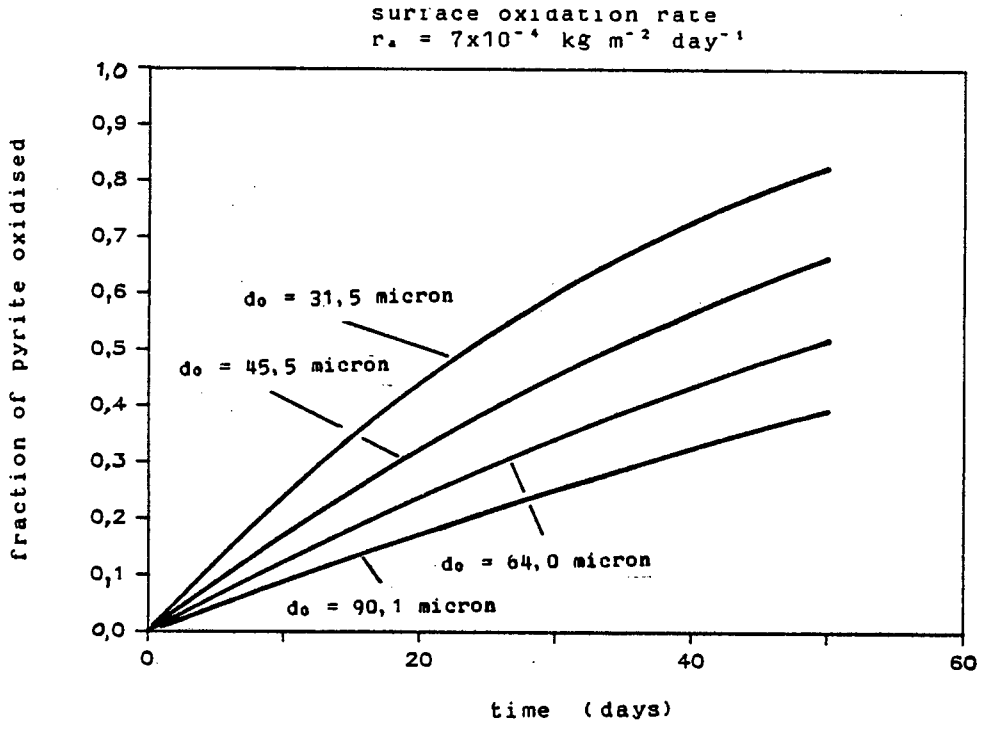

Figure 3.1: Effect of particle size. - Shrinking-particle model.

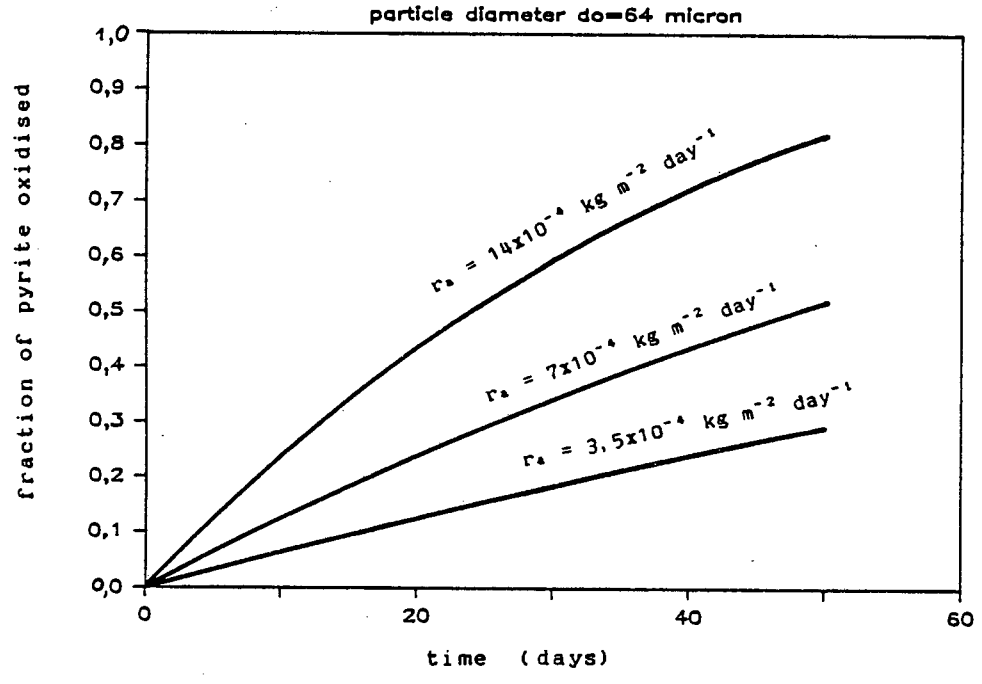

Figure 3.2: Effect of surface oxidation rate. - Shrinking -particle model (a).

Figure 3.1 shows that the fraction of pyrite oxidised increases with decreasing particle size. This implies that the volumetric oxidation rate, as defined by Equation 3.16, also increases with decreasing particle size. The shape of the curves also indicates that the first derivative of F(t) decreases steadily with time for a given particle size, and consequently the volumetric oxidation rate also decreases with time. This can also be shown by the examination of the sign of the second derivative of F(t):

$$\frac{d^2F(t)}{dt^2} = 24 \frac{r_a^2}{\rho_p^2 d_o^2} \left(2 \frac{r_a}{\rho_p d_o} t - 1\right) \qquad 3.17$$

The term $2 \frac{r_a}{\rho_p d_o} t - 1$ is always negative for the set of values of r_a, ρ_p, d_o and time used in this study and therefore the second derivative of F(t) is negative. It follows that the first derivative of F(t) decreases with time and so does the volumetric oxidation rate.
Therefore the shrinking-particle model predicts that the volumetric pyrite oxidation rate, r_v, will decrease with time as a result of the particle size decrease during the course of leaching.

The effect of the surface oxidation rate on the shrinking-particle model is depicted in Figure 3.2. Three different r_a values, $r_a = 3,5 \times 10^{-4}$, $r_a = 7 \times 10^{-4}$ and $r_a = 14 \times 10^{-4}$ kg m^{-2} day^{-1}, were used to predict the F(t) versus t curve from Equation 3.12 for a specific particle diameter, d_o = 64 micron, and density ρ_p = 5000 kg m^{-3}.

Figure 3.2 illustrates that the fraction of mineral oxidised and, therefore the volumetric mineral oxidation rate, increases with increasing surface mineral oxidation rate, r_a.

The value of t at the point of inflection of Equation 3.12 can be obtained from:

$$\frac{d^2\bar{F}(t)}{dt^2} = 0 \qquad \text{or} \qquad 3.18$$

$$-24 \frac{r_a^2}{\rho_p^2 d_0^2} (1 - 2 \frac{r_a}{\rho_p d_0} t) = 0 \qquad 3.19$$

$$\text{from which} \quad t = \frac{\rho_p d_0}{2 r_a} \qquad 3.20$$

Substituting the value of t from Equation 3.20 into Equation 3.12 gives:

$$F(t) = 1$$

which means that all the mineral has been oxidised at the time corresponding to the point of inflection. In order to calculate the time at which this happens the value of r_a has to be known. For a typical particle diameter d_0 = 64 micron, density ρ = 5000 kg m^{-3} and r_a values that differ by an order of magnitude, Equation 3.20 gives:

r_a = 7 x 10^{-4} kg m^{-2} day^{-1}	t = 228 days
r_a = 70 x 10^{-4} kg m^{-2} day^{-1}	t = 22 days
r_a = 700 x 10^{-4} kg m^{-2} day^{-1}	t = 2 days

In order for the inflection point to occur at time t = 50 days or in order for the mineral to be completely oxidised in 50 days an r_a value of 32x10^{-4} kg m^{-2} day^{-1} is required, as shown in Figure 3.3.

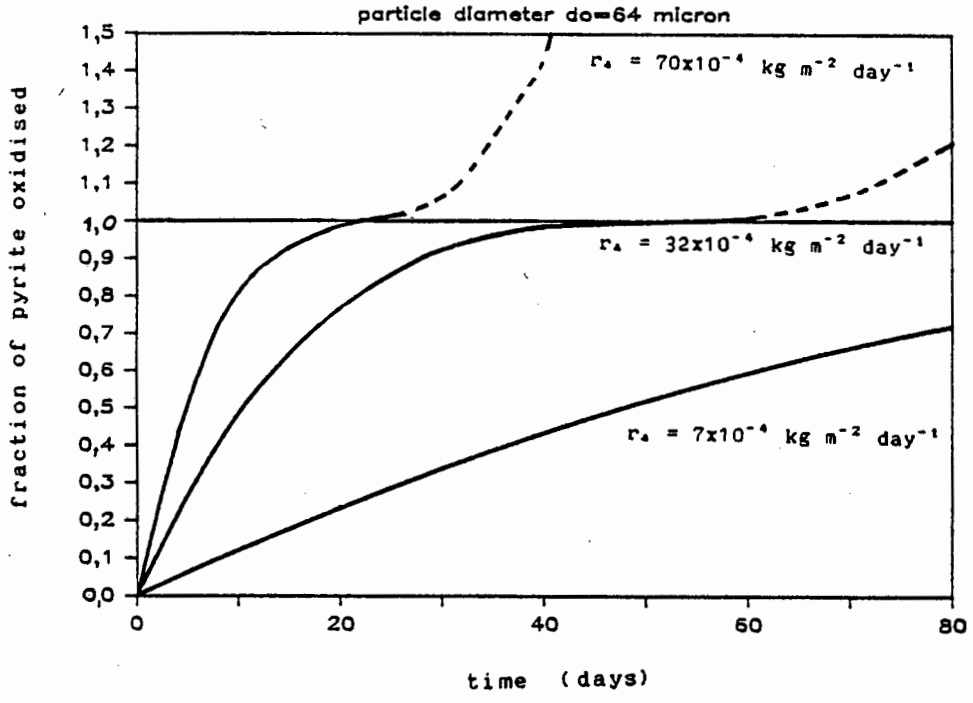

Figure 3.3: Effect of surface oxidation rate.- Shrinking -particle model (b).

3.3 Propagating-Pore Model

By examining polished sections of particles subjected to bacterial leaching Southwood and Southwood (1985) observed that bacterial leaching may take place in the pyrite particles in the following way: The bacteria oxidise the mineral, developing pores which are preferentially orientated parallel to the three crystallographic axes of the pyrite crystal lattice. The pores occur mainly in structurally disturbed regions of the pyrite crystals.

The above observations have been used in this study as the basis for the derivation of a propagating-pore model. For this purpose it is assumed that pores develop along all potential loci in the particle (active pores). The initial number of pores is therefore dependent on the number of potential avenues for pore development and will vary with the mineralogical character of the particles. However after some

time a number of pores will stop propagating (and therefore become inactive pores), either because they have penetrated through to the other side of the particle or have run into some barrier or inactive region within the particle. Consequently the number of active pores decreases with time. After some time all the pores will have become inactive and leaching via the propagating-pore mechanism will cease. Fundamental to the development of the model is the assumption that the rate of leaching in terms of the mass of pyrite leached per unit area of pore base per unit time at the leading face of the propagating pore is constant. This means that the speed with which the pores propagate is constant during the course of leaching and, if all pores are of equal diameters then they all propagate with equal velocity.

It is also assumed that there is a minimum pore length, to which pores will develop before becoming inactive, and some maximum length that pores can attain, governed largely by particle size. Therefore in a particle in which all pore leaching has been completed there will a number of inactive pores whose terminating lengths lie between a minimum and a maximum value.

3.3.1 Assumptions.

For the derivation of the propagating-pore model the following assumptions have been made:

1. The mineral particles are considered to be spheres.
2. The particles consist of a single mineral.
3. Bacterial saturation on the solids takes place rapidly.
4. The pore propagation starts rapidly. All pores start from the particle surface and the number of possible new pores formed within the particle is negligible.
5. Bacterial oxidation is confined to the leading face (closed end) of the pore. No bacterial oxidation of pore walls takes place (Southwood and Southwood, 1985).

6. The rate of mineral dissolution per unit surface area of pore base, r_p, is constant throughout the leaching process.
7. All pores have equal diameters.
8. The number of particles per unit volume of solution, n, does not change during the course of leaching.
9. Mass transfer of nutrients, oxygen and carbon dioxide to the bacteria and the pore base and of reaction products away from the pore base is not rate-limiting.
10. The products of reaction do not inhibit the growth of bacteria nor the rate of mineral leaching.
11. None of the soluble nutrients become rate-limiting.

3.3.2 Derivation of the Equations.

The volumetric pyrite oxidation rate, r_v, can be expressed as:

r_v = (pore oxidation rate) x (number of active pores per particle) x (number of particles per unit volume)

$$= (r_p\ b)\ (n_q\ \pi\ d_o^2)\ n \qquad 3.21$$

where r_p: pyrite oxidation rate at the pore base (kg m^{-2} day^{-1}), constant

b: area of the pore base (m^2), constant

n_q: number of active pores per unit surface area (m^{-2})

Since r_p and b cannot be measured easily it is more practical to express the r_v in terms of surface oxidation rate, r_a, which expresses the rate of pyrite oxidation per unit particle surface area. This oxidation occurs only at the closed end of the active pores. The r_a is expressed as a function of r_p as follows:

r_a = (pyrite oxidation rate at the pore base) x (base area of a pore) x (number of active pores per unit surface area)

$$= r_p\ b\ n_q \qquad 3.22$$

The above equation indicates that, unlike the shrinking-particle model, r_s is not constant during the course of leaching since n_q changes with time. However for the initial stage of leaching, during which all pores are active i.e. $n_q = n_{q0}$, the surface oxidation rate is constant and has its maximum value, r_{s0}:

$$r_{s0} = r_p \; b \; n_{q0} \quad \text{or}$$

$$r_p = \frac{r_{s0}}{b \; n_{q0}} \qquad 3.23$$

Substituting r_p and n from Equations 3.23 and 3.3 respectively, Equation 3.21 becomes:

$$r_v = 6 \; r_{s0} \; \frac{c_0}{\rho_p} \; \frac{1}{d_0} \; \frac{n_q}{n_{q0}} \qquad 3.24$$

The above equation indicates that the number of active pores, n_q, must be known in order to calculate the volumetric oxidation rate at any given time. This can be done as follows: assume that there is some terminating length L at which leaching stops in a pore, either because the pore has penetrated right through the particle or because the pore has reached an inactive region within the particle. Thus when the pore length is less than L the pore is active and when it becomes equal to L the pore becomes inactive. It seems unlikely that all pores will terminate at the same depth, and rather that there is some minimum depth at which pores terminate, L_i; and some maximum depth that some pores attain for a particular particle size before terminating, L_e. Between these two limits the terminating pore length L can be assumed to be distributed in some manner expressed by a distribution function f(L). It follows that if the terminating pore length distribution within the particle, f(L), is known, then the number of pores with terminating lengths less than L can be calculated.

It was assumed that the terminating pore lengths are uniformly distributed between a minimum pore length, L_i, and a maximum pore length, L_e, as described by the following function:

$$f(L) = \begin{cases} 0 & \text{for } 0 < L \leq L_i \\ \dfrac{n_{e0}}{L_e - L_i} & \text{for } L_i < L < L_e \\ 0 & \text{for } L \geq L_e \end{cases} \qquad 3.25$$

This distribution is illustrated in Figure 3.4.

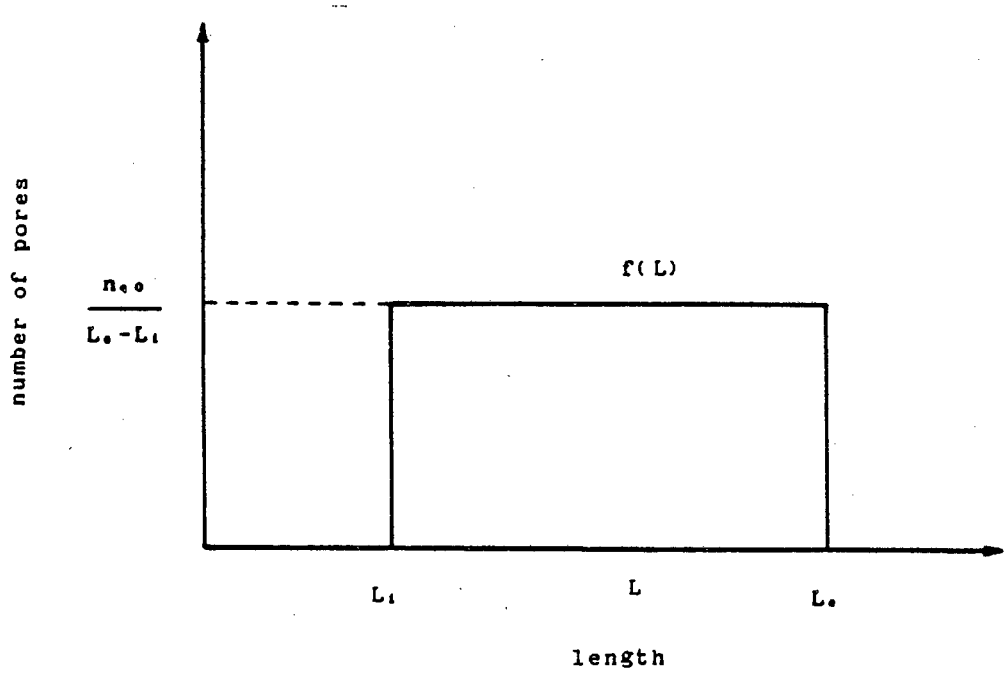

Figure 3.4: Terminating pore length distribution.

Then the number of pores per unit surface area with terminating lengths less than a value L, is given by the function $F(L) = \int_0^L f(L)\,dL$, which is expressed as follows:

$$F(L) = \int_0^L f(L)\,dL = \begin{cases} 0 & \text{for } 0 < L \leq L_i \\ \dfrac{n_{q0}}{L_e - L_i}(L - L_i) & \text{for } L_i < L < L_e \\ n_{q0} & \text{for } L \geq L_e \end{cases} \qquad 3.26$$

This new distribution is illustrated in Figure 3.5.

The time t required by the bacteria to develop a pore of length L is:

$$t = \frac{L}{v_p} \qquad 3.27$$

where $v_p = \dfrac{r_p}{\rho_p}$ is the constant velocity at which the pore propagates into the particle. At any time t all pores with terminating length less than $L = t\,v_p$ have become inactive. Therefore the number of inactive pores at time t is equal to the number of pores having terminating length less than $L = t\,v_p$, and is given by Equation 3.26. In order to obtain the number of inactive pores at any time t, the numerator and denominator of Equation 3.26, as well as the length intervals, are divided by v_p and combining with Equation 3.27 gives:

$$P(t) = \begin{cases} 0 & \text{for } t \leq T_i \\ \dfrac{n_{q0}}{T_e - T_i}(t - T_i) & \text{for } T_i < t < T_e \\ n_{q0} & \text{for } t \geq T_e \end{cases} \qquad 3.28$$

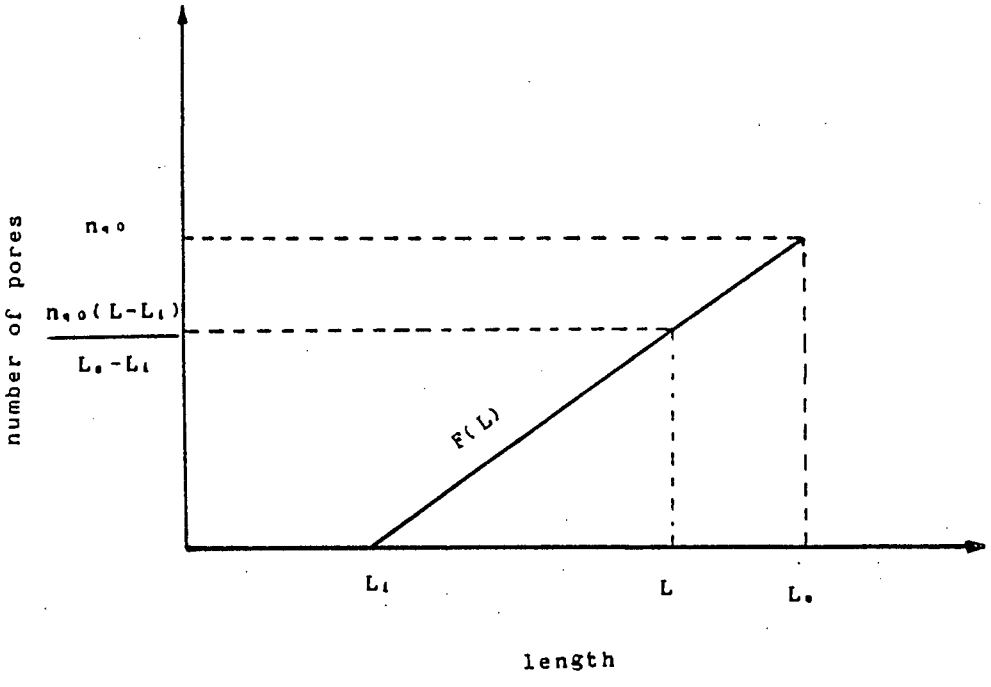

Figure 3.5: Number of pores with terminating length less than L

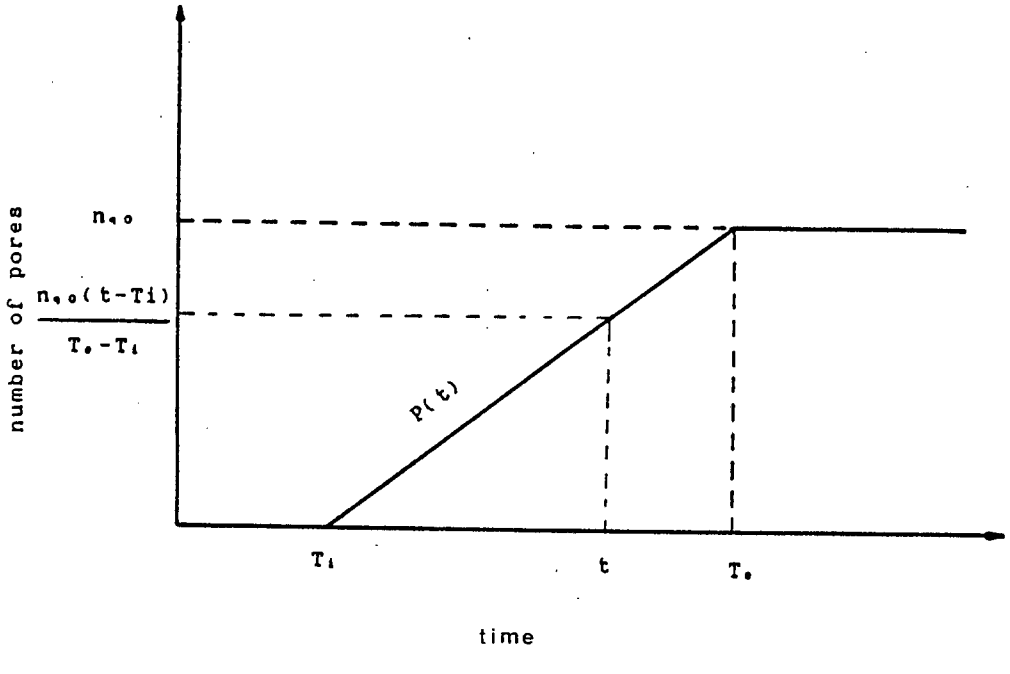

Figure 3.6: Number of inactive pores at time t.

This equation is illustrated in Figure 3.6, which indicates the following: at time $t \leq T_i$ there are no terminated pores therefore all pores are active; at time t, $T_i < t < T_e$, there are $n_{q0} (t-T_i) / (T_e-T_i)$ inactive pores and $n_q = n_{q0} - n_{q0} (t-T_i) / (T_e-T_i)$ active pores; at time $t \geq T_e$ there are n_{q0} terminated pores or n_{q0} inactive pores.

The number of active pores at any moment t is given by:

$$n_q = n_{q0} - P(t) \qquad 3.29$$

According to Equations 3.28 and 3.29 Equation 3.24 becomes:

$$r_v = 6\, r_{a0}\, \frac{c_0}{\rho_p}\, \frac{1}{d_0} \left(\frac{n_{q0} - P(t)}{n_{q0}} \right)$$

$$= 6\, r_{a0}\, \frac{c_0}{\rho_p}\, \frac{1}{d_0} \left(1 - \frac{P(t)}{n_{q0}} \right) \qquad 3.30$$

The fraction of pyrite oxidised F(t) at time t is given by Equations 3.10 and 3.11. Substituting r_v from Equation 3.30 gives:

$$F(t) = \frac{c_0 - c_t}{c_0} = \frac{\int_0^t r_v\, dt}{c_0}$$

$$= \frac{\int_0^t 6\, r_{a0}\, \frac{c_0}{\rho_p}\, \frac{1}{d_0} \left(1 - \frac{P(t)}{n_{q0}} \right)}{c_0}$$

$$= \frac{6\, r_{a0}}{\rho_p\, d_0} \int_0^t \left(1 - \frac{P(t)}{n_{q0}} \right) dt \qquad 3.31$$

The integration in Equation 3.31 will be done over the three time intervals, $t \leq T_i$, $T_i < t < T_e$, $t \geq T_e$

- $t \leq T_i$. Substituting P(t) from Equation 3.28, Equation 3.31 gives:

$$F(t) = \frac{6\ r_{a0}}{\rho_p\ d_0} \int_0^t \left(1 - \frac{0}{n_{q0}}\right) dt$$

$$= \frac{6\ r_{a0}}{\rho_p\ d_0} \int_0^t dt$$

$$= \frac{6\ r_{a0}}{\rho_p\ d_0}\ t + C \qquad 3.32$$

Since $F(t=0) = 0$, $C=0$.

Thus for $t \leq T_i$, $F(t) = \frac{6\ r_{a0}}{\rho_p\ d_0}\ t$ 3.33

$T_i < t < T_e$. Substituting $P(t)$ from Equation 3.28, Equation 3.31 gives:

$$F(t) = \frac{6\ r_{a0}}{\rho_p\ d_0} \int_0^t \left(1 - \frac{t-T_i}{T_e-T_i}\right) dt$$

$$= \frac{6\ r_{a0}}{\rho_p\ d_0} \int_0^t \frac{T_e-t}{T_e-T_i} dt$$

$$= \frac{6\ r_{a0}}{\rho_p\ d_0}\ \frac{1}{T_e-T_i} \int_0^t (T_e-t)\, dt$$

$$= -\frac{6\ r_{a0}}{\rho_p\ d_0}\ \frac{1}{T_e-T_i}\ \frac{(T_e-t)^2}{2} + C \qquad 3.34$$

In order to calculate the value of C in Equation 3.34, $F(t)$ at time T_i of Equation 3.33 is set equal to $F(t)$ at time T_i of Equation 3.34:

$$\frac{6\ r_{a0}}{\rho_p\ d_0}\ T_i = -\frac{6\ r_{a0}}{\rho_p\ d_0}\ \frac{(T_e-T_i)^2}{2\ (T_e-T_i)} + C \qquad 3.35$$

From Equation 3.35

$$C = \frac{6\ r_{a0}}{\rho_p\ d_0}\ \frac{T_e+T_i}{2} \qquad 3.36$$

Substituting the value of C from Equation 3.36 into Equation 3.34 gives:

$$F(t) = -\frac{6\ r_{a0}}{\rho_p\ d_0}\ \frac{1}{T_e-T_i}\ \frac{(T_e-t)^2}{2} + \frac{6\ r_{a0}}{\rho_p\ d_0}\ \frac{T_e+T_i}{2}$$

$$= \frac{6\ r_{a0}}{\rho_p\ d_0}\left(t - \frac{(t-T_i)^2}{2\ (T_e-T_i)}\right) \qquad 3.37$$

- $t \geq T_e$. Substituting P(t) from Equation 3.28, Equation 3.31 gives:

$$F(t) = \frac{6\ r_{a0}}{\rho_p\ d_0}\int_0^t \left(1 - \frac{n_{q0}}{n_{q0}}\right) dt$$

$$= \frac{6\ r_{a0}}{\rho_p\ d_0}\ C \qquad 3.38$$

In a similar manner the value of C in Equation 3.38 is calculated by setting F(t) at $t = T_e$ of Equation 3.37 equal to F(t) at $t = T_e$ of Equation 3.38:

$$\frac{6\ r_{a0}}{\rho_p\ d_0}\left(T_e - \frac{(T_e-T_i)^2}{2\ (T_e-T_i)}\right) = \frac{6\ r_{a0}}{\rho_p\ d_0}\ C \qquad 3.39$$

From Equation 3.39

$$C = \frac{T_e+T_i}{2} \qquad 3.40$$

Therefore Equation 3.38 becomes:

$$F(t) = \frac{6\ r_{a0}}{\rho_p\ d_0}\ \frac{T_i+T_e}{2} \qquad 3.41$$

Summarising Equations 3.33, 3.37 and 3.41 we obtain:

$$F(t) = \frac{6\ r_{a0}}{\rho_p\ d_0}\ t \qquad \text{for } t \leq T_i$$

$$F(t) = \frac{6\ r_{a0}}{\rho_p\ d_0}\left(t - \frac{(t-T_i)^2}{2\ (T_e - T_i)}\right) \qquad \text{for } T_i < t < T_e$$

$$F(t) = \frac{6\ r_{a0}}{\rho_p\ d_0}\ \frac{T_i + T_e}{2} \qquad \text{for } t \geq T_e$$

3.42

3.3.3 Discussion

It has been shown that the batch kinetics of the propagating-pore mechanism is described by Equation 3.42: the fraction of pyrite oxidised is linearly dependent on time for $t \leq T_i$; second order with time for $T_i < t < T_e$; and zero order with time for $t \geq T_e$. In terms of the volumetric pyrite oxidation rate, T_i represents the time when r_v decreases from the previously constant value r_{v0} due to partial pore deactivation, and T_e the time when r_v becomes zero due to total pore deactivation.

The values of T_i and T_e, which are related to the values of minimum and maximum terminating pore lengths, L_i and L_e, should depend on the particle size. It is expected that both L_e and L_i would increase as particle size decreases. As a result the time T_i and T_e should decrease as particle size decreases.

During the initial stage of leaching when all pores are active, ($n_q = n_{q0}$), Equation 3.24 gives:

$$r_{v0} = 6\ r_{a0}\ \frac{c_0}{\rho_p}\ \frac{1}{d_0} \qquad 3.43$$

Comparing Equations 3.14 and 3.43 one observes that during the initial stage of leaching, until pores have become

inactivated via the propagating-pore mechanism or until the surface area has significantly decreased via the shrinking-particle mechanism, both models give a similar expression for the volumetric pyrite oxidation rate.

The effect of particle size on the propagating-pore model is shown in Figure 3.7. The F(t) versus t curve was obtained at the four particle diameters, 90,5, 64,0, 45,5 and 31,5 micron (Table B1), using Equation 3.42. The pyrite density was set equal to ρ_p = 5000 kg m^{-3} and the surface oxidation rate, r_{a0} = $7x10^{-4}$ kg m^{-2} day^{-1}. The values used for the parameters T_i and T_e are given below and are approximately equal to the T_i and T_e values estimated in this study.

This figure illustrates that the fraction of pyrite oxidised, and consequently the volumetric oxidation rate, increases with decreasing particle size.

The effect of the surface oxidation rate on the propagating-pore model is illustrated in Figure 3.8. Three different r_{a0} values, r_{a0} = $3,5x10^{-4}$, r_{a0} = $7x10^{-4}$ and r_{a0} = $14x10^{-4}$ kg m^{-2} day^{-1} were used to predict the F(t) versus t curve using Equation 3.42, for a specific size fraction, d_0 = 64 micron, and density ρ_p = 5000kg m^{-3}. The above values for T_i and T_e were used.

Table 3.1: T_i and T_e values used for the calculation of the propagating-pore model curves.

particle size micron	T_i days	T_e days
90,5	15	44
64,0	13	40
45,5	11	36
31,5	9	32

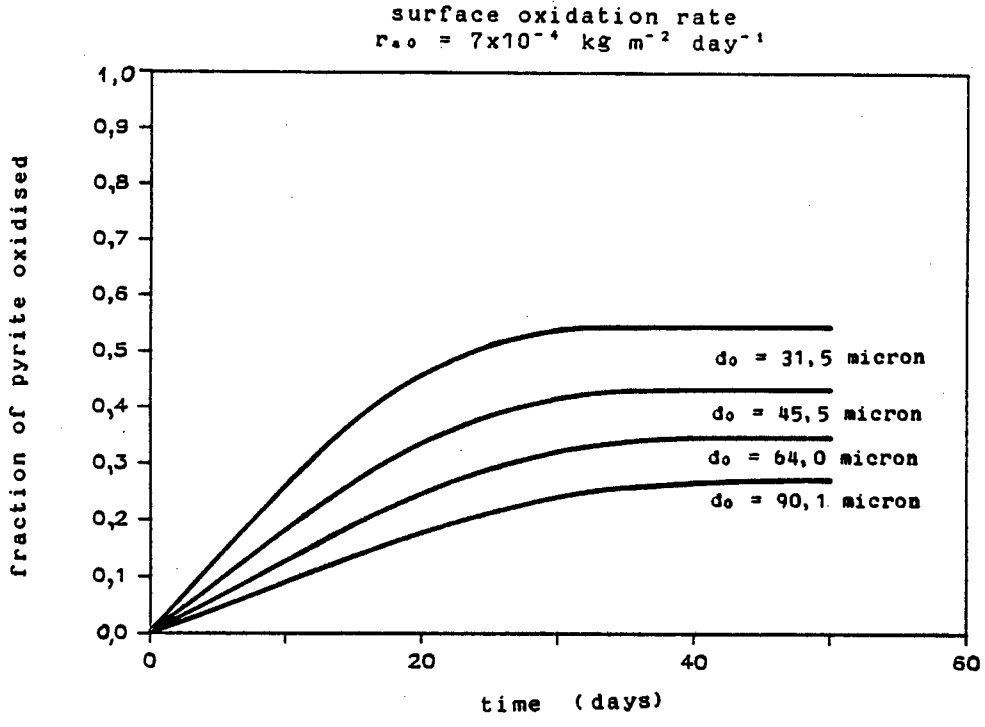

Figure 3.7: Effect of particle size. - Propagating-pore model

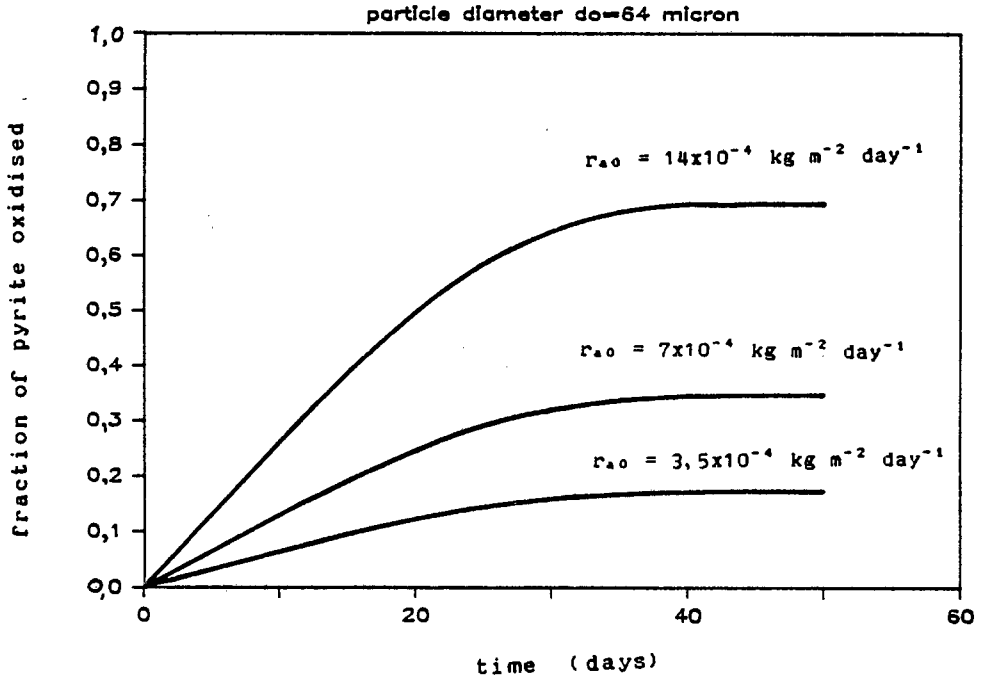

Figure 3.8: Effect of surface oxidation rate.- Propagating-pore model.

Figure 3.8 illustrates that the fraction of mineral oxidised and, consequently the volumetric oxidation rate increase with increasing surface oxidation rate, r_s.

3.4 General Comments on Theory

Two models that describe the oxidation kinetics of a sulphide mineral in a batch bacterial system were presented in this chapter: the shrinking-particle model according to which the oxidation occurs on a front defined by the external surface area of the particle; and the propagating-pore model according to which the bacteria preferentially oxidise the mineral within pores, which develop along regions of weak crystal structure and are orientated parallel to the crystallographic axes of the sulphide crystal.

The shrinking-particle mechanism suggests that the particle size, along with the surface area concentration, will continuously decrease as the bioleach progresses hence resulting in a steady decrease in the volumetric oxidation rate of the mineral during the course of leaching.

On the other hand the propagating-pore mechanism does not predict a change in particle size, unless this is a result of particle breakage due to the formation of large pores. Also the surface area available for oxidation, being mainly the leading face of the pore, may increase with time due to the development of new pores as the bacteria come in contact with new structurally weak regions within the particle. However, in the derivation of the mathematical equations for the propagating-pore model in this study the surface area available for oxidation was assumed constant during the linear phase of the process.

Both models while inferring that leaching is controlled by the action of the attached bacteria do not depend on any assumption regarding indirect or direct leaching mechanism nor do they require a measure of the attached bacteria.

Both mechanisms of oxidation have been observed separately in bacterial leach systems. The type of leaching may depend on various factors, such as the mineralogy and crystal structure of the mineral. However the two mechanisms do not exclude each other. It is possible that oxidation occurs simultaneously on the outer particle surface by the shrinking-particle mechanism and the interior of the particle by the propagating-pore mechanism although the corresponding oxidation rates could be different, Southwood and Southwood (1985).

Although Equations 3.12 and 3.42 are valid for pure minerals they also are valid when the calculations are based on one of the metals of a concentrate or an ore (i.e, iron for pyrite or copper for chalcopyrite)

In this study the calculations are based on the total-sulphur oxidised and therefore ρ represents the density of sulphur in the concentrate, and the estimated r_s the sulphur oxidation rate. The corresponding pyrite oxidation rate can be calculated from the stoichiometric relationship of sulphur in the pyrite.

CHAPTER 4

APPARATUS AND EXPERIMENTAL PROCEDURE

4.1 Introduction

In this chapter the experimental apparatus and procedures used in this study are described. Where the procedures used were standard, the appropriate reference is cited. Procedures which differed sufficiently from those described in the literature are described in full.

4.2 Origin, Preparation and Composition of the Concentrate

The pyrite concentrate used in this study originates from the Crown Mines waste ore dumps, which had previously been processed for gold recovery. A flotation pyrite concentrate was obtained from the ore dump samples and was further subjected to a gravity concentration using shaking tables at MINTEK laboratories. The concentrate was then sized into four different particle size fractions: +75-106, +53-75, +38-53 and +25-38 micron respectively. The three larger size fractions were obtained by sieving the concentrate using standard laboratory sieves. The +25-38 micron fraction was obtained by cyclosizing the -38 micron size fraction in a standard WARMAN cyclosizer.

All size fractions were cyanide leached in order to extract the non-refractory gold. A 50% slurry solution was used for the cyanidation and the pH was adjusted to 11.5 using a 10% sodium hydroxide solution. Sodium cyanide was added to give a final sodium cyanide concentration of 2% w/v (5g NaCN per 250 g solution). This suspension was bottle rolled for 24 hours, after which the solution was decanted and titrated to determine residual cyanide, CN^-. The bottle

rolling procedure was repeated. In order to remove any cyanide precipitate, the cyanided concentrates were then bottle-roll washed with 5% hydrochloric acid for 1 hour at 50% solids concentration. The washed concentrates were filtered, rinsed thoroughly with distilled water and dried so as to enable metal content analyses to be made. Analyses for iron, sulphur, arsenic, nickel, copper and gold were performed.

The iron analysis was performed as follows: the sample was fused with sodium peroxide and leached in boiling water. The hydroxide precipitate was separated by filtration. The precipitate was redissolved in hydrochloric acid and then reduced with stannous chloride solution. This solution was titrated with potassium dichromate using sodium diphenylamine as indicator (Vogel, 1961).

The sulphur analysis was performed in a LECO Sulphur Determinator, SC32 DB64, at 1350°C. At this temperature the total sulphur content of the sample is determined. An elemental sulphur analysis was also done as follows: the sample was dissolved in hot carbon tetrachloride. The liquid was separated from the insoluble portion using a continuous Soxhlet type reflux system. The solvent was evaporated and the sulphur was determined gravimetrically. The elemental sulphur was under the detection limit of the method, 0,5%, for all size fractions.

The arsenic, nickel and copper analyses were performed by acid-digesting the sample in perchloric acid and hydrofluoric acid. The resulting solution was assayed for arsenic, nickel and copper in a VARIAN MODEL 1275 Atomic Absorption Spectrophotometer. The gold was determined by a fire assay method, (Van Wyk and Dixon, 1983). The results from all the above assays are given in Table 4.1.

The feed samples prepared as described above were stored in an atmospheric environment before use. This might have resulted in surface oxidation of the pyrite. Thus, in order

to remove any acid-soluble oxide as well as to standardise the experiments, the samples were washed with an 8% hydrochloric acid solution for 2 hours prior to use (Silverman, 1967; Lau et al., 1970; Pinches et al., 1976). The samples were then filtered, rinsed thoroughly with distilled water and dried. Preliminary tests showed that the hydrochloric acid-wash did not dissolve any pyrite.

Table 4.1: Analysis of the Crown Mine concentrate after cyanidation and acid wash.

size fraction micron	Fe g/100g	S g/100g	Au g/t	As g/t	Ni g/t	Cu g/t
+75-106	44,4	50,20	4,65	2100	1380	980
+53-75	44,6	50,55	2,87	2380	1790	1200
	first series of batch experiments					
+38-53	44,9	51,05	2,51	2810	2135	1350
+25-38	43,7	52,00	1,18	1500	1100	670
	second series of batch experiments					
+38-53	45,0	51,10	2,36	3700	2140	1270
+25-38	44,8	51,80	1,44	2110	1390	479

4.3 Maintenance of Bacteria

The bacterium used was originally a pure strain of Thiobacillus ferrooxidans (ATCC 33020). It was routinely maintained on the 9K medium of Silverman and Lundgren (1959) in which the ferrous iron source was replaced by pyrite

concentrate to give a concentration of 10% (w/v) at a pH of 1.8, Table 4.2. The bacteria were transferred to fresh medium every 15 days so as to guarantee the continued existence of the bacterial culture. This period was reduced to 8 days when the culture was used as an inoculum. This procedure ensured that a culture adapted to the pyrite concentrate was available for inoculation when required.

Table 4.2: 9K growth medium

salts	amount g
$(NH_4)_2SO_4$	3,00
K_2HPO_4	0,50
KCL	0,10
$MgSO_4$	0,50
$Ca(NO_3)_2$	0,01
H_2SO_4	to give desired pH
water	up to 1 liter

Bacteria for use as inoculum were harvested from late logarithmic phase cultures. To secure a clean iron-free inoculum, the following harvesting procedure was followed: unreacted mineral particles and precipitates were allowed to settle overnight from growth suspensions. Part of the supernatant was centrifuged at 10000 rpm for 10 minutes using a SORVALL RC2-B centrifuge. The pellet, consisting of bacteria and a small amount of the undesired fine precipitate was removed. It was then resuspended in iron-free 9K medium at a pH of 1.6 and temperature 4°C, and shaken vigorously so as to enable dissolution of the precipitate. The suspension was centrifuged again and the whole procedure repeated until all the precipitate had dissolved. The clean bacterial

pellet was resuspended in iron-free 9K medium. Bacteria were used as inoculum within five hours of being washed. Cell numbers in the fresh inoculum were estimated by visual count, and the amount of inoculum used was that necessary to ensure an initial bacterial concentration of $1,0x10^8$ cells/ml in each reactor. Aseptic conditions were not followed.

4.4 Evaluation of Bacterial Growth

The estimation of the numbers of free bacteria was done by visual count using a THOMA counting chamber in a NIKON microscope under phase contrast at 400 times magnification. The number of bacteria in sixteen small squares was counted for each of three samples, and the average count multiplied by $2x10^7$ gave the bacterial concentration in solution in cells/ml.

Several methods of estimating the numbers of attached bacteria were attempted unsuccessfully. Techniques such as vibromixing the sample to detach the attached bacteria after mixing it with iso-propanol (Corrans, 1974), or immersing it into the ultrasonic bath for various periods of time, either made no difference in the numbers of the free cells or were not reproducible.

4.5 Leaching Techniques

The experiments conducted in this study were all batch experiments. No provision was made for sterilisation and maintenance of asepsis. As batch tests were lengthy the reactors constructed had to be reliable over a long period of time. The reactors employed were twelve identical polyvinyl cylindrical containers with the following dimensions: height 230 mm, diameter 190 mm, volume 5 liters, see Figure 4.1 below.

The reactors were sealed with a Perspex lid, which could easily be removed so that all the necessary measurements (pH, temperature, water loss due to evaporation, oxygen concentration) and adjustments could be done. In the centre of the lid a single-speed agitator motor was attached. The agitation was by means of a stirrer with a two-bladed impeller, as shown in Figure 4.1. An agitation rate of 1300 rpm was used. This high agitation rate was necessary so as to:

- ensure good mixing and mass transport to and from the mineral particles,
- prevent any settling of the solids at the solids concentration used and also
- prevent possible coating of the pyrite particles by any precipitates.

The reactors were maintained at 30°C by placing them in two stainless steel water baths each heated by a thermoregulator, as shown in Figure 4.2. Each water bath could accommodate 6 reactors. The baths' dimensions were: length 1000 mm, width 600 mm and height 200 mm.

The culture suspension was aerated by pumping air through a 3 mm plastic pipe that passed through the lid and almost reached the bottom of the reactor. The air supplied was first led through a humidifier at room temperature to avoid excess water evaporation from the reactor. No additional carbon dioxide was supplied.

The following procedure was adopted for preparing leach tests: a known volume of iron-free 9K medium (2,5 liters minus the volume of the inoculum), at a pH of 1.8 was put into each reactor. 250 g of the required size fraction was then added to give a final solids concentration of 10% (w/v). This was followed by the addition of the necessary volume of fresh inoculum to give an initial cell concentration of $1,0 \times 10^8$ cells/ml in solution. The pH of the suspension was adjusted to 1.8 with a few drops of concentrated sulphuric acid, and the reactors were then put into the water bath.

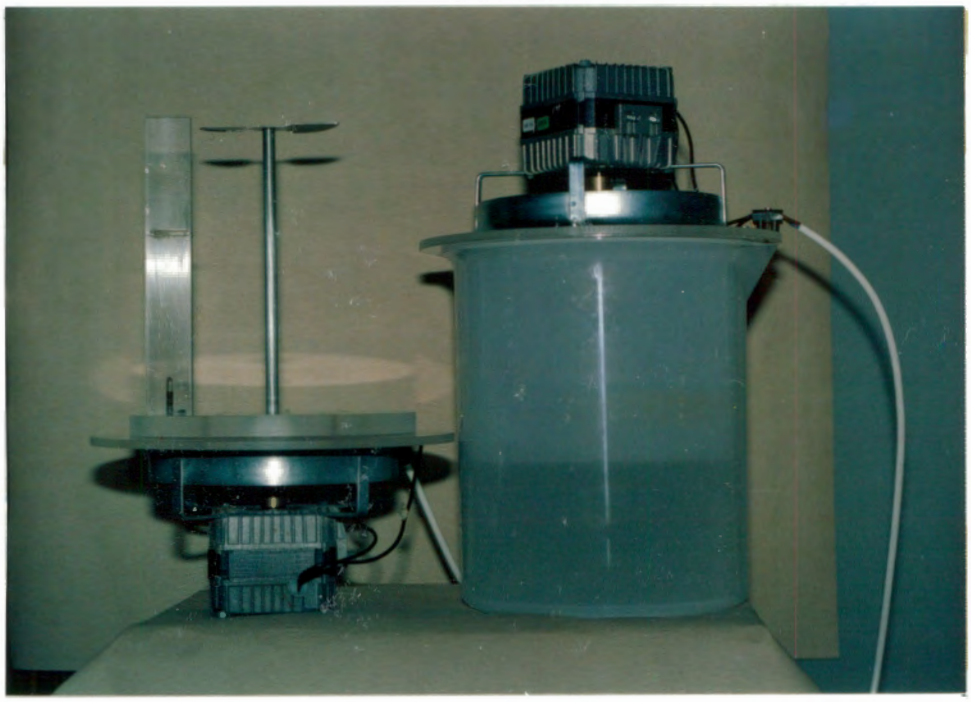

Figure 4.1: View of a reactor.

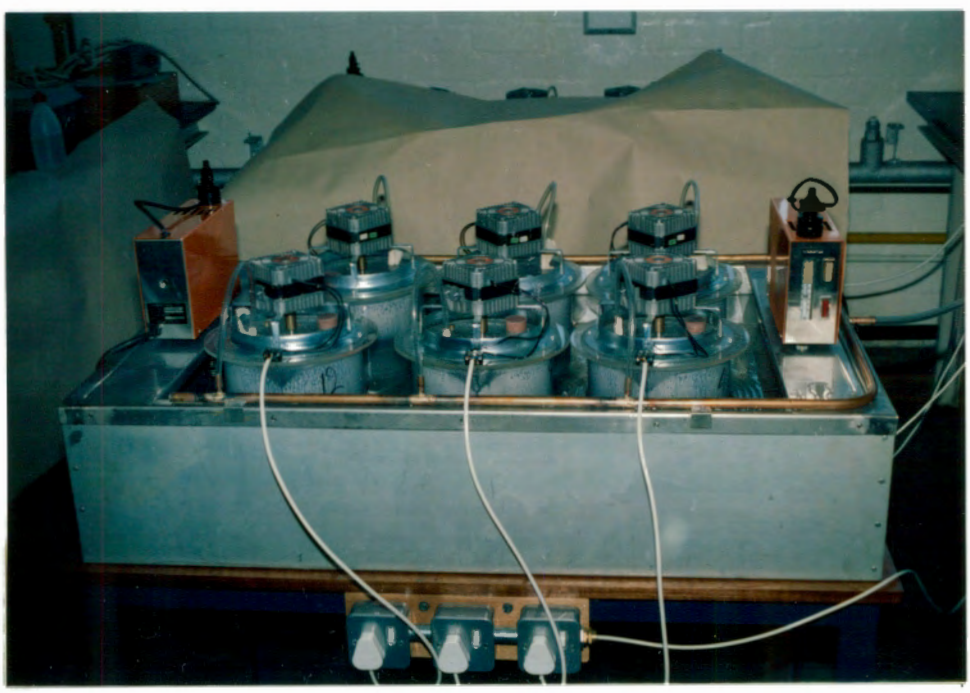

Figure 4.2: View of a water bath with 6 reactors.

A number of identical reactors were set up for each time profile batch test. The bacterial growth and leach rates were assumed identical for each reactor. A number of assumed identical reactors were used as opposed to one large reactor as the laboratory was not suitably equipped to deal with the latter. An advantage of using several reactors is the simplified sampling technique. Sampling consisted of simply removing one of the reactors from the system at the required time. The reactor's suspension was treated as described in section 4.6.2. After the liquid was separated from the solids, representative samples of each were used for the necessary analyses. A disadvantage with using several reactors is that growth conditions and leaching progress may not be identical in all reactors. However regular bacterial count checks were made on all reactors to ensure identical bacterial growth.

In order to check the effect of chemical leaching on pyrite as well as on gold liberation, sterile control experiments were carried out. These were prepared in exactly the same way as the leach tests except that no inoculum was used and instead, 10 ml of a 5% phenol solution (200 mg phenol) were added to prevent any bacterial growth.

The pH of the leach suspension was measured using a combination electrode connected to a RADIOMETER PHM 82 STANDARD pH-meter and adjusted on a daily basis using either concentrated sulphuric acid or a saturated (40% w/v) sodium hydroxide solution. Compensation for evaporation loss was done daily just before the pH adjustment using distilled water.

4.6 Sampling Procedures

4.6.1 Sampling Procedure for Bacterial Counts

Free bacteria were counted daily for the period of active growth and every 9 days after the bacterial population had stabilized. For each time profile leach test the bacterial count samples were withdrawn from the same reactor, i.e. the reactor which was incubated for the longest time. However, regular checks of the bacterial concentration in the other reactors were also done. The following procedure was adopted for the preparation of samples for bacterial counts:

- after the water loss and pH adjustments the leach suspension was stirred for ten minutes and then the solids were allowed to settle for half an hour.
- three samples of 1 ml each were then withdrawn from the supernatant and diluted with the necessary amount of water to give 5 to 10 cells in each small square of the THOMA counting chamber.
- the average count of the three samples multiplied by the dilution factor and $2x10^7$ gave the free bacterial concentration of that day in cells/ml.

The effect of sampling on the leaching process was negligible as a total of about 50 ml were withdrawn from 2500 ml of supernatant over a period of 46 days.

4.6.2 Sampling Procedure, Sample Preparations and Analyses.

The duration of the time profile leach tests was 51 days for the +25-38 micron size fraction, and 46 days for the other three size fractions. Sampling was done every 2 days during the early stages of leaching, (i.e. for the first 14 days) and every 9 days for the rest of the experiment. Because of the lack of space, two series of experiments were carried out to obtain all the necessary data for the +25-38 and +38-53 micron size fractions: the first series, a short run, lasted 13 and 14 days respectively and sampling was done

every 2 days; and the second series, a long run, lasted 51 and 46 days respectively and sampling was done every 9 days. It was found that the results from the short and the long run overlapped on the 13th and 14th days respectively, for both the above fractions, and it was therefore possible to combine the short and long run results into one set of data. For the +75-106 micron size fraction sampling was done only every 9 days.

A reactor was removed from the water bath on the sampling day only after the evaporation and pH adjustments had been made. The solid residue of the removed reactor's suspension consisted of the unreacted pyrite concentrate and the precipitates formed, basically iron precipitates; and the supernatant contained the unprecipitated leached metals, basically iron and the trace elements arsenic, nickel and copper. The following procedure was adopted for all the necessary analyses: part of the supernatant was filtered to give a filtrate volume of 50 ml. This solution was used for the determination of the concentrations of ferrous and total iron, arsenic, nickel and copper, which represented the soluble metal concentrations in the leach suspension. The residue on the filter paper from the above separation was returned to the reactor from which it had been removed. Although the pH of the leach suspension during leaching was low (<1.8), iron precipitation did occur and a very fine yellowish precipitate was formed. It was found that these precipitates could be redissolved by treating the suspension with hydrochloric acid (Pinches, 1972; Atkins, 1978). Thus the leach suspension was subsequently mixed with concentrated hydrochloric acid to give a final acid concentration of 17% and was left for 6 hours at room temperature while stirred periodically to allow redissolution of the precipitates. The acid-treated leach suspension was then filtered and the solid residue, free of any precipitate, which was considered to be the unreacted pyrite concentrate, was rinsed thoroughly with distilled water, dried and weighed. The filtrate of this separation was considered to contain the total amount of metals leached, i.e., the amount remaining in solution, as

well as the amount precipitated and was assayed for these amounts as described below.

The ferrous iron concentration in the non-acid-treated supernatant was measured using the standard potassium dichromate titration method (Vogel, 1961). Analyses for the iron, arsenic, nickel and copper concentrations in the non-acid-treated supernatant, as well as in the filtrate from the acid-treated suspension, were performed by atomic absorption spectrophotometry. A VARIAN MODEL AA-6 Atomic Absorption Spectrophotometer was used for the iron analysis and a VARIAN MODEL 1275 for the arsenic nickel and copper (MINTEK laboratories). A gold analysis of these solutions was also performed by atomic absorption in a VARIAN MODEL 1275 Atomic Absorption Spectrophotometer (MINTEK laboratories)

The solid residue was subjected to cyanidation under the conditions described in Section 4.2 for 24 hours, so that the gold liberated by bacterial action could be removed. A fire assay method was used to determine the amount of unliberated gold in the unreacted solid residue. A total sulphur and iron analysis of the leached residue was performed, as previously described. The arsenic, copper and nickel concentration of the leached residue was also determined as described previously. The leached solid residue was further subjected to a size analysis (MINTEK laboratories) to determine any changes in particle size: standard laboratory sieves were used for the +75, +53 and +38 micron size fractions and a MALVERN MODEL 3600 Particle Size Analyser for the +25 micron size fraction.

The calculations concerning the bacterial oxidation of the concentrate were based on the sulphur oxidation of the concentrate.

4.7 Miscellaneous Measurements

4.7.1 Surface Area Measurements

The BET adsorption method was used for the specific surface area measurements. The adsorbed gas was Krypton (MINTEK laboratories).

4.7.2 Density Measurements.

The density of the four size fractions was determined in a QUANTACHROME SPY-2 Stereopycnometer (MINTEK laboratories). The apparatus determines the volume of a weighed sample by the displacement of a gas with small atomic dimensions such as helium. The small gas atom size enables it to penetrate particle crevices and pores.

4.7.3 Scanning Electron Micrographs.

Feed samples and leached residues were examined in a Hitachi S450 Scanning Electron Microscope with a 25 kV accelerating voltage and a beam current of approximately $1x10^{-10}$ Amps. The samples were prepared by mounting the particles on a microscope stub using double sided adhesive tape. Before viewing they were gold coated in a POLARON E 5000 Sputter Coater to a thickness of approximately 25 nm (MINTEK laboratories).

CHAPTER 5

RESULTS AND DISCUSSION

5.1 Introduction

This chapter presents and discusses the results of batch bacterial tests performed on four particle size fractions, +75-106, +53-75, +38-53 and +25-38 micron respectively, of a gold-bearing pyrite concentrate. All the experiments were carried out under identical initial conditions, which were chosen from conditions described in the literature as well as from the observations of preliminary investigations. These conditions have been described in Chapter 4.

The objective of the experiments was to obtain kinetic data on the bacterial leaching of a refractory gold- bearing pyrite concentrate, i.e the rate and extent of pyrite oxidation, as well as the relationship between gold liberation and pyrite oxidation for various size fractions. The kinetic data for the pyrite oxidation were tested on two kinetic models, viz.; a shrinking-particle model and a propagating-pore model.

The following measurements were made for each test:

- total-sulphur oxidation of the solid residue as a function of time.
- iron oxidation of the solid residue as a function of time.
- concentration of ferrous and total iron leached in the liquors of the leach suspension prior to acid-treatment as a function of time.
- concentration of total iron leached in the liquors of the acid-treated leach suspension as a function of time.
- gold liberation as a function of time.

- arsenic, nickel and copper oxidation as a function of time.
- bacterial numbers in solution as a function of time.
- pH of the leach suspension as a function of time.

The experiments were generally carried out only once because of time constraints. However, in cases where an experiment was repeated, the fraction of total-sulphur oxidised and the bacterial growth in solution obtained for a particular size fraction showed good reproducibility. Table 5.1 shows the degree of reproducibility obtained for the leaching of the +25-38 micron size fraction in two runs.

Table 5.1: Fraction of total-sulphur oxidised in the +25-38 micron size fraction for runs A and B.

leach time days	fraction of total-sulphur oxidised +25-38 micron	
	run A	run B
3	0,049	0,052
5	0,082	0,085
7	0,138	0,133
9	0,189	0,179
11	0,229	0,235
13	0,260	0,253

The results of the batch leach tests, obtained as described in section 4.6.2, are presented in Tables 5.2 to 5.5 for the four size fractions respectively. The data relating to the oxidation of nickel and copper are given in Appendix A.

Table 5.2: Analysis of unreacted solid residue, calculated fraction oxidised and leached iron concentration. Size fraction: +75-106 micron.

	UNREACTED SOLID RESIDUE					FRACTION OXIDISED			LEACHED IRON CONCENTRATION	
						a	b	c	d	e
leach time days	mass g	sulphur conc. g/100g	iron conc. g/100g	gold conc. g/t	arsenic conc. g/t	sulphur	gold	arsenic	soluble iron conc. g/l	total iron conc. g/l
0	250,00	50,2	44,4	4,65	2100	0,000	0,000	0,000	0,00	0,00
10	226,27	50,4	44,0	1,94	1000	0,104	0,622	0,569	3,62	4,44
17	202,87	50,4	43,5	1,14	840	0,185	0,801	0,675	6,10	9,40
28	177,20	50,9	41,1	0,68	700	0,278	0,896	0,764	6,45	15,09
37	168,53	49,6	41,7	0,59	600	0,332	0,914	0,807	6,42	15,75
42	160,80	50,0	42,2	0,70	640	0,359	0,903	0,804	6,60	17,52
46	158,00	50,4	43,0	0,60	600	0,366	0,918	0,819	6,51	18,11

a: calculated as (mass of total-sulphur in the feed - mass of total-sulphur in the acid-washed solid residue) / mass of total-sulphur in the feed.

b: calculated as (mass of refractory gold in the feed - mass of gold in the acid-washed and cyanided solid residue) / mass of refractory gold in the feed.

c: calculated as (mass of arsenic in the feed - mass of arsenic in the acid-washed solid residue) / mass of arsenic in the feed.

d: calculated by atomic absorption on the leach liquors prior to acid-treatment.

e: calculated by atomic absorption on the liquors of the acid-treated leach suspension.

Table 5.3: Analysis of unreacted solid residue, calculated fraction oxidised and leached iron concentration. Size fraction: +53-75 micron.

	UNREACTED SOLID RESIDUE					FRACTION OXIDISED			LEACHED IRON CONCENTRATION	
						a	b	c	d	e
leach time days	mass g	sulphur conc. g/100g	iron conc. g/100g	gold conc. g/t	arsenic conc. g/t	sulphur	gold	arsenic	soluble iron conc. g/l	total iron conc. g/l
0	250,00	50,55	44,6	2,87	2380	0,000	0,000	0,000	0,00	0,00
4	242,60	50,70	43,5	2,24	1600	0,025	0,243	0,348	1,05	1,93
6	236,89	50,90	43,8	1,85	1300	0,045	0,389	0,482	2,22	2,48
8	227,10	52,00	43,7	1,52	1100	0,066	0,519	0,580	3,90	5,32
10	220,60	50,90	43,3	1,37	1100	0,110	0,579	0,592	5,34	6,23
12	207,00	51,60	43,5	1,00	960	0,155	0,711	0,666	6,30	8,00
14	202,10	51,30	43,3	0,96	730	0,180	0,730	0,752	6,50	9,17
19	187,00	50,70	42,6	0,75	730	0,250	0,805	0,771	6,84	12,70
28	163,50	50,70	41,8	0,38	650	0,342	0,913	0,821	6,96	16,30
42	147,20	50,60	41,5	0,39	610	0,411	0,920	0,849	6,76	20,33
46	144,16	51,00	42,1	0,42	630	0,420	0,916	0,847	6,80	20,55

a, b, c, d and e: as explained in Table 5.2.

Table 5.4: Analysis of unreacted solid residue, calculated fraction oxidised and leached iron concentration. Size fraction: +38-53 micron.

	UNREACTED SOLID RESIDUE					FRACTION OXIDISED			LEACHED IRON CONCENTRATION	
leach time days	mass g	sulphur conc. g/100g	iron conc. g/100g	gold conc. g/t	arsenic conc. g/t	[a] sulphur	[b] gold	[c] arsenic	[d] soluble iron conc. g/l	[e] total iron conc. g/l
	first series of batch experiments									
0	250,00	51,05	44,9	2,51	2810	0,000	0,000	0,000	0,00	0,00
4	240,10	52,00	44,5	1,92	1900	0,022	0,353	0,351	1,11	2,37
6	228,82	52,60	44,5	1,69	1300	0,056	0,468	0,577	3,39	4,80
8	216,02	52,30	43,6	1,46	940	0,115	0,573	0,711	4,70	6,90
10	207,03	52,90	44,1	1,24	1100	0,142	0,613	0,675	5,58	7,80
12	195,14	52,60	44,2	1,17	1000	0,196	0,689	0,722	6,06	10,87
14	186,77	52,40	43,6	0,82	1060	0,232	0,756	0,718	6,88	12,61
	second series of batch experiments									
0	250,00	51,10	45,0	2,36	3700	0,000	0,000	0,000	0,00	0,00
14	185,30	52,30	42,0	0,85	1300	0,243	0,733	0,739	6,70	14,50
19	171,48	52,60	42,1	0,55	890	0,301	0,840	0,835	6,43	15,33
28	151,78	52,20	41,7	0,40	860	0,379	0,897	0,859	6,85	19,44
37	141,64	52,10	42,7	0,37	890	0,426	0,911	0,864	6,80	21,51
46	132,55	52,40	42,7	0,38	900	0,459	0,915	0,871	6,85	23,02

a, b, c, d and e: as explained in Table 5.2.

Table 5.5: Analysis of unreacted solid residue, calculated fraction oxidised and leached iron concentration. Size fraction: +25-38 micron.

	UNREACTED SOLID RESIDUE					FRACTION OXIDISED			LEACHED IRON CONCENTRATION	
						[a]	[b]	[c]	[d]	[e]
leach time days	mass g	sulphur conc. g/100g	iron conc. g/100g	gold conc. g/t	arsenic conc. g/t	sulphur	gold	arsenic	soluble iron conc. g/l	total iron conc. g/l
	first series of batch experiments									
0	250,00	52,0	43,7	1,18	1500	0,000	0,000	0,000	0,00	0,00
1	247,80	52,2	44,6	0,91	1400	0,005	0,236	0,075	0,40	0,48
3	241,20	51,3	44,2	0,80	1200	0,049	0,346	0,228	1,51	1,52
5	230,60	51,9	44,2	0,79	1000	0,082	0,382	0,385	3,14	3,25
7	218,10	51,4	44,0	0,53	1000	0,138	0,608	0,418	4,90	5,44
9	206,00	51,2	44,2	0,48	1000	0,189	0,665	0,450	6,84	7,49
11	195,20	51,4	43,9	0,61	860	0,229	0,596	0,552	6,90	9,80
13	188,20	51,2	44,9	0,48	830	0,260	0,694	0,583	6,76	10,68
	second series of batch experiments									
0	250,00	51,8	44,8	1,44	2110	0,000	0,000	0,000	0,00	0,00
13	189,80	51,3	45,5	0,61	1000	0,248	0,680	0,640	6,75	11,13
17	158,25	51,7	46,5	0,41	810	0,369	0,820	0,757	6,70	16,78
26	145,00	50,7	45,3	0,38	710	0,431	0,847	0,805	6,60	18,88
35	134,80	50,0	45,5	0,32	660	0,479	0,880	0,831	6,90	20,69
43	123,90	50,8	45,5	0,28	610	0,514	0,904	0,857	6,56	22,96
51	121,92	50,5	42,5	0,28	590	0,524	0,905	0,864	6,76	23,32

a, b, c, d and e: as explained in Table 5.2.

The results of the leach tests have been plotted as fraction of element oxidised, F(t), versus time, t. However, since the volumetric oxidation rate can at any time be calculated from $\frac{dF(t)}{dt}$ x (initial element concentration in the leach suspension), the rate is often used in the discussion of the results.

5.2 Total-sulphur oxidation.

The oxidation of the concentrate was expressed in terms of the fraction of total-sulphur oxidised and was calculated as:
(mass of total-sulphur in the feed - mass of total-sulphur in the unreacted residue) / (mass of total-sulphur in the feed), i.e.
(250 g x concentration of total-sulphur in the feed - mass of unreacted solid residue after acid-wash x concentration of total-sulphur in the residue) / (250 g x concentration of total-sulphur in the feed).

The total-sulphur oxidation data given in Tables 5.2 to 5.5, is plotted versus time and is shown in Figure 5.1. From this figure it can be seen that there is an initial lag time of 1 to 2 days during which no significant oxidation takes place. This lag time is also depicted in Figure 5.32, a plot of the log of the free bacteria numbers versus time. Once oxidation starts it proceeds at an almost constant rate for about 10 to 15 days. After this period the rate drops off slowly, so that after about 45 days 35% to 50% of the total-sulphur has been oxidised, depending on the particle size.

The initial total-sulphur oxidation rate increases with decreasing particle size. This is in agreement with observations in a number of studies, where various size fractions of several sulphide minerals were subjected to bacterial leaching *viz.* molybdenite (Bryner and Anderson,

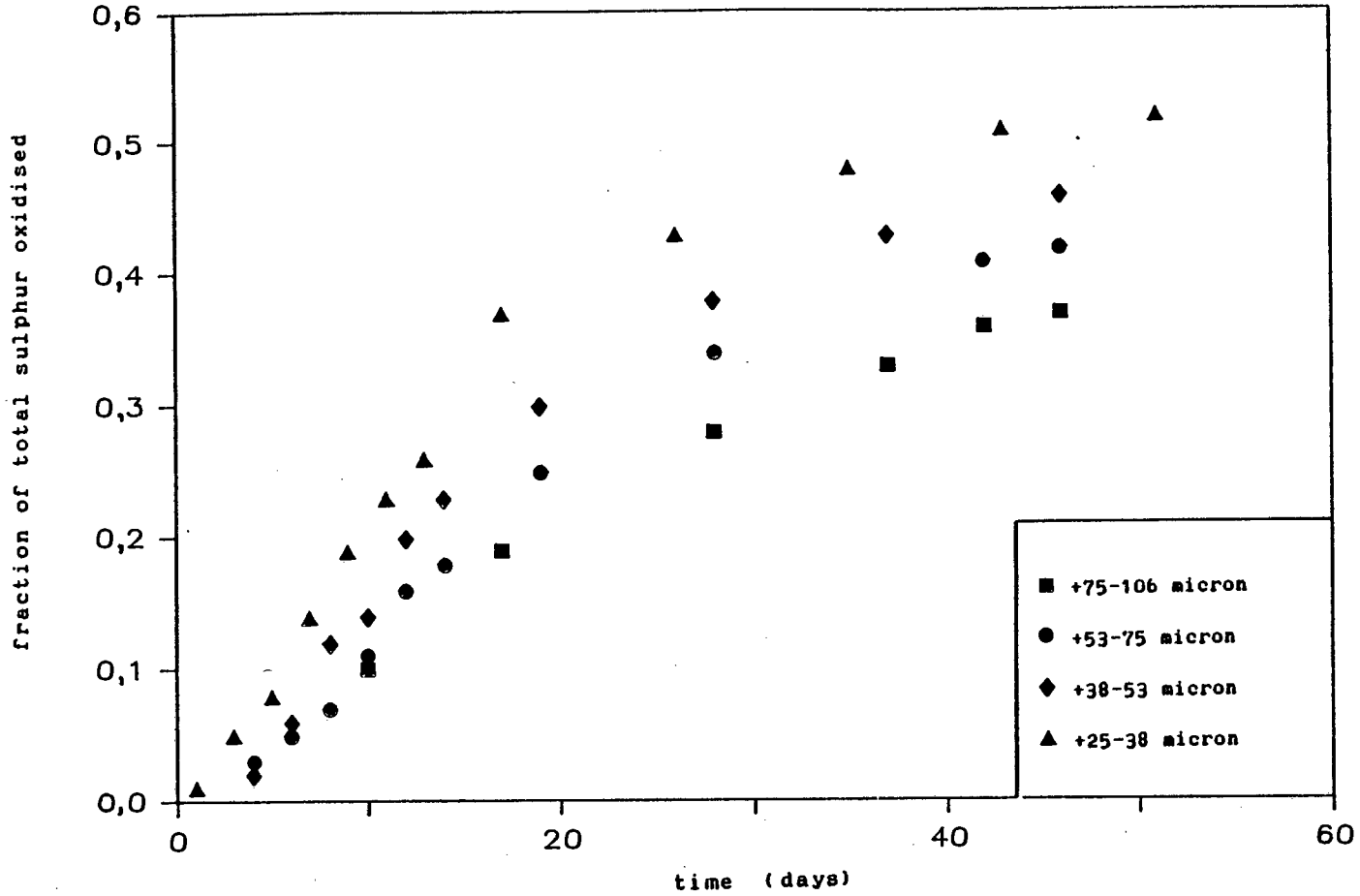

Figure 5.1: Total-sulphur oxidation versus time

1957), pyrite (Malouf and Prater, 1961), various sulphuritic materials (Silverman et al., 1961), chalcopyrite (Duncan et al., 1966; Bruynesteyn and Duncan, 1974) and synthetic copper sulphide (Ehrlich and Fox, 1967). Figure 5.1 also shows that the smaller particle size fractions are leached to a greater extent than the larger ones. This too is in agreement with the data presented by the above authors.

The fraction of total-sulphur leached chemically during the sterile tests was found to be less than 0.01 for all size fractions over a period of 30 days, and was thus considered negligible in the evaluation of the results.

5.2.1 Fitting of the Models to the Experimental Data. - Comparison of the two Models with regard to Goodness of Fit.

The applicability of the two models described in Chapter 3 was tested by fitting them to the experimental data as follows: a Nelder-Mead optimisation routine (Nelder and Mead, 1965) was used to obtain the parameter values that gave the best fit of the total-sulphur time profile data to the two kinetic models. The variable parameters in each model were:
- surface oxidation rate, r_s and lag time, T_L, in the shrinking-particle model and,
- surface oxidation rate, r_{s0}, lag time, T_L, time at which pore deactivation starts, T_i, and time at which all pores have become inactive, T_e, in the propagating-pore model.
The program listing of the Nelder-Mead routines as well as a brief accompanying explanation are given in Appendix B.

The estimated Nelder-Mead model parameters are given in Table 5.6. The fitted model curves for each size fraction are shown in Figures 5.2 to 5.5 respectively. The sum of errors squared are given in Table 5.6.

Table 5.6: Model parameters estimated by the Nelder -Mead optimisation routine for the propagating -pore and the shrinking-particle models.

	PROPAGATING-PORE MODEL					SHRINKING-PARTICLE MODEL		
size fraction micron	surface oxidation rate r_{so} kg m^{-2} day^{-1} x 10^4	T_L days	T_i days	T_o days	sum of errors squared	surface oxidation rate r_s kg m^{-2} day^{-1} x 10^4	T_L days	sum of errors squared x 10^4
+75-106	4,52	2,45	16,33	47,51	3,46	3,88	1,9400	34
+53-75	4,00	2,37	15,51	45,17	6,40	3,46	1,9800	89
+38-53	3,54	2,13	13,25	38,59	17,30	2,73	0,0005	133
+25-38	3,36	1,91	11,19	32,66	49,40	2,25	0,0020	389

From Figures 5.2 to 5.5 it can be seen that the propagating-pore model gives a good fit to the experimental data. The linear phase predicted by the model, during which all pores are active, generally fits the experimental data well. During this phase the constant volumetric oxidation rate, r_{vo}, can be calculated from the slope of the F(t) versus t curve. The second order phase predicted by the model, during which pore deactivation takes place, also gives a good fit to the experimental data. For the zero order phase predicted by the model, after total pore deactivation has occurred, there is not sufficient experimental data to test the goodness of fit of the model. However the last leach data point from each leach test suggests that leaching does not cease entirely but continues at a much lower rate. This may suggest, as noted in section 3.4, that both mechanisms of leaching occur simultaneously: at the beginning of the leaching process the propagating-pore mechanism predominates, since there is an abundance of active sites where the bacteria will preferentially attack and oxidise the mineral; as leaching progresses and the more resistant compact pyrite has been left unoxidised, the leaching may continue via the shrinking-particle mechanism.

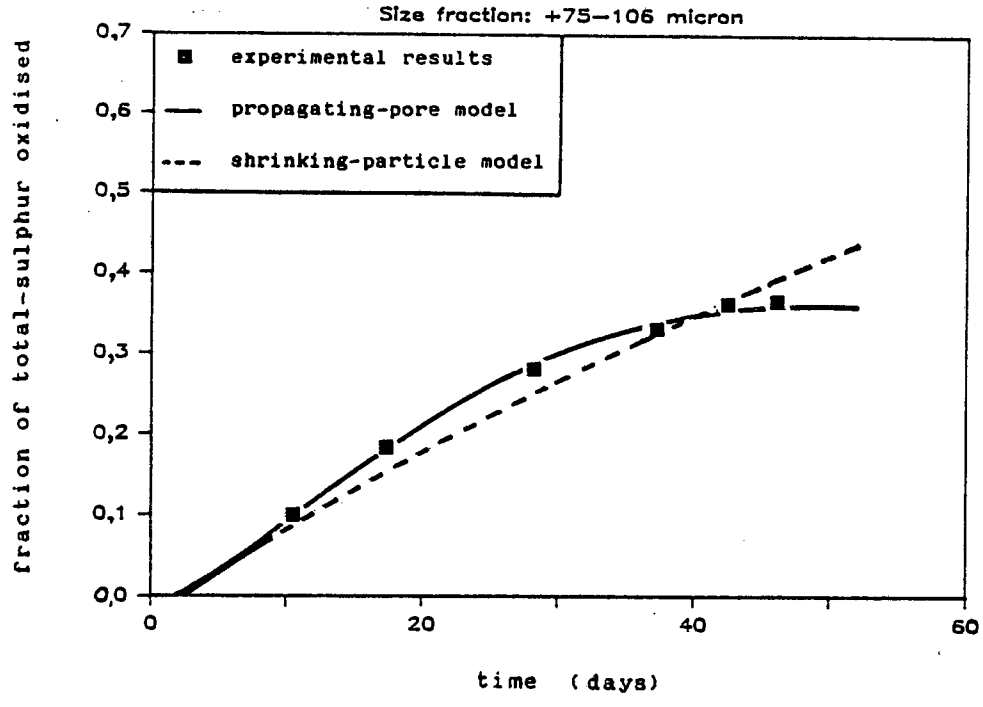

Figure 5.2: Total-sulphur oxidation versus time: experimental data and predicted curves by the propagating-pore and the shrinking-particle models.

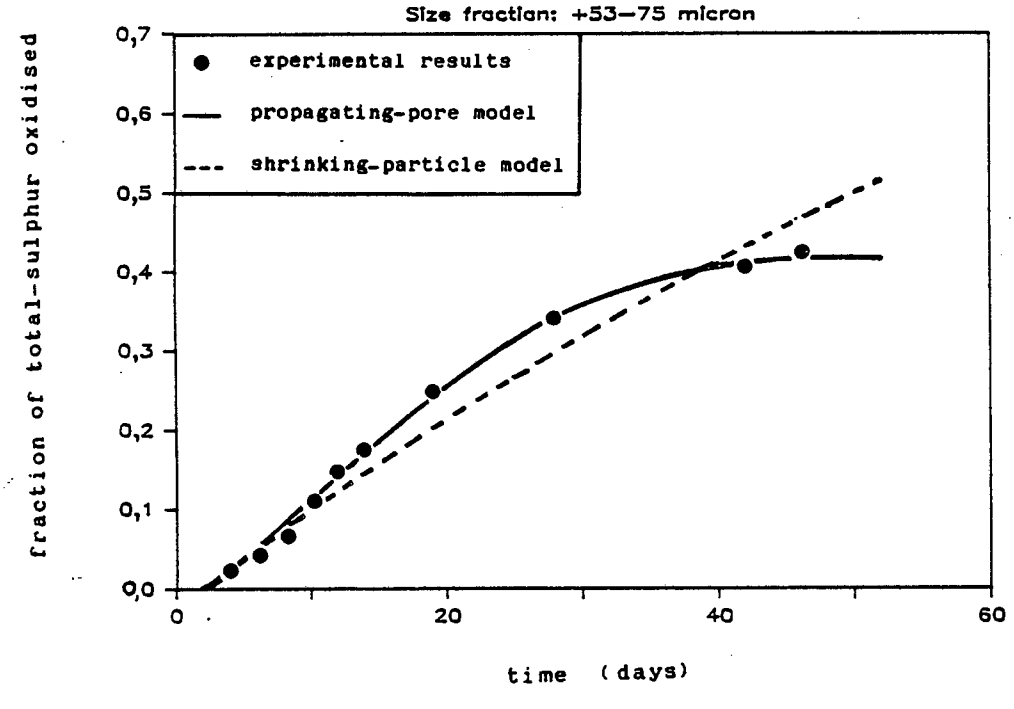

Figure 5.3: Total-sulphur oxidation versus time: experimental data and predicted curves by the propagating-pore and the shrinking-particle models.

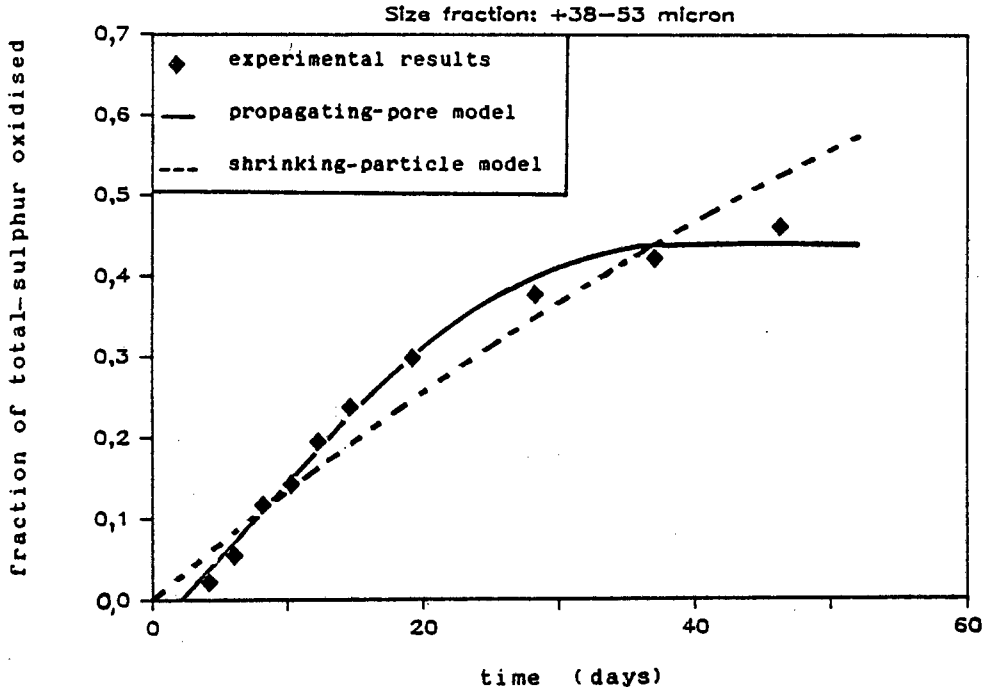

Figure 5.4: Total-sulphur oxidation versus time: experimental data and predicted curves by the propagating-pore and the shrinking-particle models.

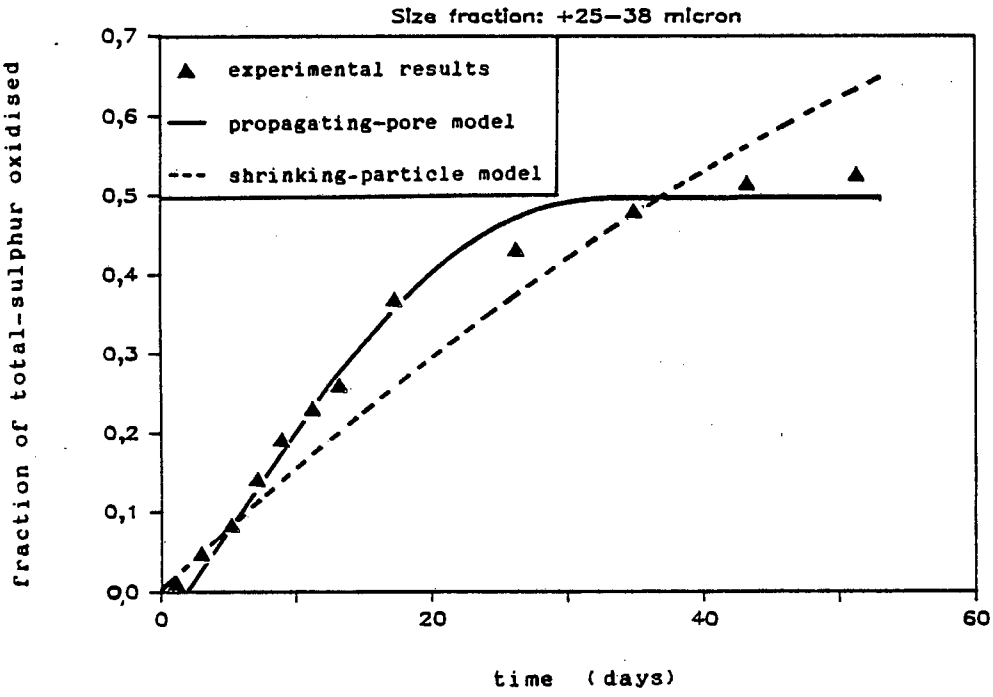

Figure 5.5: Total-sulphur oxidation versus time: experimental data and predicted curves by the propagating-pore and the shrinking-particle models.

On the other hand the shrinking-particle model does not give a good fit to the experimental data in any region of the leach curve. Table 5.6 shows that for all size fractions the sum of errors squared is approximately ten times larger for the shrinking-particle model than for the propagating-pore model.

It must be noted that the shrinking-particle model is a two parameter model, (r_a and T_L) and therefore not as flexible as the propagating-pore model. The lag time parameter, T_L, can be used to shift the curve along the horizontal axis, while the surface oxidation rate parameter, r_a, can be used to change the shape of the curve. The experimental data require a levelling off of the curve F(t) versus t between the 35th and 50th day, at which time the experimental F(t) values lie approximately between 0,50 and 0,35 depending on the particle size. In the Theory section 3.2.3, it was shown that the shrinking-particle model predicts a levelling off of the F(t) versus t curve at F(t) = 1,00. For a particle diameter d_0 = 64 micron and surface oxidation rate $r_a = 7 \times 10^{-4}$ kg m^{-2} day^{-1} the F(t) = 1,00 point is predicted to occur at about t = 228 days. In order for this model to predict a levelling off on the 50th day, the r_a would have to be equal to 32×10^{-4} kg m^{-2} day^{-1} (see Figure 3.3), which is in general higher than the values for mineral surface oxidation rate calculated from data in the literature. In this case the predicted F(t) will be equal to 1,00 on the 50th day as opposed to the experimental 0,35 to 0,50. Therefore the shrinking-particle model cannot satisfactorily explain the leaching behaviour of this particular ore under the leaching conditions employed.

On the other hand examination of the leach residues in the scanning electron microscope shows pore development, as will be described in section 5.4, and the curve fit of this model was found to give a reasonably good fit. Therefore, the propagating-pore model both on a curve-fitting basis and from evidence from the scanning electron micrographs appears to satisfactorily describe the leaching process, i.e. the

propagating-pore mechanism seems to be the predominant mechanism over the time period tested.

The calculated best fit values for the parameter r_s and r_{s0}, which are given in Table 5.6 are estimates of the surface oxidation rate. This is discussed in detail in section 5.2.2.

The calculated best fit values for the parameters T_i and T_e predicted by the propagating-pore model are consistent with the theory on this model (see section 3.3.3), i.e T_i and T_e decrease with decreasing particle size.

The lag time parameter, T_L, which was used as a variable in both models, has to be taken into account since a lag phase is almost always observed in batch biological processes. An estimate of the lag time can be calculated in various ways depending on how the lag time is defined. In this study an estimate of the lag time could be obtained in one of the following ways:

1. from the free bacteria growth curve.
2. from a linear regression through the early leach data.
3. directly from the Nelder-Mead minimisation routine where T_L is estimated as a model parameter.

The free bacteria counts were done only on a 24-hour basis and therefore the first method was discarded as inaccurate, (see Figure 5.32). The second method was also discarded as little data was available at the early stages of the +75-106 micron size fraction leach test. Therefore the third method was used for the estimation of the lag time parameter and the estimated T_L values are given in Table 5.6.

5.2.2 Surface Oxidation Rate

The volumetric oxidation rate of the metal leached from an ore or concentrate, r_v, has traditionally been used to characterise a leaching system. However this parameter is often unsuitable for characterising the leaching behaviour of

a concentrate or for comparing different leach systems, as it is dependent on both solids concentration and particle size. On the other hand the surface oxidation rate, r_a, as described in Chapter 3, is a fundamental parameter and it is therefore reasonable to assume that it is independent of solids concentration and particle size. Thus it can probably be used to characterise the leaching behaviour of certain ores and concentrates.

The surface oxidation rate ($kg\ m^{-2}\ day^{-1}$), can be estimated from the volumetric oxidation rate ($kg\ m^{-3}\ day^{-1}$) and the surface area concentration ($m^2\ m^{-3}$). Therefore the value of r_a depends on the way the surface area is measured, since different surface area determination methods give different measurements. There are various ways of determining surface area:

1. Methods based on the geometrical characteristics of the particles and the density of the mineral. The simplest measure of surface area is the surface area based on a mean particle diameter and the assumption that the particles are uniform spheres. This method is used later and is referred to as the geometrical surface area.

2. Methods that are based on gas adsorption onto the particle surface, such as the BET method. This method gives a measure of the external as well as the additional (internal) surface area due to pores, cracks and fissures. This method is also used in this work and is referred to as the BET surface area.

3. Methods that measure only the external surface area and are based on a permeability cell (Lawrence, 1974; Pinches et al., 1976; Sanmugasunderam, 1981).
The advantages and disadvantages of each method are a consequence of what each method is actually measuring.

The appropriate surface area on which the surface oxidation rate is to be based must be chosen carefully since it is linked to the leaching mechanism taking place, i.e.:

- If the classical shrinking-particle mechanism applies, it seems reasonable that leaching would take place over the external surface area exposed to the leach liquor. Therefore the external surface area would be an appropriate surface area measurement on which to base the surface oxidation rate.
- If the propagating-pore mechanism applies, the leaching will take place mostly over the surface of the pore base. The surface area of existing cracks, pores or fissures in the feed material particles will not affect the number of axes along which leaching takes place but will contribute significantly to a BET surface area measurement. Therefore the external surface area or even the geometrical surface area would be an appropriate surface area measurement on which to base the surface oxidation rate.

The question of the dependence of the surface oxidation rate on particle size or surface area concentration is of great importance in the bacterial leaching of concentrates. The $r_{s,o}$ values estimated by the Nelder-Mead optimisation routine for the propagating-pore model are given in Table 5.6. These values decrease with decreasing particle size. It is not possible to determine from the data available whether this trend represents an inherent dependence of the surface oxidation rate on particle size. The observed trend may be due to slight changes in the surface nature of the size fraction or be an artifact of the curve-fitting procedure.

The constant volumetric sulphur oxidation rate, $r_{v,o}$, during the linear phase of the propagating-pore model, was calculated for each size fraction from the slope of the predicted F(t) versus t curve multiplied by the initial total-sulphur concentration in the leach suspension. These values are given in Table 5.7 together with the geometrical and BET surface area concentration of each size fraction, (Appendix C). The $r_{v,o}$ values were plotted against geometrical surface area concentration and BET surface area concentration, as shown in Figure 5.6.

Table 5.7: Initial volumetric oxidation rate; - geometrical and BET surface area concentration.

size fraction micron	initial volumetric oxidation rate kg m^{-3} day^{-1}	geometrical surface area concentration m^2 m^{-3}	BET surface area concentration m^2 m^{-3}
+75-106	0,615	1364	8500
+53-75	0,753	1888	15000
+38-53	0,941	2669	25000
+25-38	1,290	3832	10000

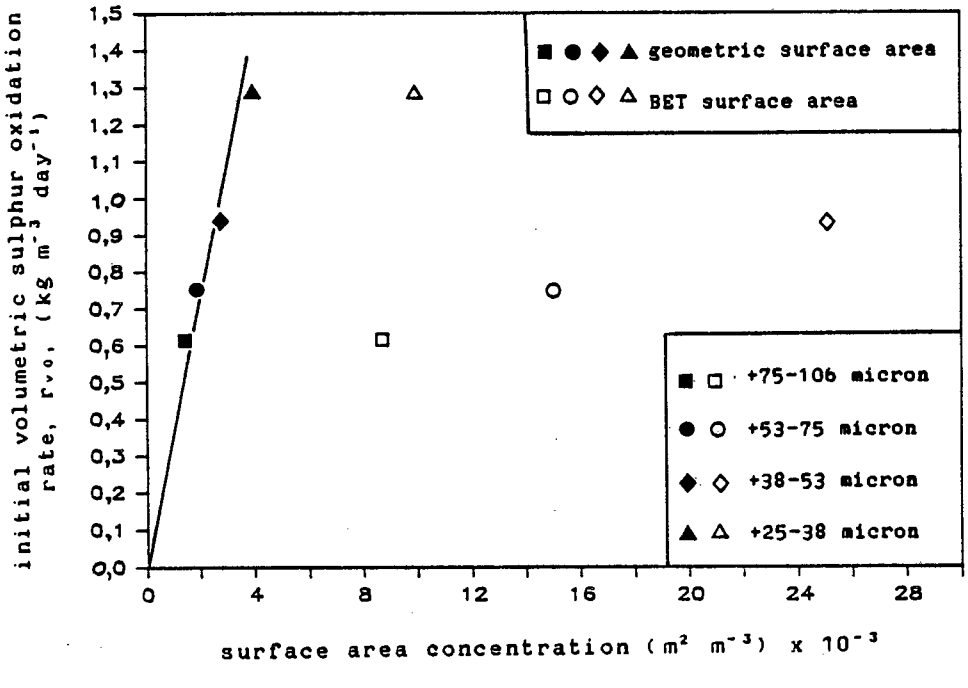

Figure 5.6: Initial volumetric sulphur oxidation rate versus geometrical and BET surface area concentration.

In this figure the plot of the volumetric oxidation rate versus geometrical surface area concentration gives a straight line with a non-zero intercept. Forcing the line to give a zero intercept the data still give a reasonable straight line. This suggests that the initial volumetric oxidation rate is linear with surface area concentration and that the surface oxidation rate, which is represented by the slope of the straight line, is virtually independent of surface area concentration (or particle size). On the other hand the plot of r_{v0} versus BET surface area concentration in the same figure presents anomalous behaviour in the +25-38 micron size range: the BET surface area of this fraction is smaller than the value suggested by the trend of the three larger size fractions. This inconsistency is shown more clearly in Figure 5.7, a plot of the BET and the geometrical surface area concentration versus the inverse of mean particle diameter, $1/d_0$.

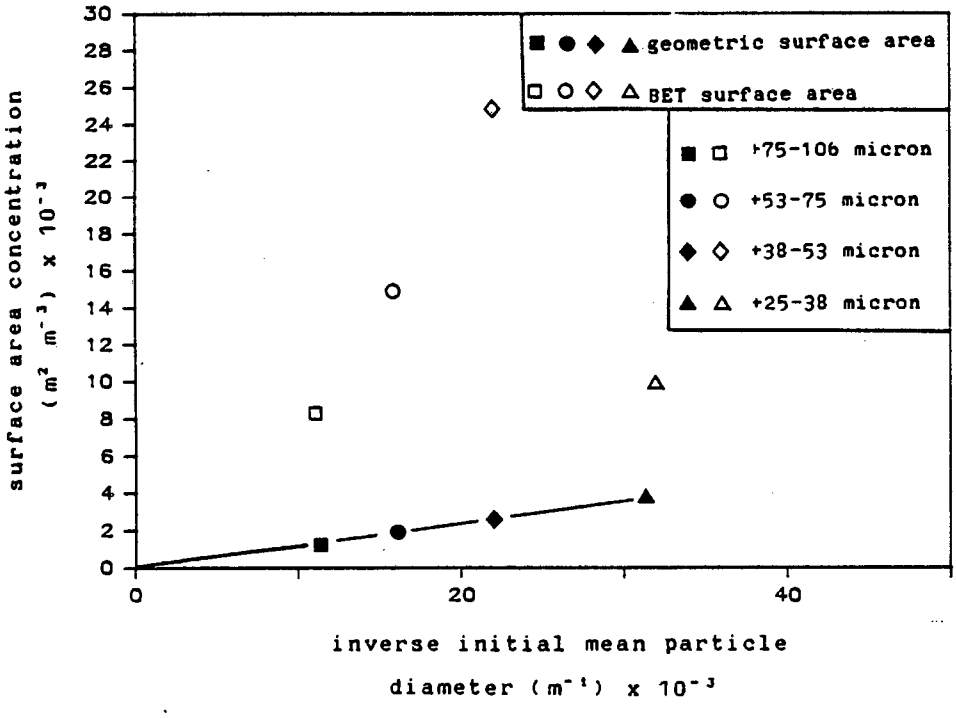

Figure 5.7: Geometrical and BET surface area concentration versus inverse initial mean particle diameter.

This anomaly could be due to the presence of fine particles or particles with very irregular surface in the three larger size fractions, which would then result in a larger measured BET surface area.

In order to investigate this anomaly, samples of the four feed fractions were examined in the scanning electron microscope and the micrographs taken are presented and discussed here. In Figure 5.8. micrographs of random fields of the feed material for each of the four size fractions are shown. From these micrographs it can be seen that most of the particles in all the samples present a fresh surface with no significant irregularities in surface texture. However a portion of particles, which will be referred to as etched particles, with very irregular surface texture can also be observed. A probe analysis of these particles showed that they consist of Fe and S. This etching appears to be of different types, examples of which are shown in Figure 5.9 a, b and c. An example of an unetched particle is shown in Figure 5.9 d. From these photographs it is not easy to conclude whether this is a primary or a secondary surface texture. It seems more likely that it is a secondary texture resulting from varying degrees of corrosion. Given that the feed material comes from an old dump it is reasonable to assume that various types of leaching might have taken place. Some of these particles for example present only a surface etching, Figure 5.9 c, while others show a high degree of corrosion, Figure 5.9 a.

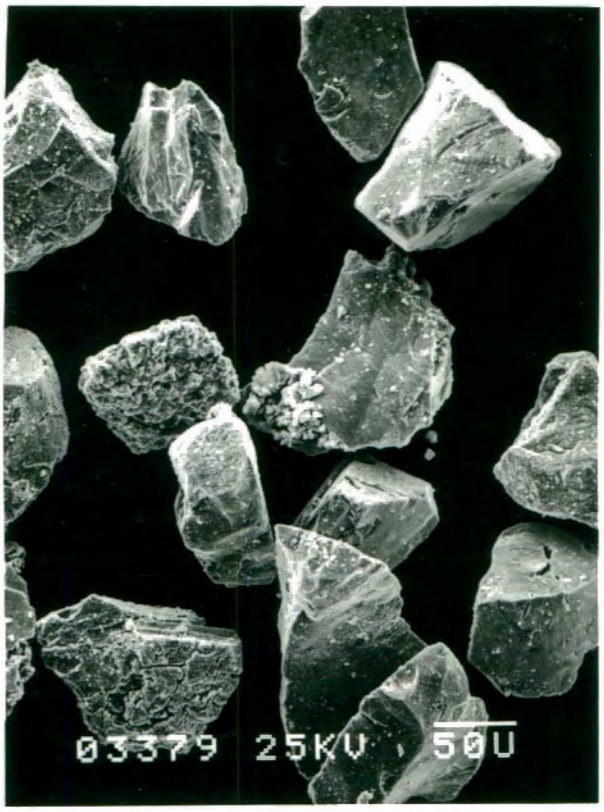

a. +75-106 micron

b. +53-75 micron

c. +38-53 micron

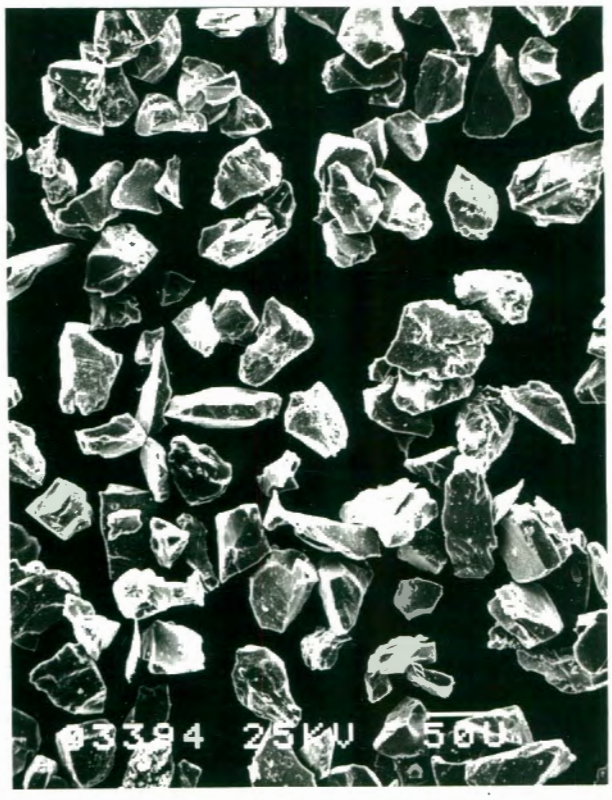

d. +25-38 micron

Figure 5.8: Micrographs of samples from the feed material.

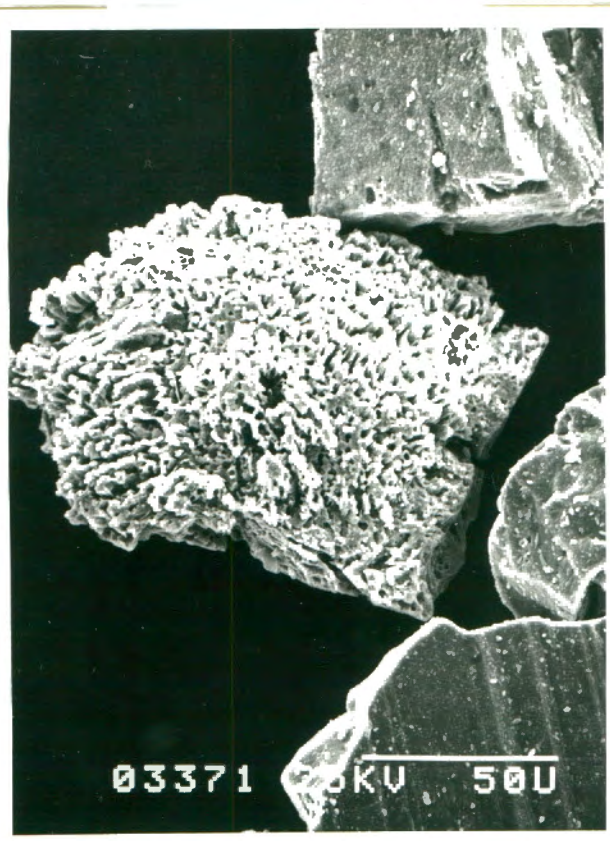

a. highly etched particle

b. highly etched particle

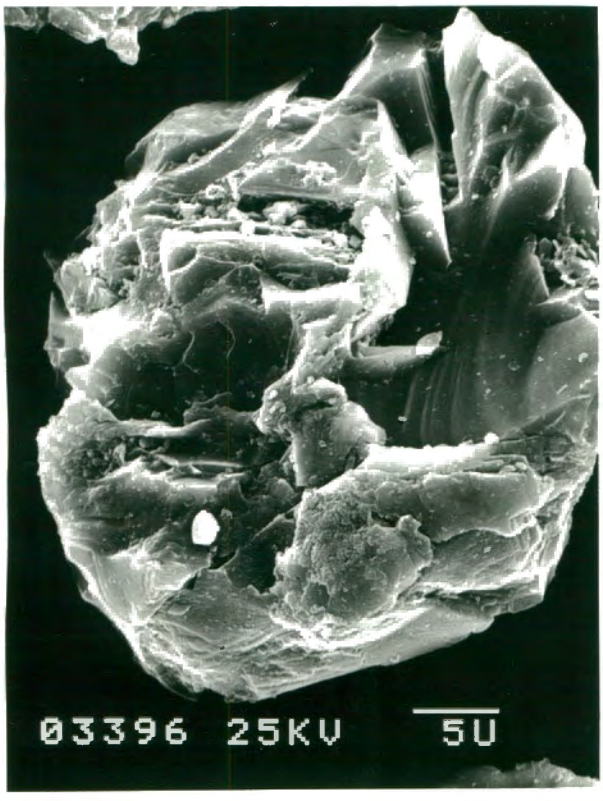

c. particle with only surface etching

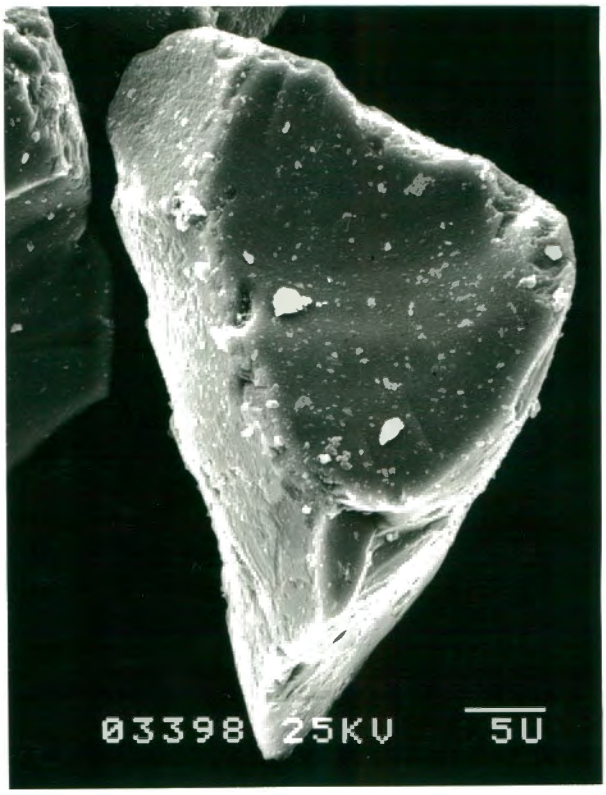

d. particle with unetched surface

Figure 5.9: Types of particles in the feed material.

The proportion of the etched particles appears to be significantly lower in the smaller size range than in the other three size ranges. In an attempt to quantify the proportion of the etched particles, the total number of particles and the number of etched particles were counted in four micrographs for each size range. The results are given in Table 5.8, where it can be seen that the proportion of etched particles in the small fraction is about 5%, while in the other fractions is about 15%, 20% and 25% respectively.

Table 5.8: Proportion of etched particles in each size fraction

size fraction micron	total number of particles	number of etched particles	proportion of etched particles %
+75-106	53	14	26,4
+53-75	92	19	20.6
+38-53	146	23	15,7
+25-38	480	26	5,4

The reason for the etched particles appearing in larger proportions in the three larger size fractions is in all likelihood the different separation technique used to obtain these fractions: the +75-106, +53-75, +38-25 micron fractions were obtained from a bulk concentrate by sieving (size separation), while the +25 micron fraction was obtained by cyclosizing the -38 micron size fraction (size and density separation). In sieving the only parameter that determines the separation is the particle size. On the other hand, in the cyclosizing tecnique both the particle's size and density determine the separation. In the cyclosizer the specific gravity of the etched and compact particles would differ

hence explaining the small proportion of etched particles in the separated size fraction.

The abovementioned observations seem to explain the inconsistency presented in Figures 5.6 and 5.7. These observations also suggest that the BET surface area is not an appropriate measurement on which to base the estimation of the surface oxidation rate. The geometrical surface area was therefore considered a better basis for this estimation. From the slope of the straight line in Figure 5.6 one obtains:
$r_{s,o} = 3,5 \times 10^{-4}$ kg S m^{-2} day^{-1}.

In conclusion, Figure 5.6 suggests that the volumetric leach rate $r_{v,o}$ is linear with surface area concentration. Thus the surface oxidation rate is independent of surface area concentration (or particle size) at least for the range of surface area concentrations plotted. However more research is needed to prove this over a wider range of surface area concentrations.

The abovementioned results are in agreement with data in the literature, where it has been shown that the volumetric leach rate is linearly dependent on surface area concentration. However the concept of a surface oxidation rate has not been previously considered. A comparison of the surface oxidation rate calculated in the present study and the corresponding values as calculated by data available in the literature was attempted. It must be noted however that different methods of calculating surface area have been used in the literature and therefore a direct comparison was not always possible. Where the data was available in the literature the surface oxidation rate calculation was based on the geometrical surface area.

Pinches (1972) in studying the bacterial leaching of a pyrite-arsenopyrite concentrate, plotted the volumetric iron leach rate versus surface area concentration of the pyrite in the concentrate. The plot showed a linear relationship over

the whole range of surface area concentrations plotted (0 - 10000 $m^2\ m^{-3}$). This fact indicates that the surface oxidation rate calculated from the slope of the straight line is constant. This value is $0,9x10^{-4}$ kg Fe $m^{-2}\ day^{-1}$ or expressed in terms of the corresponding pyrite-sulphur, $1,0x10^{-4}$ kg S $m^{-2}\ day^{-1}$. This value is lower than the value $3,5x10^{-4}$ kg S $m^{-2}\ day^{-1}$ found in this study, but of the same order of magnitude. This could be due to: a) the preferential oxidation of arsenopyrite at the cost of the oxidation of pyrite in Pinches' study. This would result in a lower r_v value for pyrite-iron than in the case of a pure pyrite ore; b) the existence of the highly etched particles in the feed material of this study. In the case where this material is leached faster than the compact particles one would expect higher r_{v0} values and therefore higher r_a value than in the case of a homogenous feed material with only compact particles; and c) the different mineralogical characteristics of the pyrite-arsenopyrite concentrate and the pyrite used in the present study. In the same study (Pinches, 1972) the arsenic leach rate was plotted versus surface area concentration of the arsenopyrite in the concentrate (0 - 10000 $m^2\ m^{-3}$). The relationship was linear for a short range of surface area concentrations after which it started levelling off to a constant r_v value. The surface arsenic oxidation rate calculated from the linear section of the curve is $11,5x10^{-4}$ kg As $m^{-2}\ day^{-1}$ (corresponding sulphur oxidation rate: $4,9x10^{-4}$ kg S $m^{-2}\ day^{-1}$)

A linear relationship between the volumetric leach rate of zinc and the surface area concentration of a zinc sulphide concentrate was also observed by Gormely (1973) in a continuous bacterial leaching study of a zinc sulphide concentrate. A straight line was obtained for the whole range of surface area concentrations (0 - 100000 $m^2\ m^{-3}$) with an intercept close to zero. If this non-zero intercept is ignored the surface oxidation rate calculated from the slope of the line is 2,7 kg Zn $m^{-2}\ day^{-1}$ (corresponding sulphur rate, $1,3x10^{-4}$ kg S $m^{-2}\ day^{-1}$). The BET method was used for the surface area determination in the above study, and since

no data is available to calculate the surface oxidation rate on the basis of a geometrical surface area, it is impossible to compare the above value with the $r_{a,o}$ value calculated in the present study.

Torma et al. (1970) also studied the relationship between the volumetric leach rate of zinc and the surface area concentration of a zinc sulphide concentrate in batch tests for a wide range of surface area concentrations (0 - 1200000 $m^2\ m^{-3}$). He found a linear relationship up to a certain surface area concentration after which the straight line started levelling off. The surface oxidation rate calculated from the linear part of the curve is $0,6x10^{-4}$ kg Zn m^{-2} day^{-1}, (corresponding sulphur rate, $0,3x10^{-4}$ kg S m^{-2} day^{-1}). The surface area determination was also done by the BET method and once again it is impossible to compare the above value to the $r_{a,o}$ value calculated in this study. The surface sulphur oxidation rate calculated from Torma's data is lower than the one obtained from Gormely's data. This can be either due to the different reactor systems employed, batch versus continuous, or due to mineralogical differences in the two zinc sulphides employed.

A similar relationship was observed when two chalcopyrite ores with different origins and different leach characteristics were subjected to bacterial leaching in batch tests (Pinches et al., 1976). When the volumetric leach rates were plotted versus surface area concentration (0 - 50000, 0 - 100000 $m^2\ m^{-3}$ respectively), a linear relationship was obtained up to a certain surface area concentration for both chalcopyrite ores, after which the line started levelling off. The surface area determination was done by the cell permeability method. Data for the calculation of the geometrical surface area were available in the above study and therefore the r_a values calculated on the basis of the geometrical surface area were found to be: $1,0x10^{-4}$ kg Cu m^{-2} day^{-1}, (corresponding sulphur rate, $1,0x10^{-4}$ kg S m^{-2} day^{-1}) and, $4,5x10^{-4}$ kg Cu m^{-2} day^{-1}, (corresponding sulphur rate, 4,5 kg S m^{-2} day^{-1}), for the less and more amenable to

bacterial leaching chalcopyrite ores respectively. Both of the above values are of the the same order of magnitude as the value calculated in our study, $3,5x10^{-4}$ kg m^{-2} day^{-1} with $4,5x10^{-4}$ kg m^{-2} day^{-1} lying relatively close to this value.

All the above data suggest that there is a linear relationship between volumetric oxidation rate and surface area concentration and therefore a constant surface oxidation rate, at least for a range of surface area concentrations, irrespective of the way the surface area is determined. However it is difficult to compare the reported surface area concentration ranges for which this occurs, since they have been determined differently by each researcher. These data also suggest that the surface oxidation rate does not only vary with different concentrates but with the mineralogical characteristics of each concentrate as well.

5.3 Gold Liberation

The results of gold liberation from the batch leach tests are given in Tables 5.2 to 5.5 for each size fraction respectively.

The gold liberation is expressed as fraction of gold liberated versus time and is determined as:

(mass of refractory gold in the feed - mass of gold in the unreacted and cyanided residue) / (mass of refractory gold in the feed), i.e.
(250 g x refractory gold concentration in the feed - mass of unreacted leach residue after acid-wash x gold concentration in the unreacted acid-washed and cyanided leach residue) / (250 g x refractory gold concentration in the feed)

The gold in solution was found less than 0,002 g m^{-3} over the entire leach period for all size fractions.

The gold liberation versus time plot is shown in Figure 5.10. From this figure it can be seen that gold liberation increases rapidly with time and levels off after about the 30th day. This behaviour appears to be similar for each size fraction. The final extent of gold liberation seems to be independent of particle size and lies between 90% and 92%.

The gold liberation and total-sulphur oxidation versus time are presented in Figures 5.11 to 5.14. It can be seen that gold liberation increases with time much more rapidly than the total-sulphur oxidation in all four plots and therefore, the extent of gold liberation is much higher than the extent of total-sulphur oxidation.

The relationship between gold liberation and total-sulphur oxidation is more clearly shown in Figure 5.15, where the fraction of gold liberated is plotted against the corresponding fraction of total-sulphur oxidised.

The data in Figure 5.15 suggest that the relationship between total-sulphur oxidation and gold liberation is non-linear for all size fractions. All four curves level off at about the 0,3 fraction of total-sulphur oxidation, for which the corresponding gold liberation is about 0,9, i.e. no more gold is liberated after 30% of the total-sulphur has been oxidised. The gold liberation-sulphur oxidation relationship seems to be independent of particle size over the size range examined.

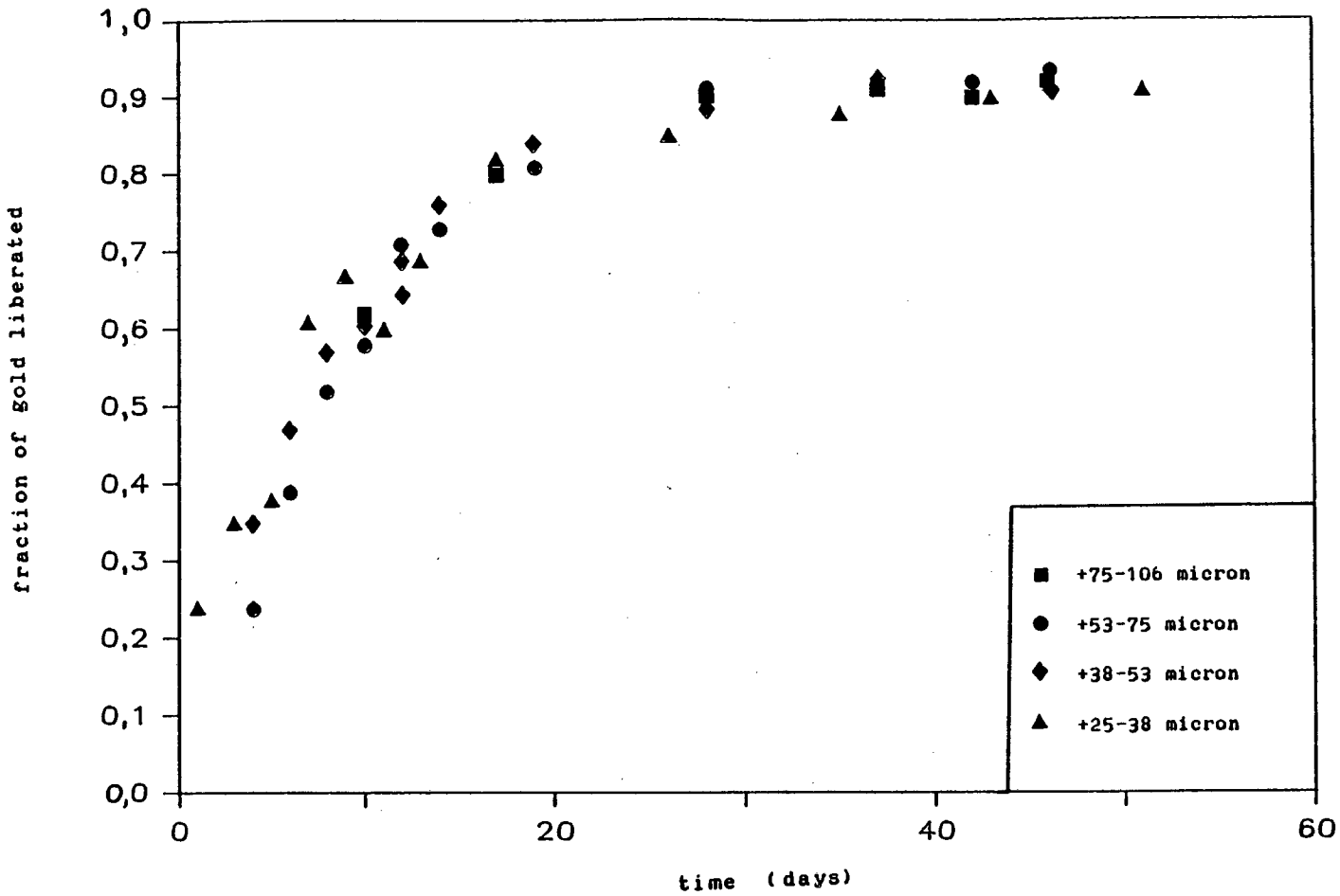

Figure 5.10: Gold liberation versus time

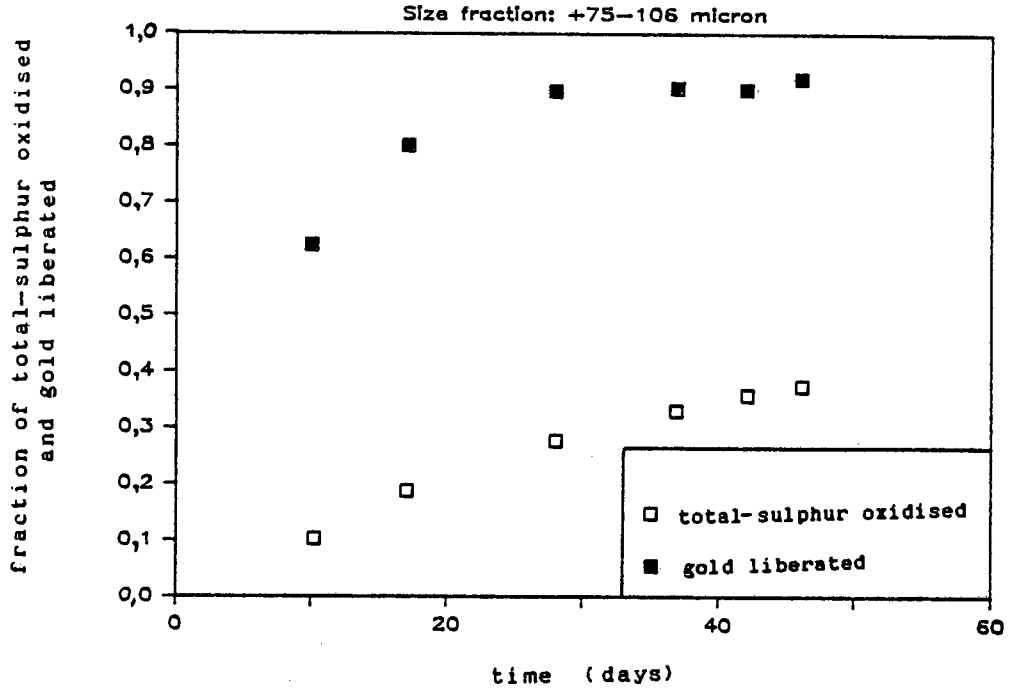

Figure 5.11: Total-sulphur oxidation and corresponding gold liberation versus time.

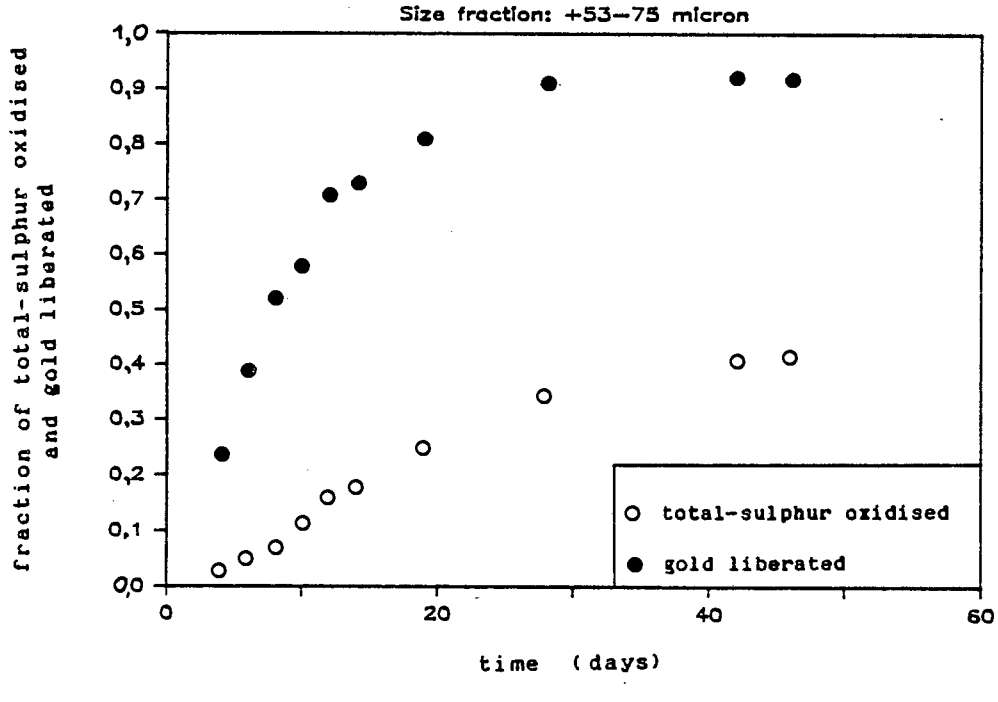

Figure 5.12: Total-sulphur oxidation and corresponding gold liberation versus time.

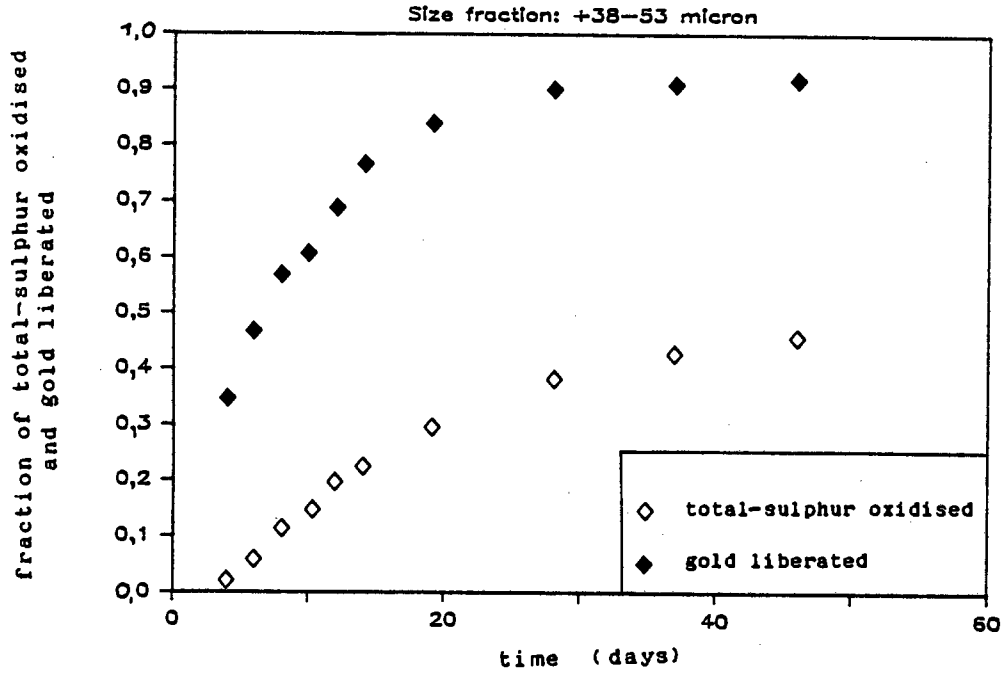

Figure 5.13: Total-sulphur oxidation and corresponding gold liberation versus time.

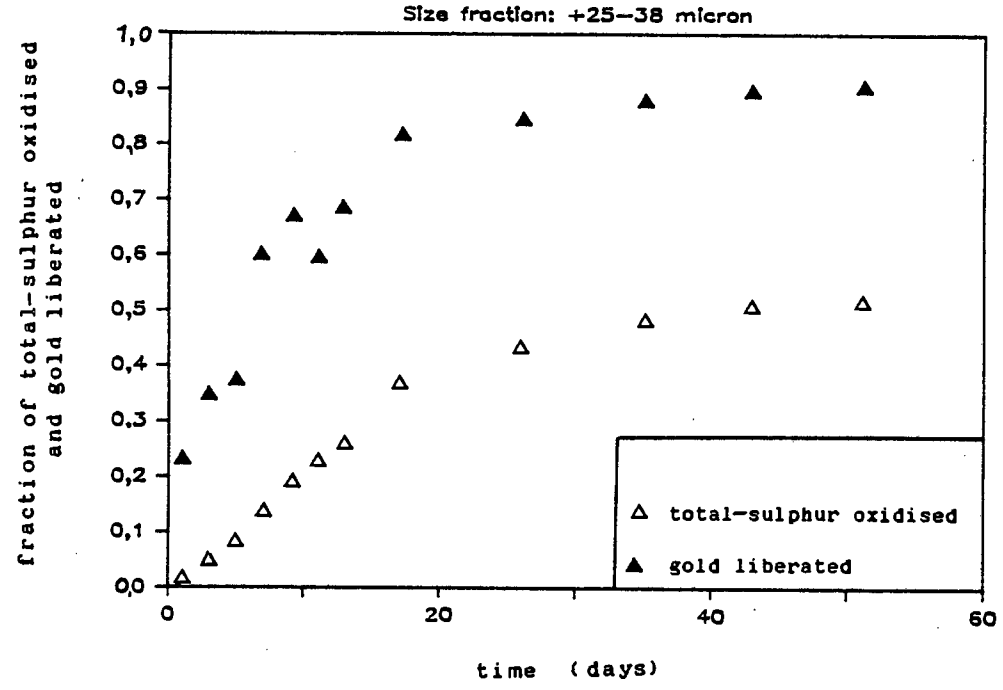

Figure 5.14: Total-sulphur oxidation and corresponding gold liberation versus time.

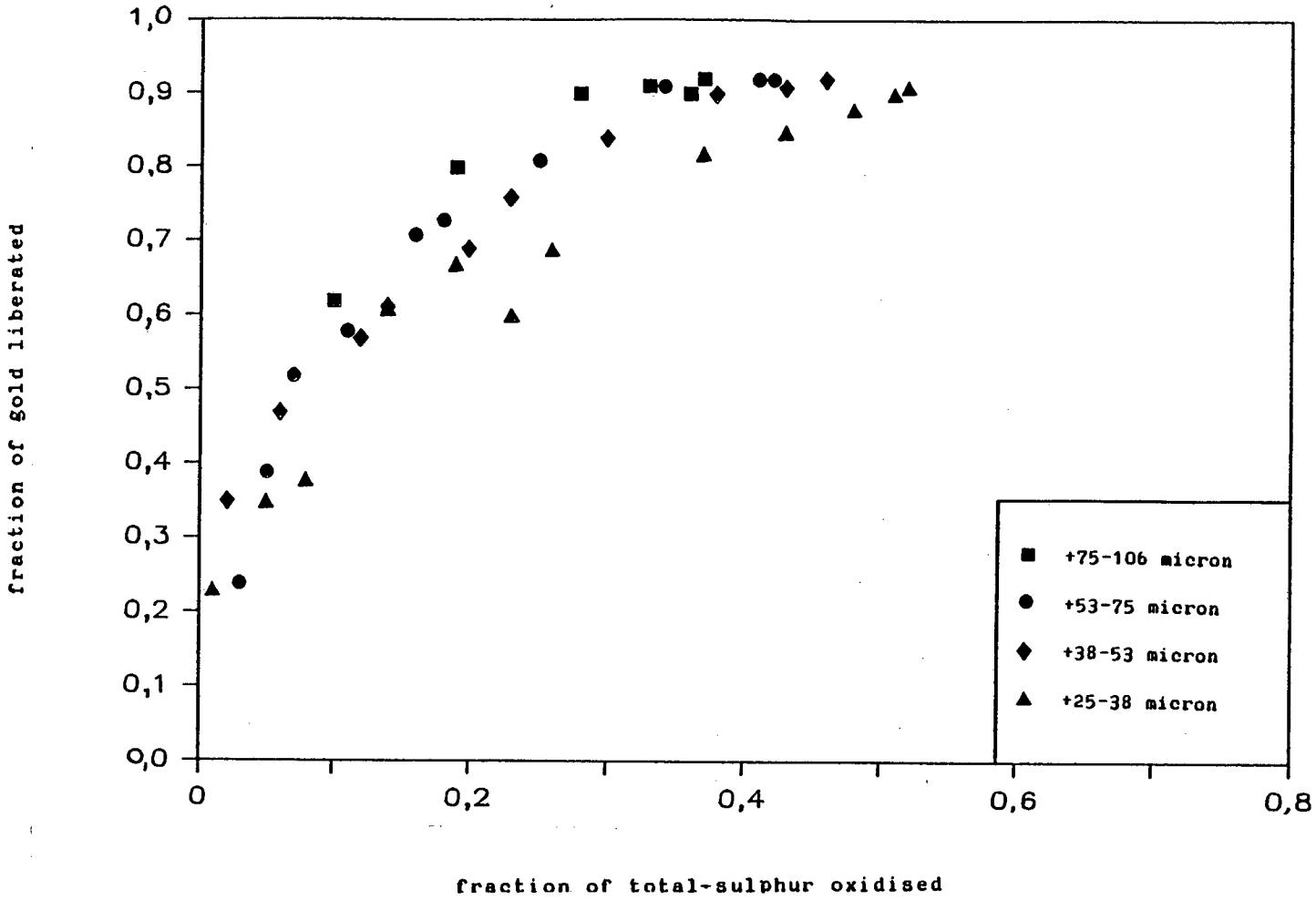

Figure 5.15: Gold liberation versus total-sulphur oxidation

The screen analysis of the leached residues (Appendix D) has shown that the particle size decreases during the course of leaching. The change of the particle size distribution with time during the batch leach tests is shown in Figures 5.16 to 5.18 for the three larger size fractions. Attempts to obtain the corresponding measurements for the +25-38 micron size fraction were unsuccessful since the different sizing method used, a Particle Size Analyser, did not give comparable results to sieving. The particle size diminution is mainly attributed to the mechanical effects rising from agitation.

The breakage of the particles stemming from mechanical effects results in partial gold exposure and subsequently gold liberation. Therefore the gold liberation presented in Figures 5.10 to 5.15 is the overall gold liberation in the system due to bacterial action and mechanical effects. It must be noted however, that in a bioleach stirred reactor it is of no meaning to separate the two effects since they both lead to gold liberation. Therefore the gross gold liberation as presented in the above figures is considered the most important. However, qualitative information about the difference between the gold liberation in the bacterial tests and the gold liberation in the sterile tests (Appendix E) can be obtained from Figures 5.19 to 5.22. The dashed curve in these figures represents the difference between gold liberation in the bacterial tests and gold liberation in the sterile tests. This curve was obtained by fitting a fourth order polynomial curve to each of the two sets of gold liberation data, in the sterile and bacterial tests, and by subtracting the two curves.

Comparing Figures 5.19 to 5.22 with Figures 5.11 to 5.14 one observes that the dashed curves rise much steeper than the corresponding total-sulphur oxidation curves i.e., that even in the case where the gold liberation is calculated as the difference between the bacterial tests and the sterile tests, it is higher than the corresponding total-sulphur oxidation.

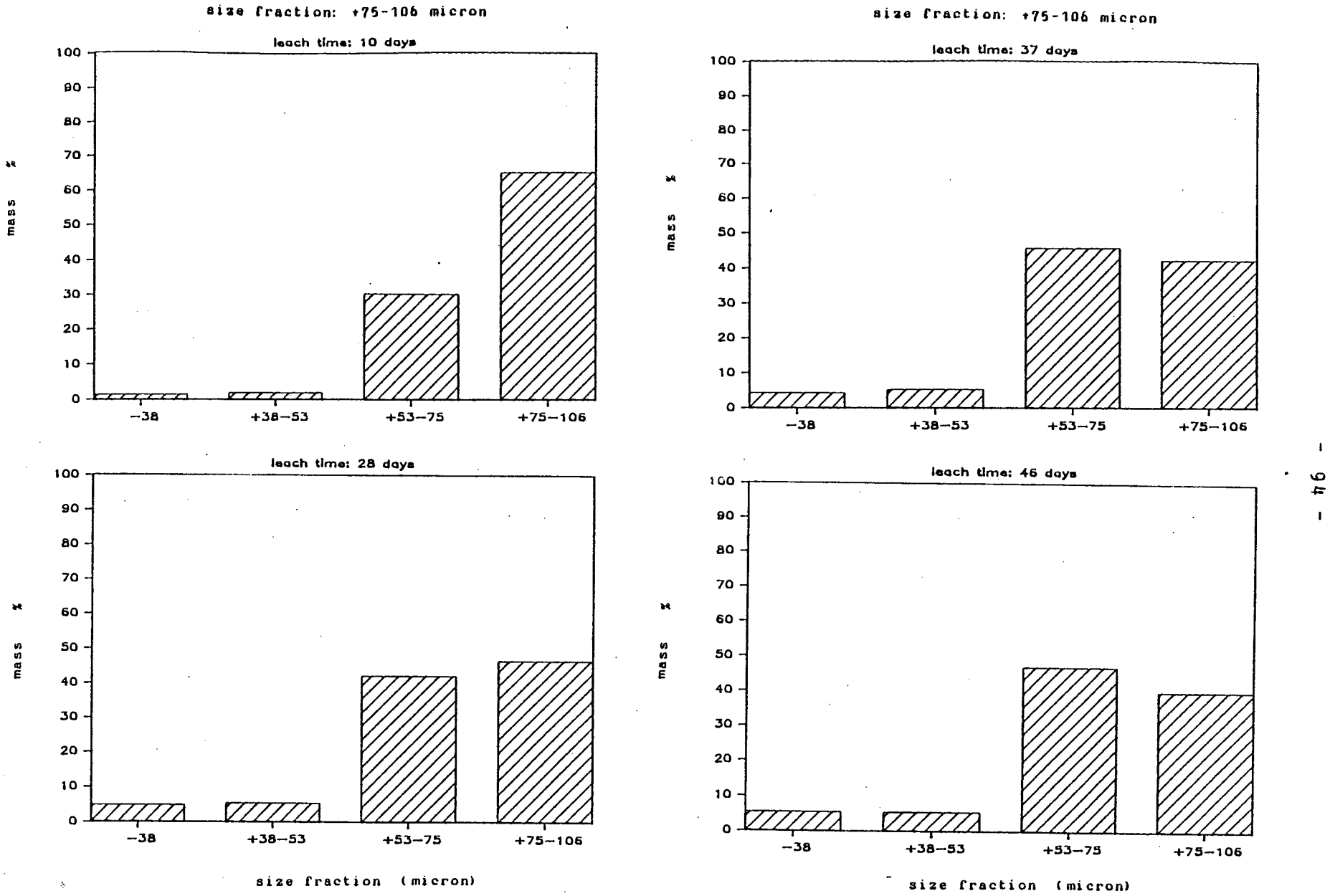

Figure 5.16: Particle size distribution versus time.

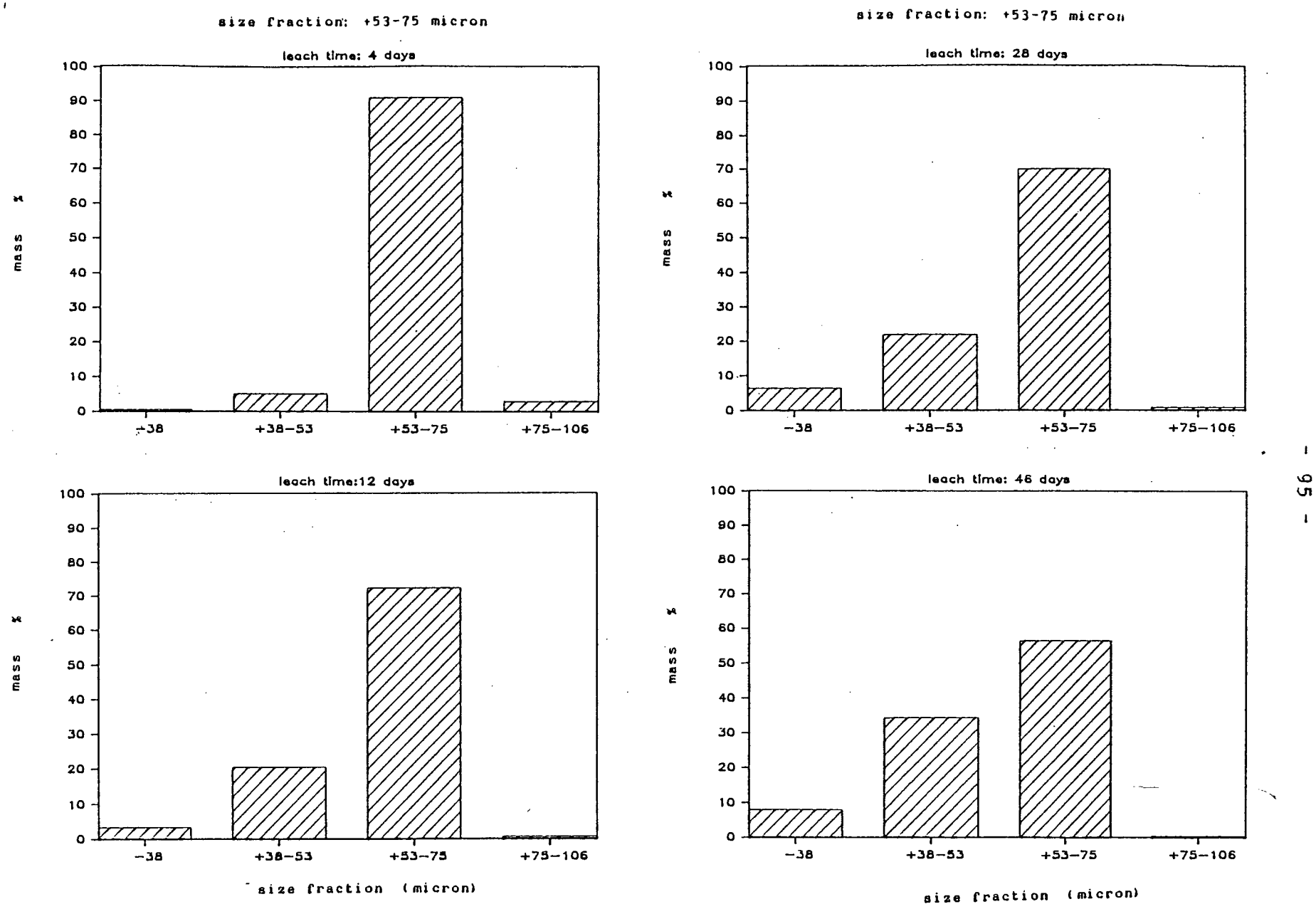

Figure 5.17: Particle size distribution versus time.

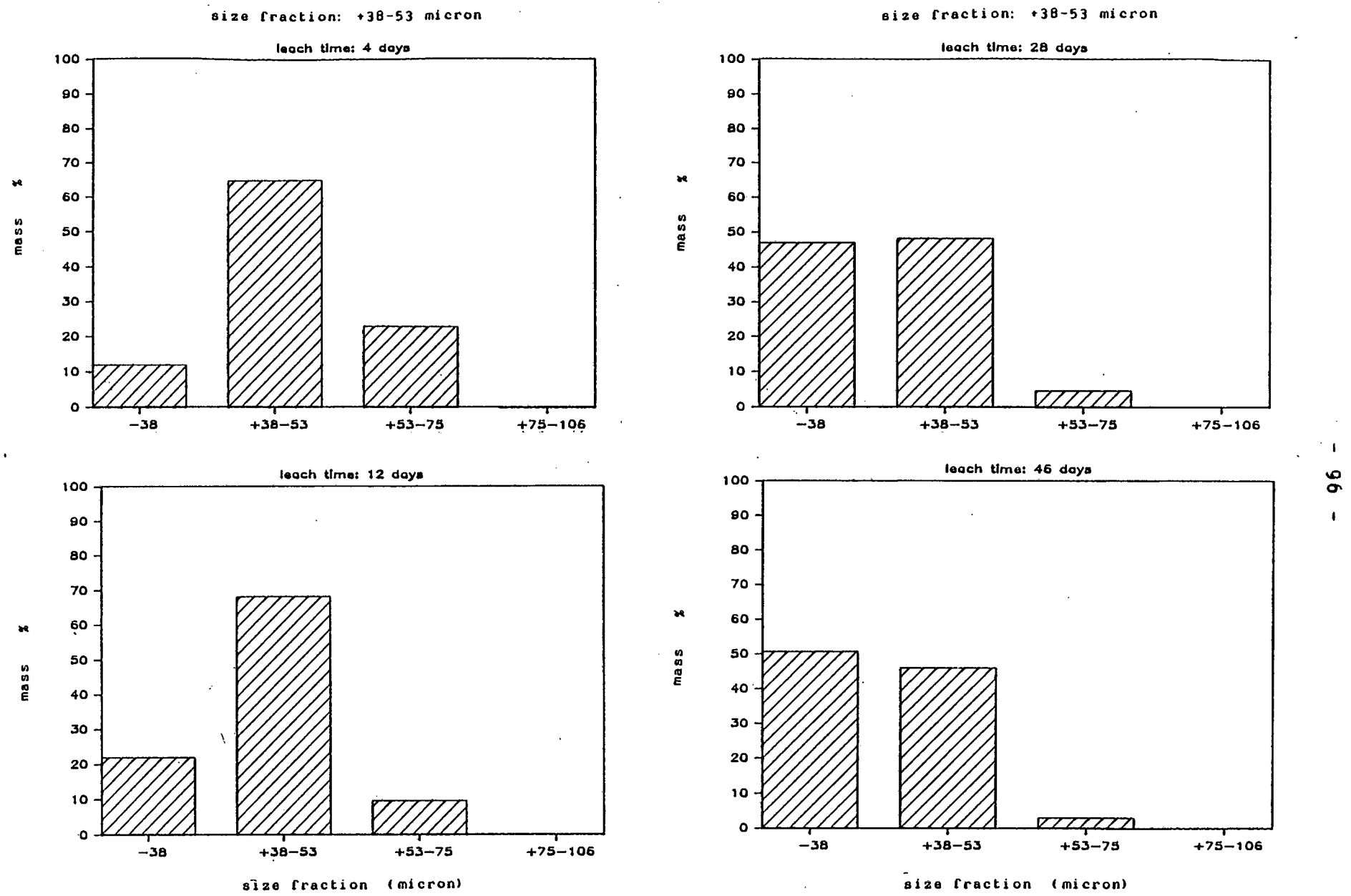

Figure 5.18: Particle size distribution versus time.

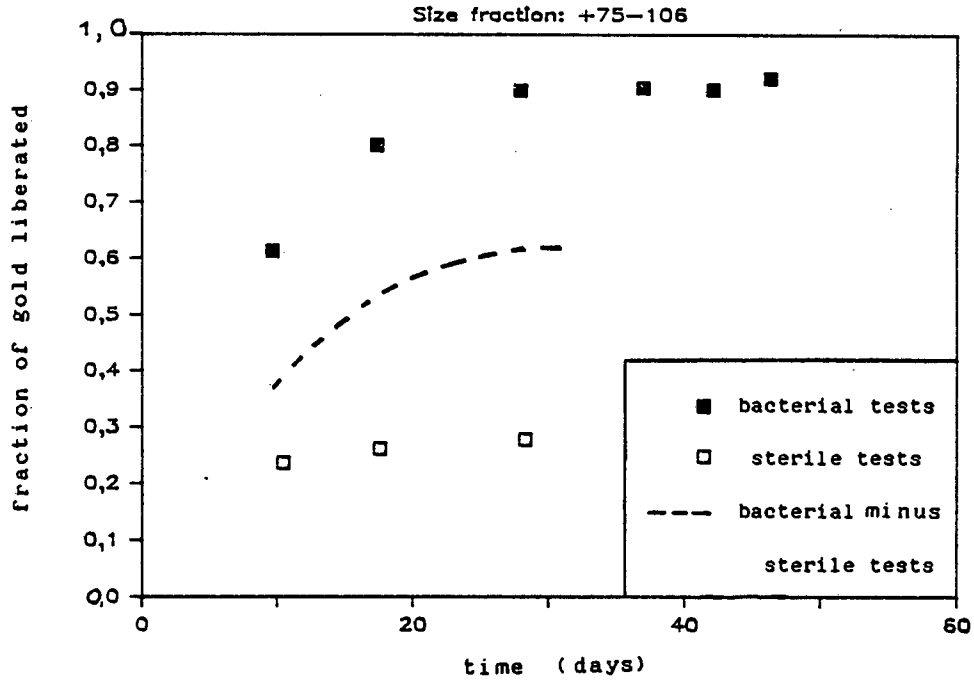

Figure 5.19: Gold liberation in the bacterial tests — gold liberation in the sterile tests.

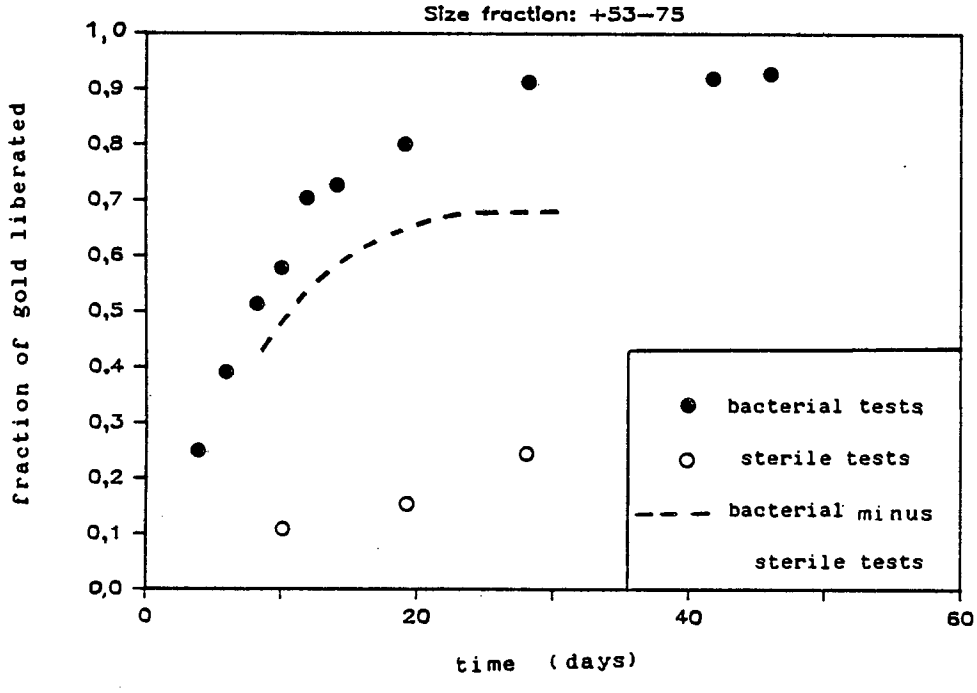

Figure 5.20: Gold liberation in the bacterial tests — gold liberation in the sterile tests.

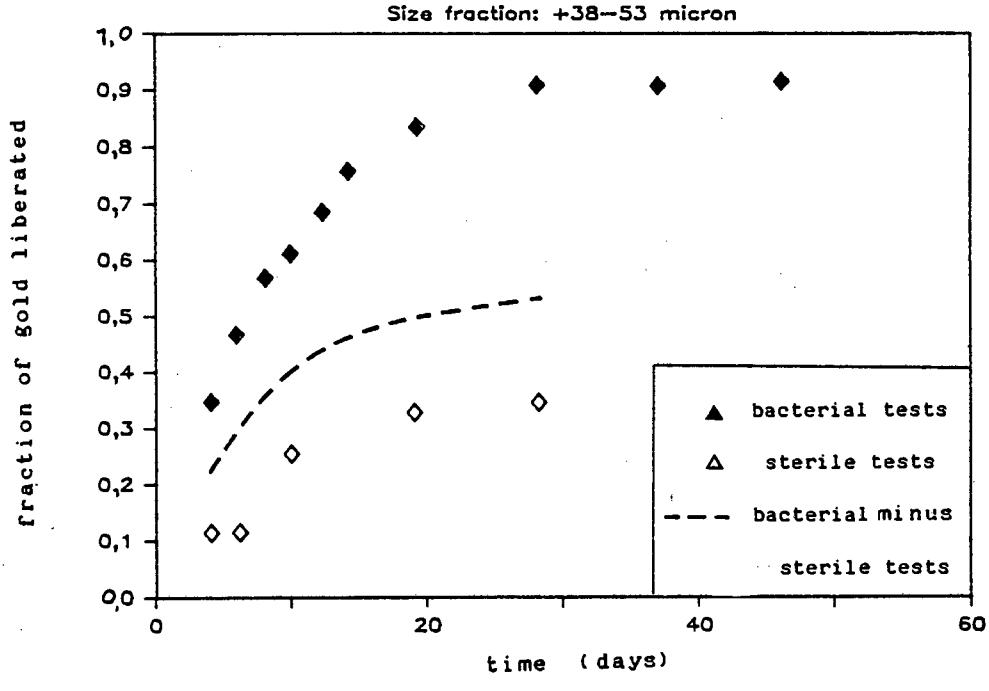

Figure 5.21: Gold liberation in the bacterial tests — gold liberation in the sterile tests.

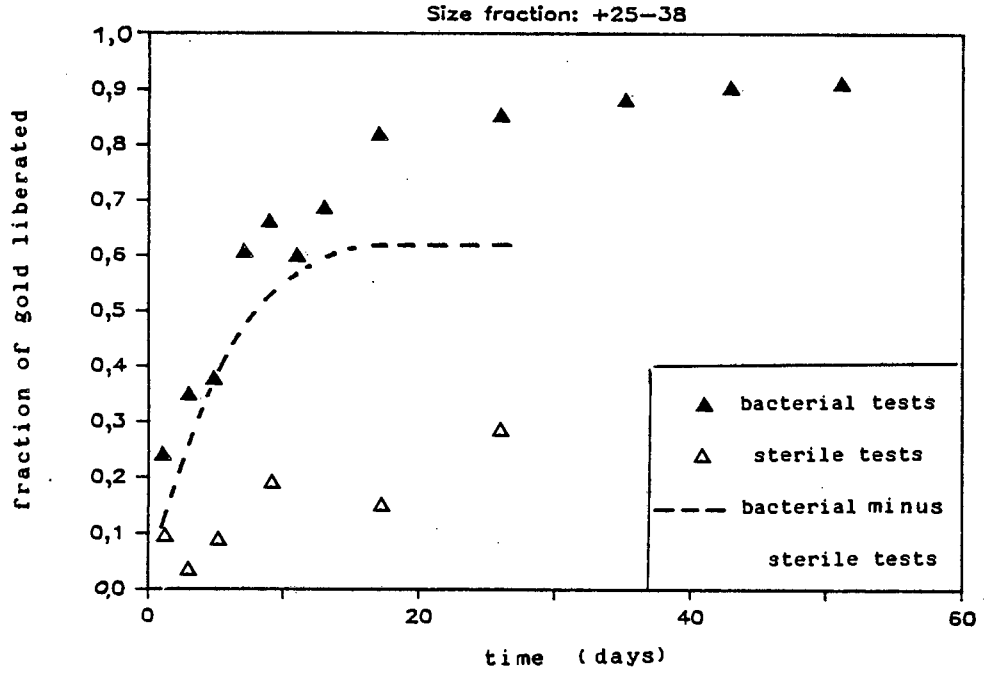

Figure 5.22: Gold liberation in the bacterial tests — gold liberation in the sterile tests.

The above results viz. the higher degree of gold liberation in comparison to the degree of total-sulphur oxidation, can be interpreted in the light of the modes of gold occurrence in the pyrite which have been described in the Literature Survey 2.3.4. Since little information is available about the occurrence of gold in the examined pyrite concentrate, the results presented above can be explained in a number of ways: if the gold was in a solid solution form in the pyrite it would be expected that the fraction of sulphur oxidised and gold liberated at a given time were equal. However this is not the case. It might be argued that the higher gold liberation might be due to a higher gold concentration close to the surface of the particles. However this is unlikely since a microprobe analysis of the sample showed a random distribution of the gold in the pyrite grain (Southwood, 1986).

It appears then that the pyrite is oxidised by the bacteria in regions where the gold is preferentially located, thus resulting in enhanced gold liberation. It has been mentioned in section 2.3.4. that discrete gold particles are possibly located in crystal dislocations in the pyrite grains. On the other hand, there is evidence in the literature to suggest that the bacteria preferentially oxidise the mineral along crystal dislocations (see section 2.3.1). Furthermore, evidence suggesting the oxidation of pyrite by a propagating-pore mechanism has been given in this study and is supported by the scanning electron micrographs which are discussed in section 5.4: the bacteria oxidise the pyrite developing pores, which seem to follow directions of dislocations within the crystal, parallel to the crystallographic axes; these dislocations very likely contain most of the discrete gold particles (Southwood and Southwood, 1985).

However, this is not the only possible explanation for higher gold liberation than sulphur oxidation. The pyrite concentrate contained trace amounts of arsenic. The arsenic content of the feed material was less than 0,4%. A

microprobe analysis of the sample showed that most of the arsenic was in a solid solution form in the pyrite and the rest was in the form of arsenopyrite (Southwood, 1986).

The arsenic oxidation during the batch leach tests is expressed as fraction of arsenic oxidised and is presented in Tables 5.2. to 5.5.

The arsenic leach data are shown together with the gold liberation data in Figures 5.23 to 5.26. These figures show that gold liberation and arsenic oxidation follow similar kinetics. It is known (see section 2.3.4), that there is a positive correlation between gold and arsenic-bearing sulphide minerals. It might therefore be possible that the liberated gold is associated with the arsenopyrite particles or the arsenic-containing phases of the pyrite. It is also known that arsenopyrite is leached faster than pyrite (Pinches, 1972) and this could result in enhanced gold liberation. Although the possibility of gold occurring in solid solution in the pyrite was excluded, it is possible that the gold is associated with the arsenic-containing phases of the pyrite, which are less refractory than the non-arsenic phases (Southwood, 1985). In the absence of a thorough mineralogical analysis the above results indicate that gold and arsenic might occur in association.

The above results suggest that gold recovery from refractory pyrite ores can be considerably enhanced after a bacterial pre-oxidation treatment of the ore. This is in agreement with work from B.C. Research (Lawrence and Bruynesteyn, 1985), where in a number of refractory gold-bearing pyrite concentrates gold recovery was greatly improved after they were subjected to bacterial leaching pretreatment. In contrast to the non-linear relationship between gold liberation and total-sulphur oxidation found in the present study, Lawrence found a proportional relationship between gold liberation and pyrite oxidation: for 84% pyrite oxidation the gold recovery achieved was 81% compared with only 24% by direct cyanidation.

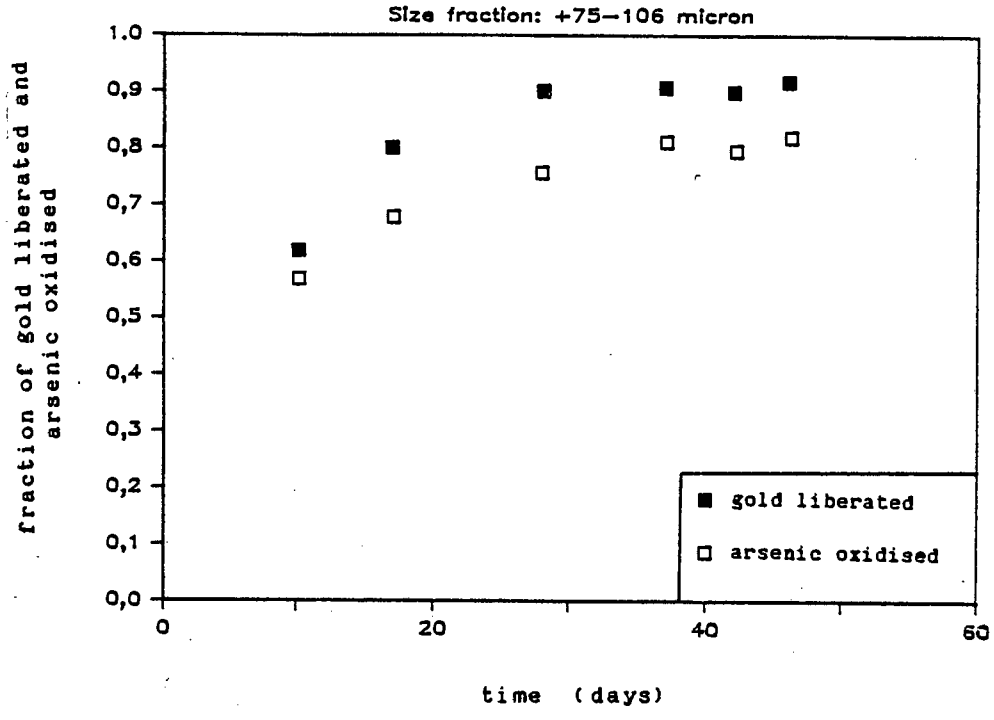

Figure 5.23: Arsenic oxidation and gold liberation versus time

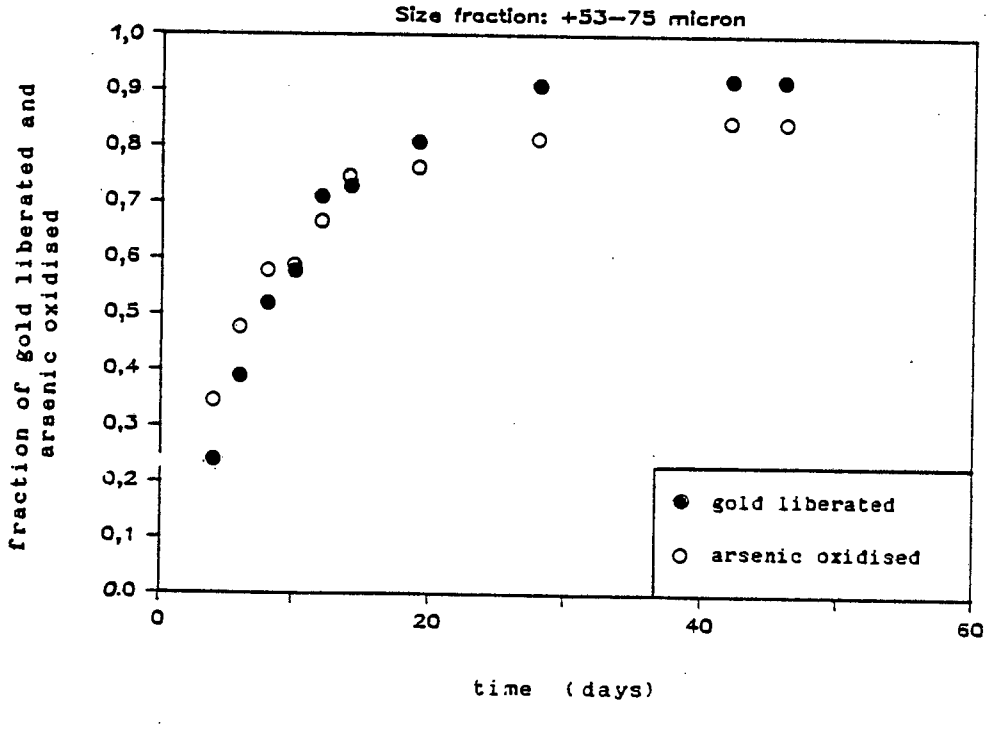

Figure 5.24: Arsenic oxidation and gold liberation versus time

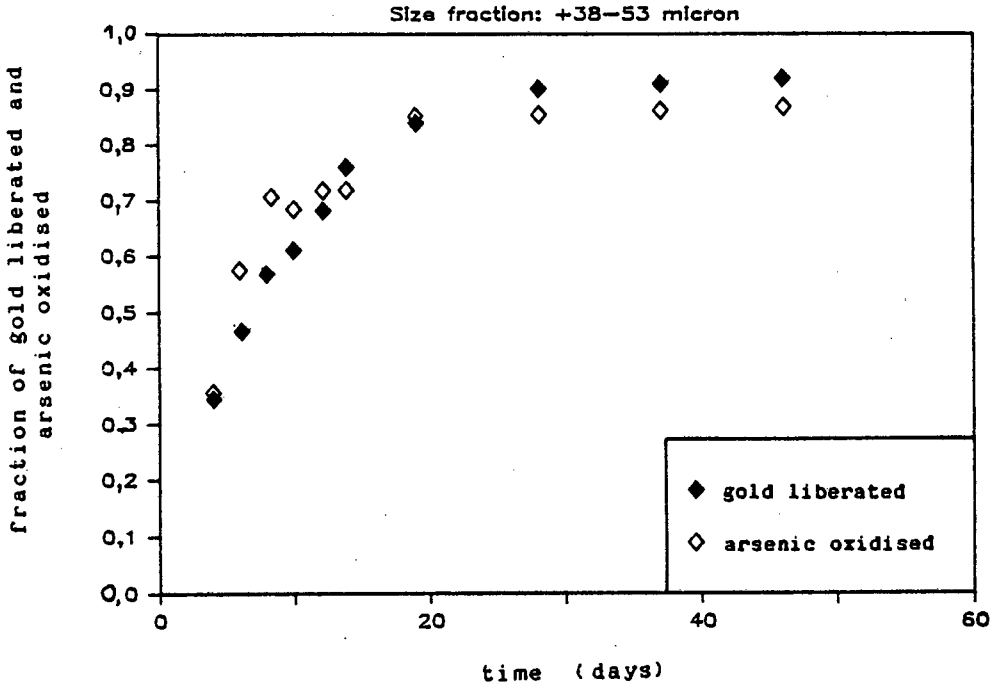

Figure 5.25: Arsenic oxidation and gold liberation versus time

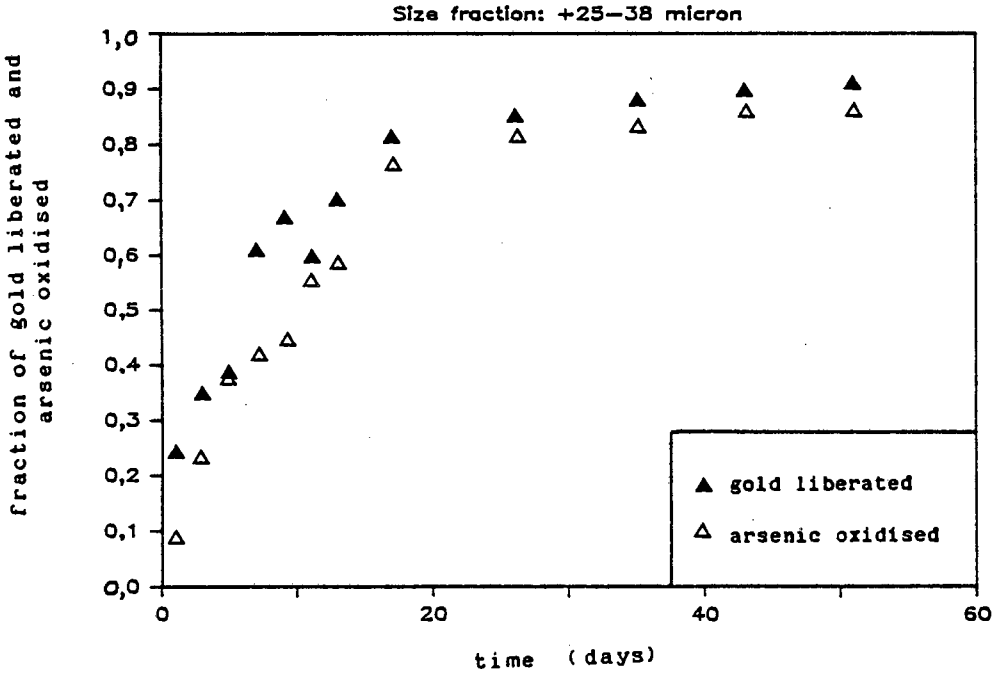

Figure 5.26: Arsenic oxidation and gold liberation versus time

The different relationship observed in Lawrence's study and this study can either be attributed to a different leaching mechanism taking place or to a different mode of gold occurrence in the two pyrite concentrates.

5.4 Scanning Electron Micrograph Observations on Pyrite Concentrate Particles before and after Leaching

Samples from feed material, bacterial leach residues and sterile control residues were examined in the scanning electron microscope so that any changes in the particle texture during leaching could be observed. The micrographs taken were of the +53-75 micron size fraction and are presented and discussed in this section. Similar observations were made for the other three size fractions.

In Figure 5.27 micrographs from feed material and bacterial leach residues after 12, 28 and 42 days of leaching respectively are shown. These micrographs show that almost all the particles in the leach residues present a leached texture. By a more careful examination of this texture it can be observed that the degree of leaching is not uniform for all the particles nor is it always uniform for a given single particle, i.e. there are particles or parts of particles which are more intensely leached than others in the same sample. The type of etching observed in most of the leached particles is different to that observed in Figure 5.9. a, b and c. Grooves, pits and holes that propagate through the particles can be observed in almost all the leached particles.

In Figure 5.28 micrographs of feed material, bacterial leach residue after 28 days of leaching, and sterile control residue after 28 days of leaching respectively, are shown.

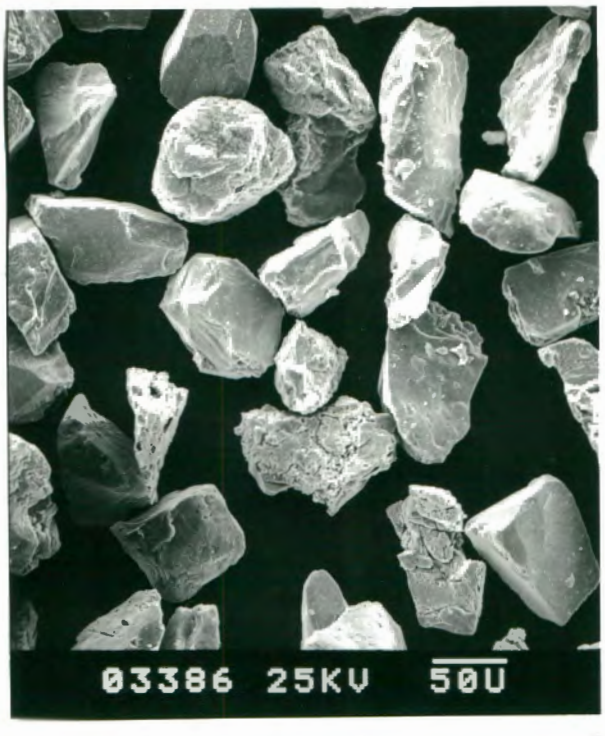

a. feed material

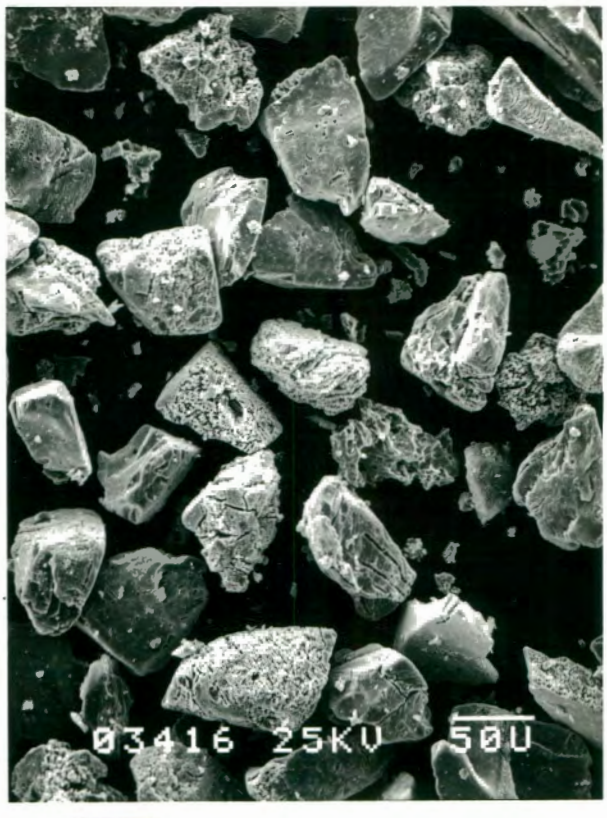

b. 12 days of leaching

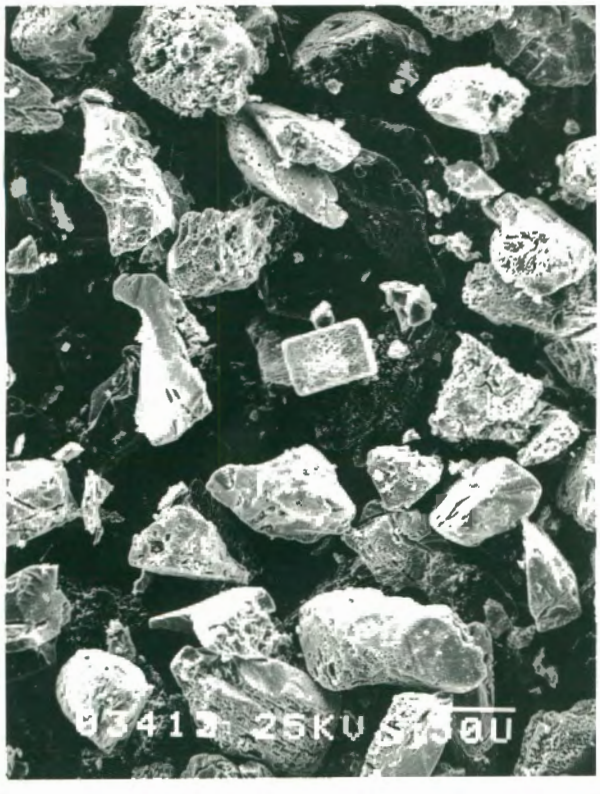

a. 28 days of leaching

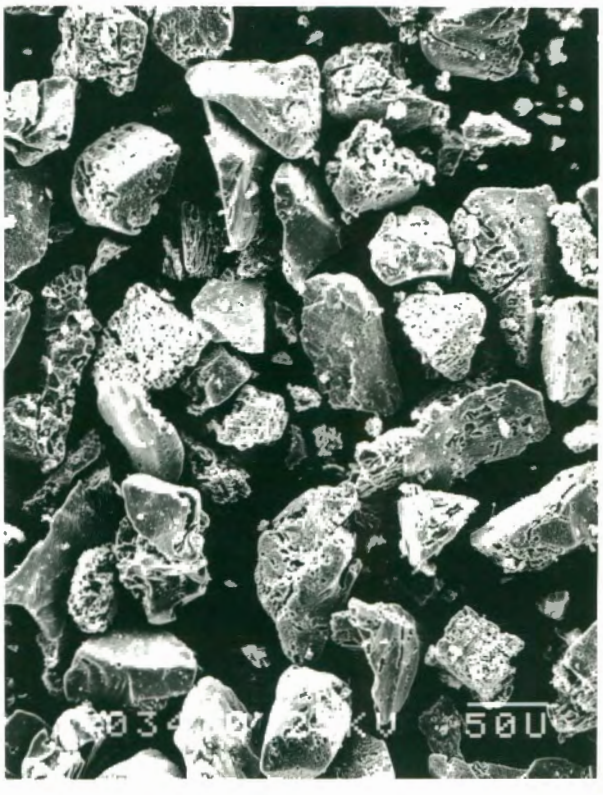

d. 42 days of leaching

Figure 5.27: Samples from feed material and bacterial leach residues. Size fraction: +53-75 micron.

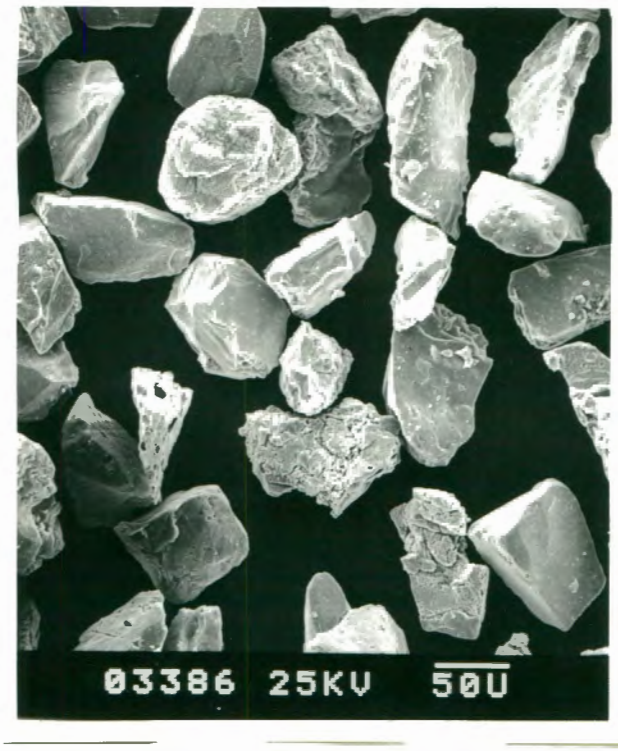

feed material

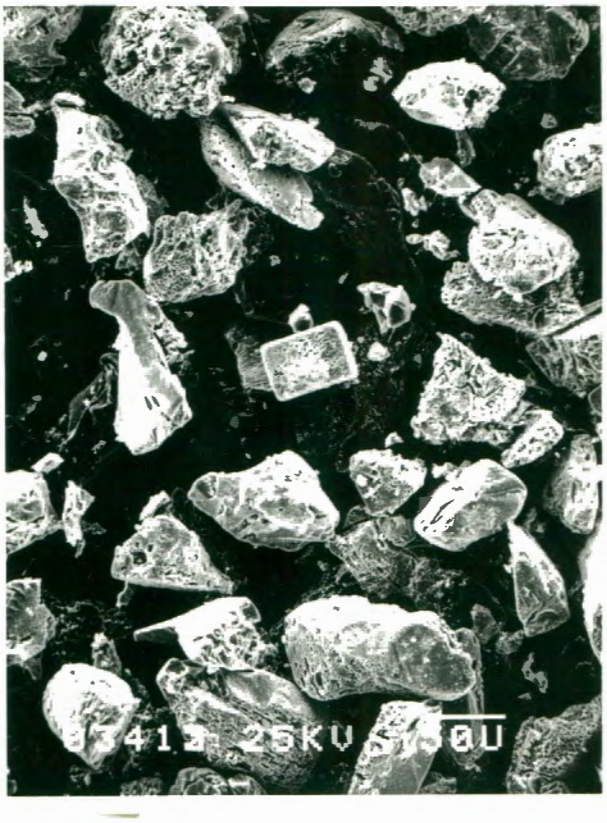

leach residue,
28 days of leaching

sterile residue,
28 days of leaching

Figure 28: Feed material, bacterial leach residue and sterile control residue. Size fraction: +53-75 micron.

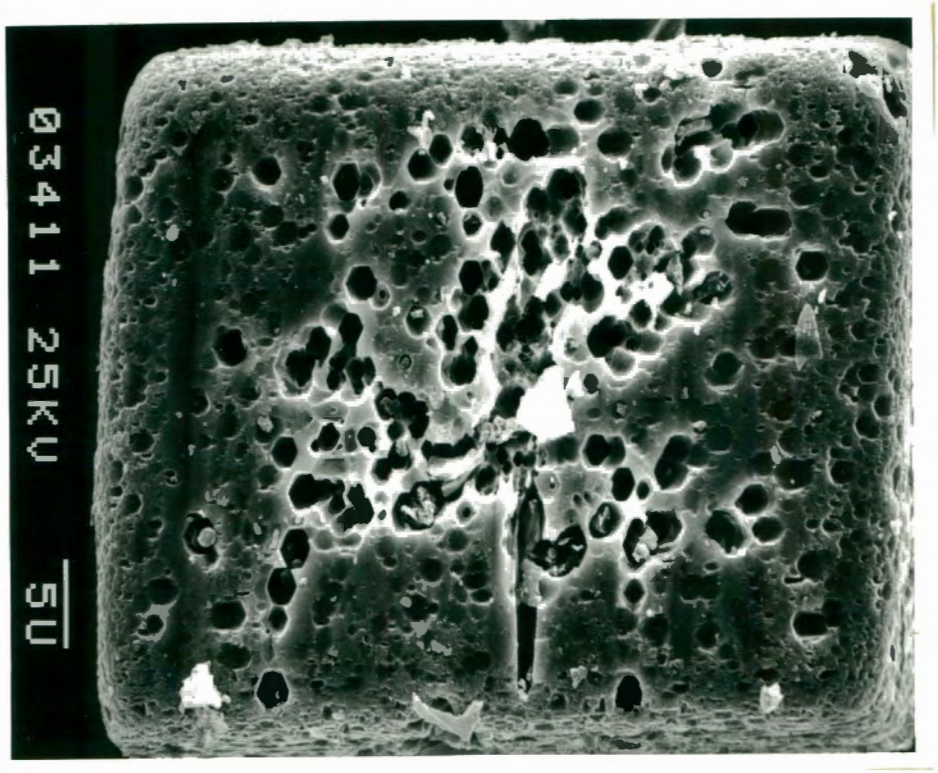

Figure 5.30: Pyrite crystal leached for 28 days, showing pore formation along three possible directions. Most of the pores present an hexagonal cross-section. Size fraction: +53-75 micron.

Furthermore some of the holes on this plane have an hexagonal cross-section. It is known that screw dislocations in a cubic crystal occur on the (111) plane (Amelinckx, 1964) and manifest themselves as hexagons. It is therefore possible that these pores with hexagonal cross-sections were formed by bacterial action along screw dislocations.

In Figure 5.31 a pyrite crystal from a sample that has been leached for 42 days is shown. In this crystal a type of surface leaching, pitting, together with some pore development along two perpendicular directions has occurred. The diameter of the surface holes is about 1 micron.

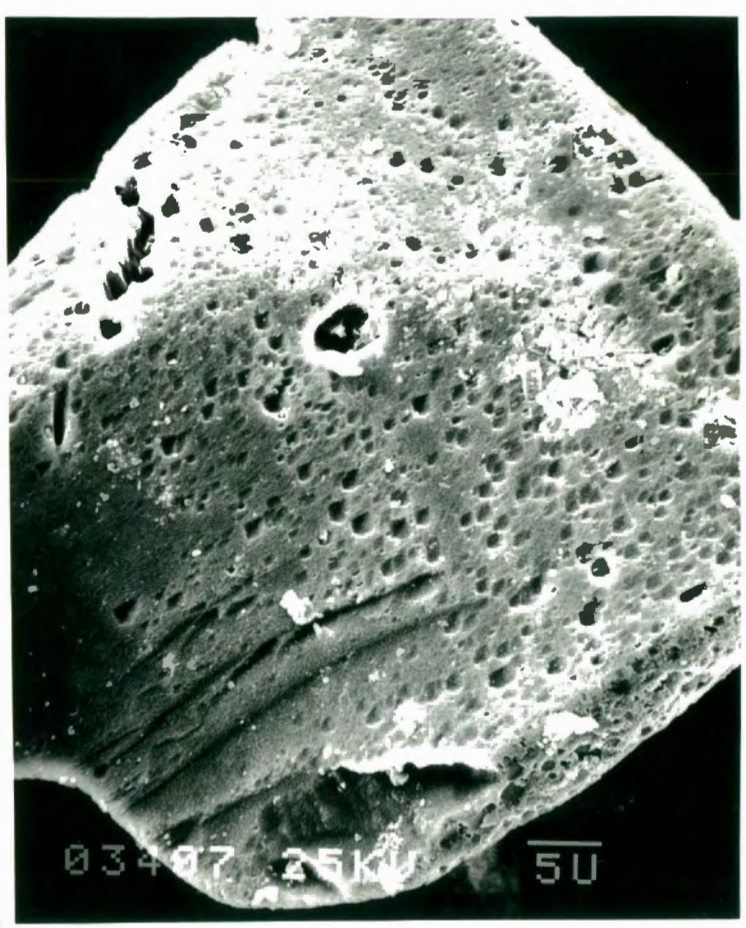

a

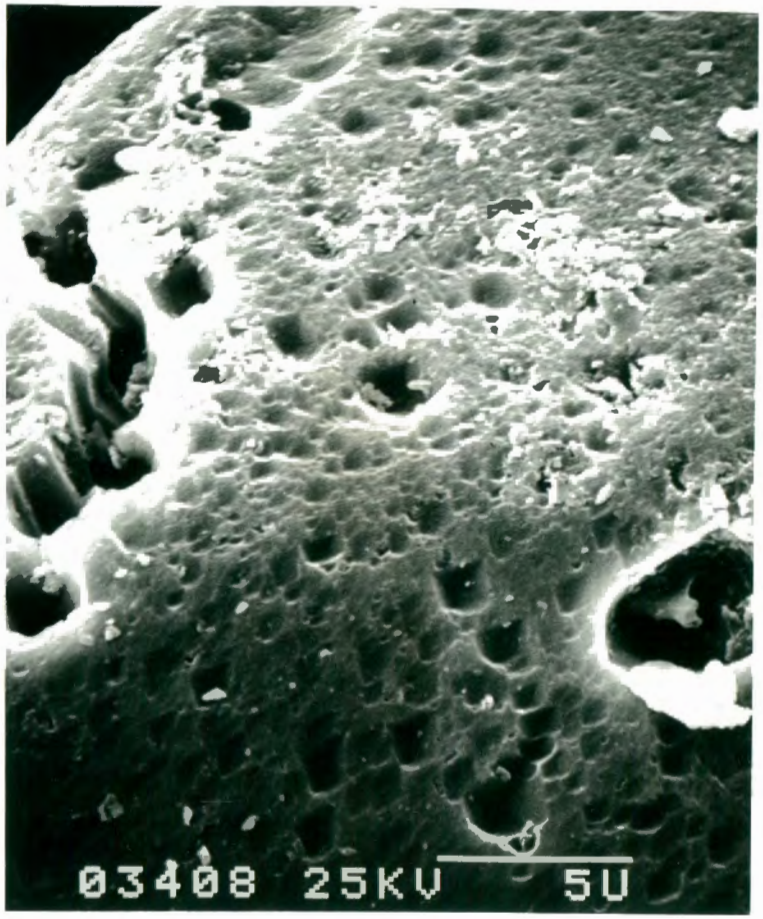

b

Figure 5.31: Pitting and pore formation along a possible plane of weakness in a crystal leached for 42 days. Size fraction: +53-75 micron.

In this figure one observes that the surface texture of the particles in the sterile control leach residue is very similar to that of the feed material, i.e. the surface of the particles has remained unreacted and retains the characteristics it had before leaching. The above observations lead to the conclusion that the large difference observed in the particle texture before and after leaching, as well as between the bacterial and sterile control leach residues, is the result of bacterial action.

A more detailed observation of the particles' surface texture in the bacterial leach residues was attempted by taking micrographs of selected particles showing a rather regular crystal shape, under higher magnification. Figures 5.29, 5.30 and 5.31 show some of these details. Figure 5.29 shows a cubic pyrite crystal that has been leached by bacteria for 42 days. Holes that penetrate through the crystal can be observed on all three crystal planes shown in the micrograph. The diameter of these holes (on what it is believed to be the (100) plane) is 1 to 6 microns. This is in agreement with data reported by Southwood and Southwood (1985), where the mean pore diameter observed in two bacterially leached pyrite concentrates was 4,5 and 8,0 micron respectively. The direction of the pores within the pyrite crystal cannot be clearly seen, since it is mainly the surface of the particles that is observed in these photographs. A detail of one of these holes is shown in Figure 5.29 b.

In Figure 5.30 a pyrite crystal penetrated by pores is shown. The sample has been leached for 28 days. The plane represents most probably the (110) plane in the pyrite crystal. Two directions along which pores propagate seem to exist; one followed by the pores on the left hand-side of the plane and another followed by the pores on the right hand-side of the plane. A third possible direction of pore propagation is found in the middle of the crystal perpendicular to the two previous ones.

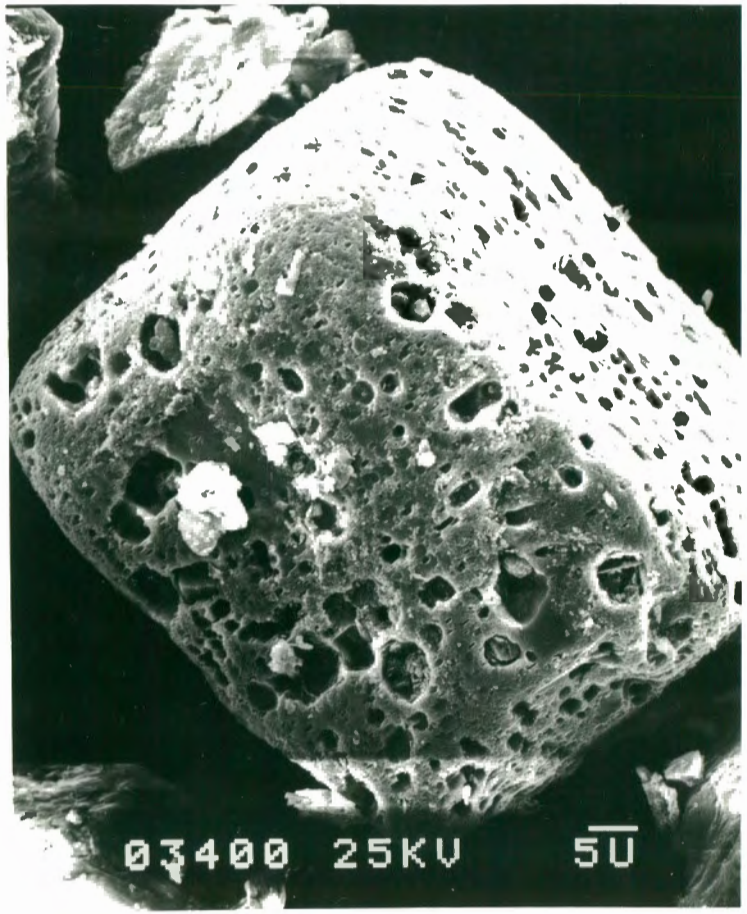

a

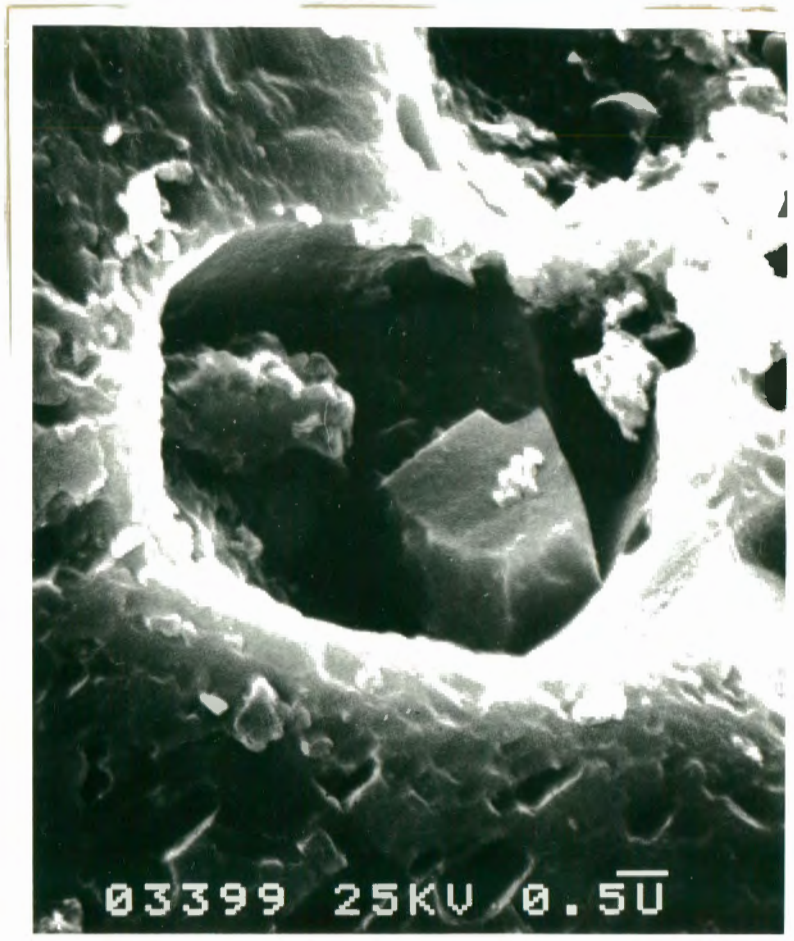

b

Figure 5.29: Pore formation in a cubic pyrite crystal leached for 42 days. Size fraction: +53-75 micron.

5.5 Bacterial Growth during Batch Leaching

The change in the numbers of free bacteria with time is presented in Table 5.9. The log of the numbers of the free bacteria has been plotted versus time and is shown in Figure 5.32.

From this figure it can be seen that there is a lag time of about one day for the three smaller size fractions. For the largest size fraction the lag time appears to be about two days. The lag time calculated from the batch leach data using the Nelder-Mead routine was generally higher than those values.

During the preliminary experiments it was found that in order to mininise the lag phase in bacterial growth and to maximise the rate of pyrite oxidation, an inoculum age of eight days was optimal, i.e. an inoculum in its late active growth phase. This is in agreement with data published by Blancarte-Zurita *et al.* (1985). The lag time appears to be a function of the adaptation of the bacteria to the ore and the inoculum size used. The effect of inoculum size was not examined in this study; instead, in order to determine the optimum inoculum size, data from the literature were taken into account. The effect of inoculum size on the lag time and leach rates of a pyrite-arsenopyrite concentrate was examined by Pinches (1972). Pinches found that the inoculum size, varied from $1,5 \times 10^6$ to $2,7 \times 10^7$ cells/cm^2 of oxidisable surface area/ml of solution, did not have any significant effect on either the bacteria growth rates or the metal leach rates. However the lag time decreased from about 70 hours for the small inoculum size to about 10 for the larger. Atkins (1978) also found that varying the inoculum size from 6×10^5 to 6×10^9 cells/ml had no effect on the leach rate, but it affected the lag time. However, when an inoculum size of 6×10^{10} cells/ml was used, an anomalous behaviour in the leach rate was observed.

Table 5.9: Numbers of free bacteria versus time.

leach time days	+75-106 cells/ml x 10^{-6}	+53-75 cells/ml x 10^{-6}	+38-53 cells/ml x10^{-6}	+25-38 cells/ml x 10^{-6}
0	1,00	1,00	1,00	1,00
1	0,46	0,93	1,20	0,94
2	0,99	2,13	3,21	2,56
3	2,53	6,10	8,92	6,32
4	6,85	8,52	17,80	10,90
5	11.00	11,50	21.10	14,40
6	14,60	12,30	22,00	21,30
7	17,40	17,00	30,40	23,70
8	22,90	20,80	29,30	26,50
9	25,30	24,00	31,70	30,30
10	28,30	27,50	29,00	27,00
11	26,50	23,60	28,00	29,40
12	28,90	28,50	31,00	28,00
13	28,60	26,70	27,00	29,80
19	28,20	29,80	30,50	31,00
28	27,50	27,00	29,00	30,50
37	26,00	27,50	27,00	28,00
46	26,50	26,70	25,80	29,00

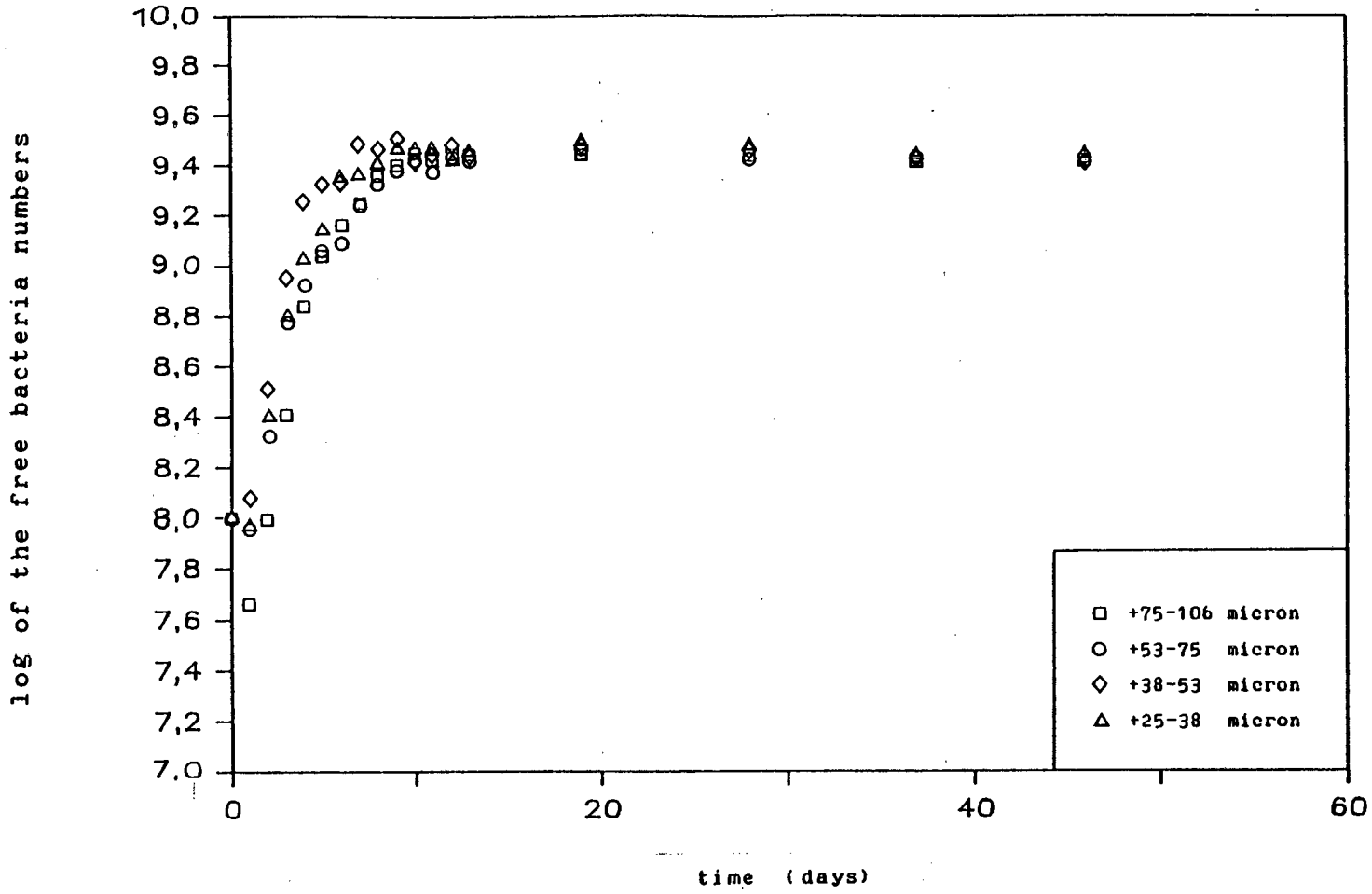

Figure 5.32: Log of the free bacteria numbers versus time

From the above work it appears that to minimize the lag time a large inoculum size, of the order of 10^9 cells/ml, is needed. Due to lack of the necessary equipment, such a large inoculum could not be used in this study and instead an inoculum size that gave a cell concentration of $1,0x10^8$ cells/ml in each reactor after inoculation was used.

From the initial value of $1,0x10^8$ cells/ml the free bacteria concentration increased with time until, after about 10 days, it reached its maximum value of about $2,8x10^9$ cells/ml. This value was approximately the same for all particle size ranges. Thereafter the concentration of the free bacteria remained close to this value.

The curve of bacterial numbers in solution versus time found in this work is generally consistent with data published in the literature. Corrans (1974), found that the growth of bacteria in solution during batch leach tests of pendladite increased linearly with time after a lag time of 3 to 4 days. The bacterial population in solution reached its maximum value of $1,2x10^9$ cells/ml after about 17 days, after which it remained constant for the rest of the experiment. The longer lag time observed by Corrans may be due to the smaller inoculum size used, $1x10^7$ cells/ml, or due to inadequate adaptation of the bacteria to the substrate. The longer time required for the bacterial population to reach its maximum value may be due to the different substrate and the different leaching conditions used (e.g. 5% pulp density).

A similar pattern for the growth of free bacteria in solution versus time was found in batch leach tests of pyrite by Wakao *et al.* (1984) The free bacterial population, initially inoculated at a concentration of $1,5x10^7$ cells/ml, increased to about 10^{10} cells/ml after about 6 days. This large number is probably due to the surface active agent used which resulted in the release of cells from the solid surfaces.

No routine measurements of attached bacteria were done in this study. It is recognised however that a growth curve of the attached bacteria numbers versus time would be important in elucidating the role of the free and attached bacteria in the leaching of pyrite. A few selected samples were analysed for attached bacteria at GENCOR laboratories using the micro-Kjeldahl nitrogen method (McGoran et al., 1969). The samples used, from the +38-53 micron size range, had been leached for 18 and 43 days. It was found that 80% and 75% of the total bacterial population respectively (viz. 3 to 4 times more bacteria) was attached to the solids.

The maximum free bacteria concentration observed in the present study, $2,8 \times 10^9$ cells/ml, is also consistent with the value 4×10^8 to 4×10^9 of free cells/ml observed by Le Roux et al. (1973). Le Roux found 6 times as many attached bacteria. Groudev (1979) also observed that the free cell concentration in his studies exceeded 5×10^8 cells/ml. The attached bacteria concentration was 1,5 or 4 times higher than the free depending on the strain.

The above observations suggest that most of the bacteria in a pyrite bioleach system are attached to the solids and that the attached bacteria are 4 to 6 times more numerous than the free bacteria.

5.6 Leached Iron Concentration versus Time

During the bacterial oxidation of pyrite only a portion of the iron produced remains in solution, the rest precipitating according to the hydrolysis reactions described in section 2.2. The concentration of ferrous iron in solution during the batch leach tests, measured as described in section 4.6.2, never exceeded 0,4 g/l. The total soluble iron concentration increased up to a value of about 7g/l, (as it can be seen from Figures 5.33 to 5.36), and hence it can be concluded that the leached iron was mainly in the ferric form.

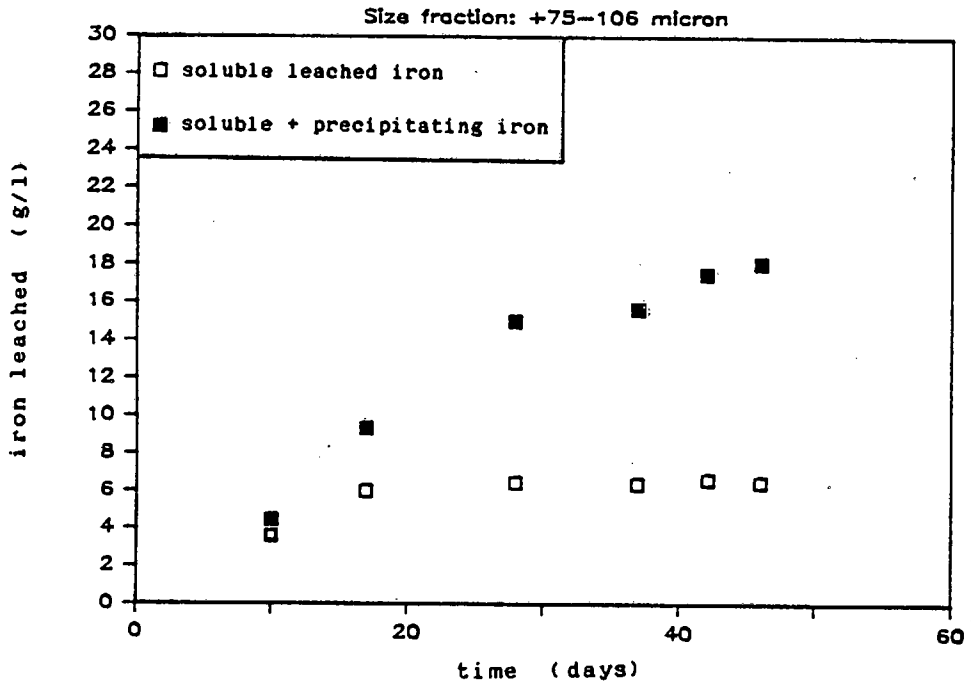

Figure 5.33: Leached iron concentration versus time.

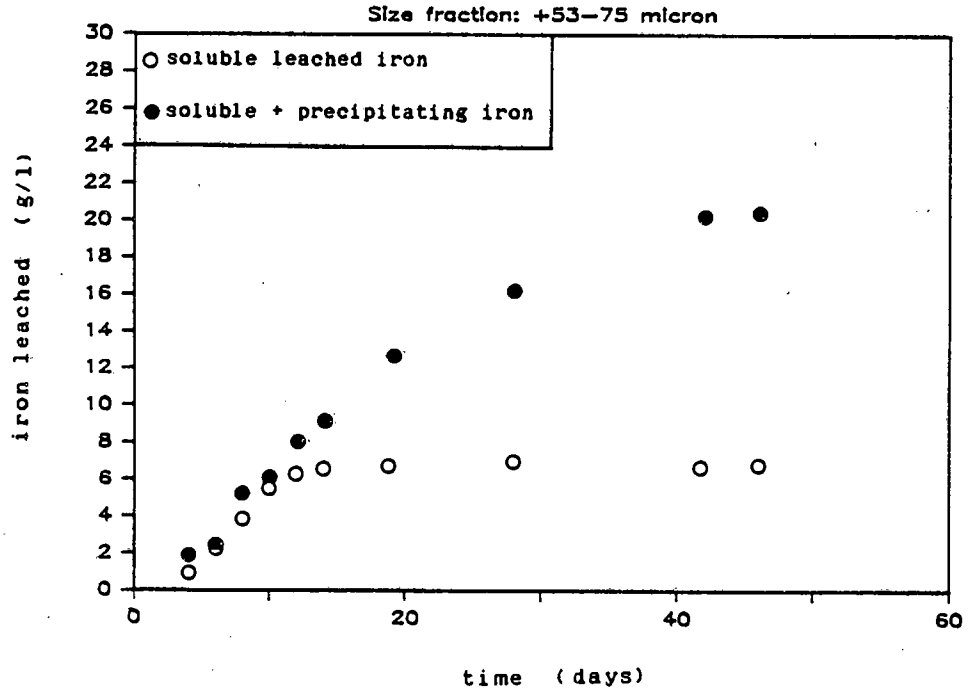

Figure 5.34: Leached iron concentration versus time.

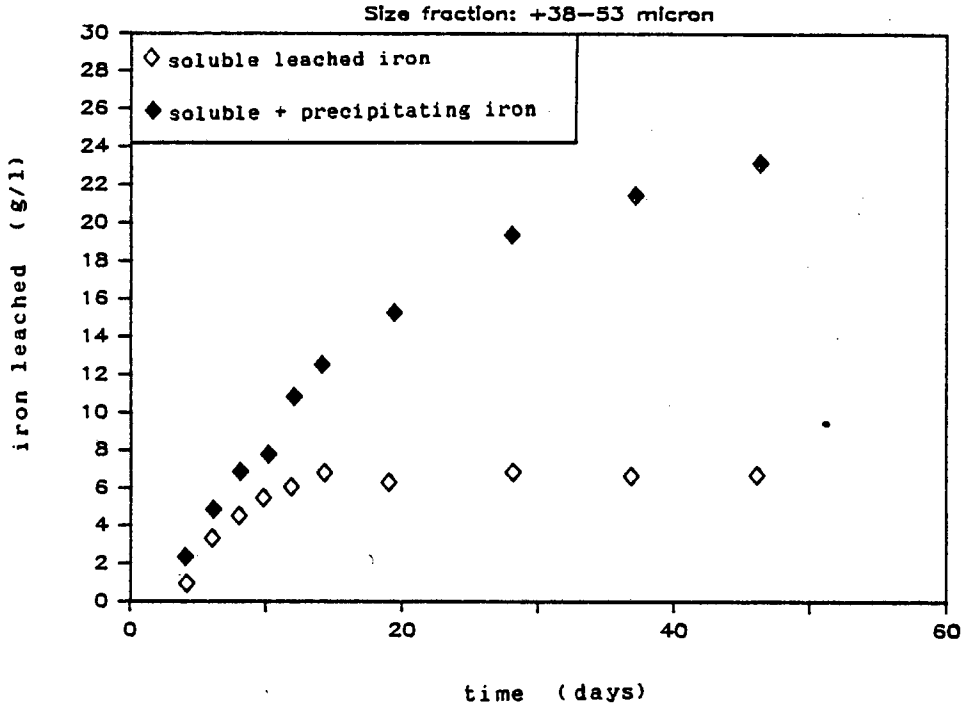

Figure 5.35: Leached iron concentration versus time.

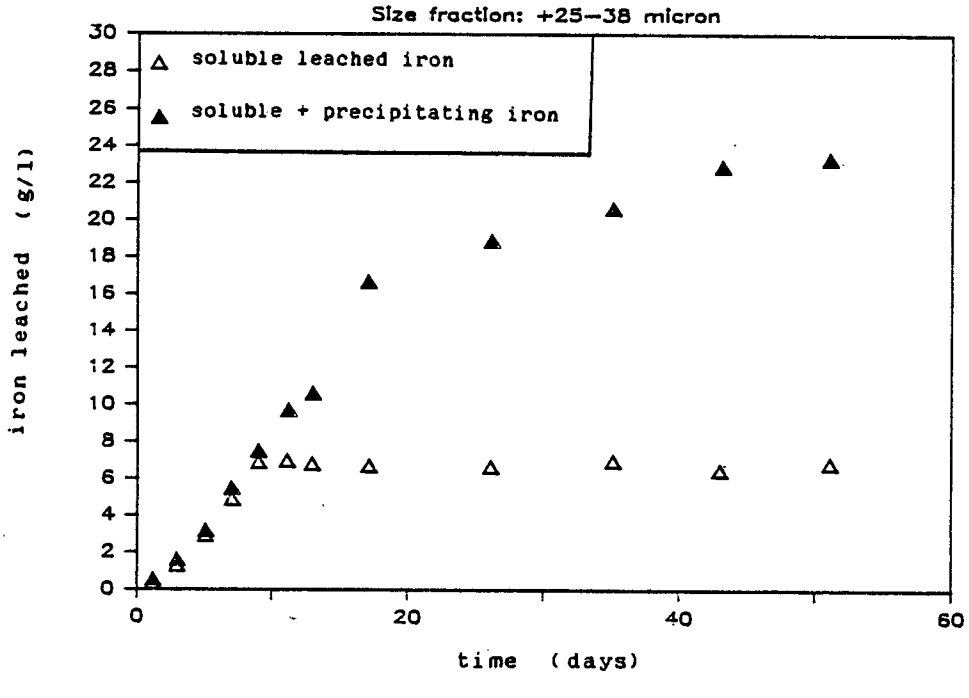

Figure 5.36: Leached iron concentration versus time.

The total iron leached (soluble and precipitating) as well as the soluble iron leached, measured as described in section 4.6.2 are presented in Tables 5.2 to 5.5. These values have been plotted versus time and are shown in Figures 5.33 to 5.36.

These figures show that, at the beginning of the leaching process when the amount of leached iron is still low, essentially all the iron produced remains in solution. As the total amount of leached iron increases, the amount of precipitating iron also increases, while the soluble iron concentration levels off at a constant concentration which is virtually the same for all size fractions (6,5 to 7,0 g/l). The remaining iron concentration in solution depends on the solubility constant of the iron hydroxides and the hydrogen ion activity. This constant concentration value found, seems to be the saturation concentration for ferric ion concentration in solution under the conditions employed.

The effect of the ferric iron produced on the oxidation of pyrite was not examined. Although it is recognised that this issue is of importance it was beyond the scope of this work. A study on the chemical leaching of pyrite by ferric sulphate has been presented by Dutrizac (1974).

5.7 pH versus Time

The pH of the leach suspension was adjusted daily to 1.8, as described in section 4.5. The pH plot versus time is shown in Figure 5.34 for the +25-38 micron size range. Similar graphs were obtained for the other size ranges.

Figure 5.34 shows that during about the first 6 days the pH decreases daily to 1.70 prior to adjustment, while during the next 20 days it was found to decrease to 1.58. Thereafter only minimal adjustment was required. The pH decrease is the result of the sulphuric acid production, which is produced both due to pyrite oxidation and ferric iron precipitation, (see section 2.2).

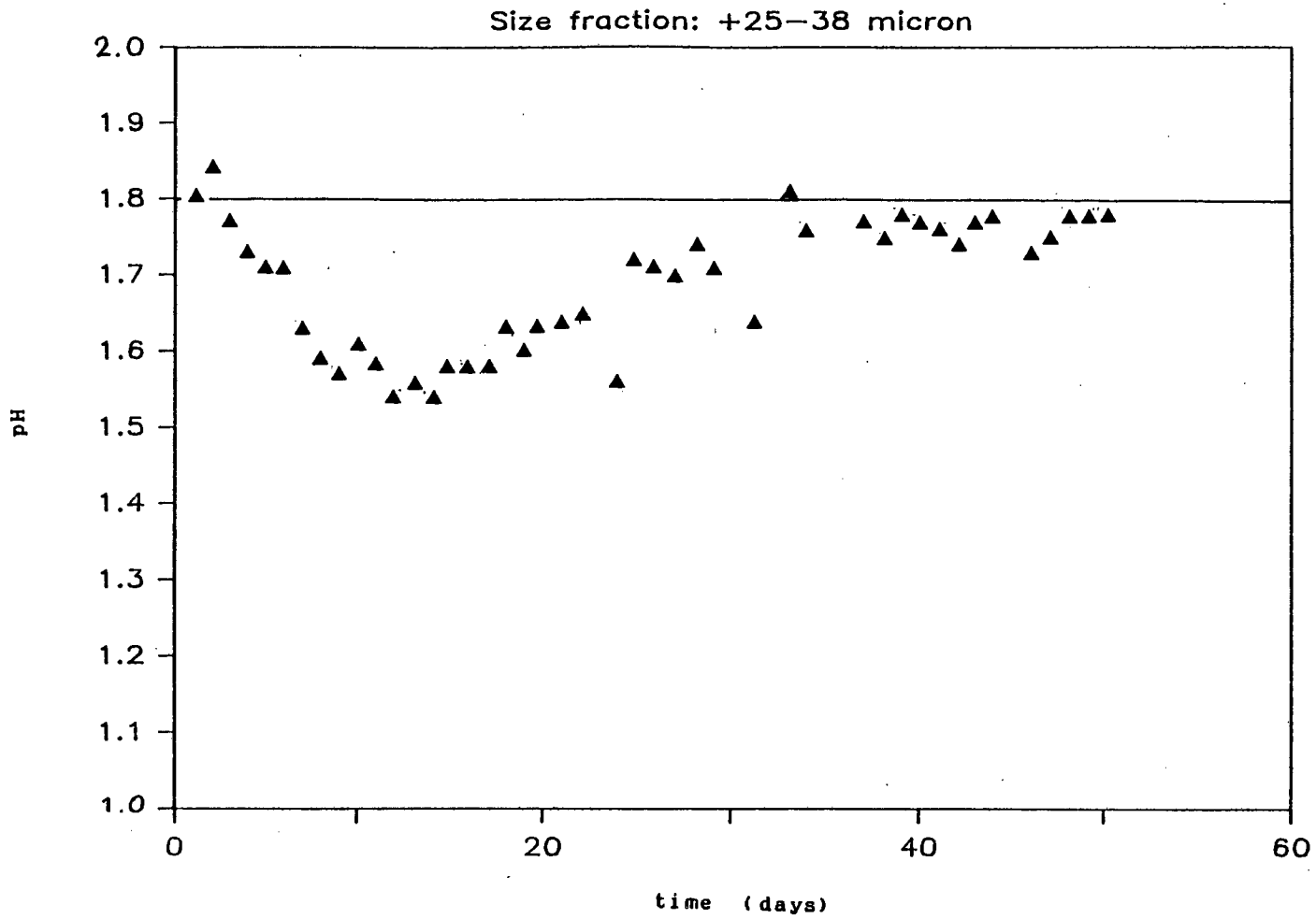

Figure 5.37: pH versus time

The pH decrease of about 0.1 units during the first 6 days of the leaching seems to correspond with the pyrite oxidation only. After this period the iron leached started to precipitate leading to a higher pH decrease until about the 20th day. Thereafter the pyrite leach rate as well as the iron precipitation rate dropped off. Thus the amount by which the pH dropped daily decreased.

5.8. Mass Balance

In order to check the results obtained during the batch leach tests two mass balances were completed. The first consisted of an elemental iron balance and the second an overall mass balance. The results and intermediate calculations of these balances are tabulated in Tables 5.10 to 5.13.

The elemental iron balance was based on the premise that the mass of iron oxidised from the solid residue should be equal to the mass of iron leached into the solution. The ratio between the iron lost by the solids and that gained by the solution should be equal to 1,000. The last column of Tables 5.10 to 5.13 indicates that the ratios were close to 1,000 for all size fractions. Ratios deviating by up to 20% from 1,000 are to be found but these occur at the early stages of the leach where small masses are involved.

The overall mass balance was based on the assumption that the total mass loss of the solids was only due to oxidation of iron and sulphur. The total solids mass loss was then compared to the sum of the iron and sulphur oxidised. The ratio of these values is given in the sixth column of Tables 5.10 to 5.13. Again the ratios calculated are close to 1,000 for most of the samples taken, thus confirming the mass balance.

The ratio of moles of sulphur oxidised to the moles of iron oxidised was calculated and is given in the seventh

column of the tables. It is observed that these values do not lie very close to 2, the stoichiometric ratio for pyrite.

Table 5.10. Mass balance of the +75-106 micron size fraction

leach time days	a mass of sulphur oxidised g (1)	b mass of iron oxidised g (2)	c mass loss g (3)	d mass loss g (4)	ratio (4)/(3)	moles S oxid moles Fe oxid from (1) and (2)	e mass of iron oxidised g (5)	ratio (5)/(2)
0	0,00	0,00	0,00	0,00		1,97	0,00	
10	13,11	11,56	23,73	24,67	1,040	1,98	11,10	0,960
17	23,19	22,69	47,13	45,88	0,974	1,78	23,50	1,036
28	34,90	38,25	72,80	73,15	1,005	1,59	37,72	0,986
37	41,68	40,26	81,47	81,94	1,006	1,81	39,38	0,978
42	45,00	43,06	89,20	88,06	0,987	1,82	43,80	1,017
46	45,87	43,06	92,00	88,93	0,966	1,86	45,26	1,05

a: calculated from the sulphur mass fraction in the feed and the unreacted solid residue.

b: calculated from the iron mass fraction in the feed and the unreacted solid residue.

c: calculated by subtracting the mass of the unreacted solid residue from the mass of the feed.

d: sum of (1) and (2).

e: measured by atomic absorption on the liquors of the acid-washed leach suspension.

Table 5.11. Mass balance of the +53-75 micron size fraction.

leach time days	a mass of sulphur oxidised g (1)	b mass of iron oxidised g (2)	c mass loss g (3)	d mass loss g (4)	ratio (4)/(3)	moles S oxid moles Fe oxid from (1) and (2)	e mass of iron oxidised g (5)	ratio (5)/(2)
0	0,00	0,00	0,00	0,00		1,98	0,00	
4	3,18	5,79	7,40	8,97	1,210	0,96	4,83	0,834
6	5,75	7,69	13,11	13,44	1,025	1,30	6,20	0,806
8	8,34	12,30	22,80	20,64	0,905	1,18	13,31	1,082
10	13,89	15,81	29,40	29,70	1,010	1,53	15,58	0,958
12	19,59	21,45	43,00	41,04	0,954	1,59	20,00	0,932
14	22,75	24,03	47,90	46,78	0,977	1,65	22,93	0,954
19	31,57	30,53	63,00	62,10	0,986	1,80	31,74	1,039
28	43,23	42,94	86,50	86,17	0,996	1,76	40,76	0,949
42	52,00	50,49	102,80	102,49	0,996	1,80	50,82	1,006
46	52,94	50,88	105,84	103,82	0,981	1,81	51,37	1,009

a: calculated from the sulphur mass fraction in the feed and the unreacted solid residue.

b: calculated from the iron mass fraction in the feed and the unreacted solid residue.

c: calculated by subtracting the mass of the unreacted solid residue from the mass of the feed.

d: sum of (1) and (2).

e: measured by atomic absorption on the liquors of the acid-washed leach suspension.

Table 5.12: Mass balance of the +38-53 micron size fraction.

leach time days	a mass of sulphur oxidised g (1)	b mass of iron oxidised g (2)	c mass loss g (3)	d mass loss g (4)	ratio (4)/(3)	moles S oxid moles Fe oxid from (1) and (2)	e mass of iron oxidised g (5)	ratio (5)/(2)
0	0,00	0,00	0,00	0,00		1,98	0,00	
4	2,83	5,45	9,90	8,28	0,836	0,91	5,93	1,088
6	7,18	10,34	21,18	17,52	0,827	1,21	12,00	1,161
8	14,68	18,07	33,98	32,75	0,964	1,42	17,26	0,955
10	18,13	20,96	42,70	39,09	0,915	1,51	19,53	0,932
12	25,06	26,06	54,86	51,12	0,931	1,68	27,18	1,043
14	29,64	30,72	63,23	60,36	0,955	1,68	31,53	1,026
19	38,80	40,09	78,52	78,89	1,005	1,69	38,32	0,956
28	48,80	49,12	98,22	97,92	0,997	1,73	48,60	0,989
37	54,77	53,29	108,36	108,06	0,997	1,79	53,76	1,009
46	59,06	57,04	117,45	116,10	0,989	1,80	57,77	1,013

a: calculated from the sulphur mass fraction in the feed and the unreacted solid residue.

b: calculated from the iron mass fraction in the feed and the unreacted solid residue.

c: calculated by subtracting the mass of the unreacted solid residue from the mass of the feed.

d: sum of (1) and (2).

e: measured by atomic absorption on the liquors of the acid-washed leach suspension.

Table 5.13: Mass balance of the +25-38 micron size fraction.

leach time	a mass of sulphur oxidised	b mass of iron oxidised	c mass loss	d mass loss	ratio (4)/(3)	moles S oxid moles Fe oxid	e mass of iron oxidised	ratio (5)/(2)
days	g (1)	g (2)	g (3)	g (4)		from (1) and (2)	g (5)	
0	0,00	0,00	0,00	0,00		2,05	0,00	
1	0,54		2,20				1,20	
3	6,37	2,73	8,80	9,10	1,034	0,41	3,80	1,392
5	10,63	7,59	19,40	18,22	0,939	2,44	8,13	1,071
7	17,95	13,33	31,90	31,28	0,981	2,35	13,60	1,020
9	24,53	18,20	44,00	42,73	0,971	2,35	18,73	1,029
11	29,77	23,65	54,80	53,42	0,975	2,19	24,50	1,036
13	33,24	24,84	61,80	58,08	0,940	2,33	26,70	1,075
17	47,81	38,53	91,75	86,34	0,941	2,16	41,96	1,089
26	55,69	46,31	105,00	102,00	0,970	2,10	47,20	1,019
35	62,00	50,57	115,20	112,57	0,977	2,14	51,73	1,022
43	66,51	55,58	126,20	122,09	0,967	2,09	57,42	1,033
51	67,89	60,15	128,08	128,04	0,999	1,97	58,32	0,970

a: calculated from the sulphur mass fraction in the feed and the unreacted solid residue.

b: calculated from the iron mass fraction in the feed and the unreacted solid residue.

c: calculated by subtracting the mass of the unreacted solid residue from the mass of the feed.

d: sum of (1) and (2).

e: measured by atomic absorption on the liquors of the acid-washed leach suspension.

CHAPTER 6

CONCLUSIONS AND RECOMMENDATIONS

6.1 Conclusions

The objectives of this work as outlined in Chapter 1. were:

a) to investigate the kinetics of the bioleaching of a refractory gold-bearing pyrite concentrate by deriving mathematical models, and then to test these models against time profile data obtained for four size fractions and,

b) to establish the relationship between sulphide breakdown and corresponding gold liberation during the batch bacterial tests.

The observations and conclusions from this work can be summarised as follows:

1. The total-sulphur oxidation of the pyrite concentrate during the batch tests was found to be linearly dependent on time during the early stages of leaching, i.e for about the first 10 to 15 days depending on particle size. After this period the oxidation rate dropped off slowly, so that after the 46th day 36% to 52% of the total-sulphur had oxidised depending on the particle size .

2. The rate and extent of total-sulphur oxidation was found to increase with decreasing particle size.

3. A propagating-pore model for the bioleaching of ores was derived and tested against the experimental batch leach data. The model gave a reasonably good fit to the experimental data.

4. Examination of feed material, bacterial leach residues and sterile leach residues in the SEM, showed a highly

leached texture only in the bacterial leach residues. Pore development was characteristic of this texture and this evidence supports the above mentioned propagating-pore mechanism for the bioleaching of ores.

5. A shrinking-particle model for the bioleaching of ores was also derived and tested against the batch leach data. This model did not give a good fit to the experimental data.

6. Calculation of the surface oxidation rate in this study suggested that it may be independent of particle size or surface area concentration for a particular ore. Data from the literature was used to calculate the surface oxidation rates for other ores. These data confirm that the surface oxidation rate is independent of surface area concentration (at least over a range of surface area concentrations), thus suggesting that the surface oxidation rate may be a useful parameter of characterising the leaching behaviour of ores.

7. The relationship between gold liberation and total-sulphur oxidation was non-linear, the sulphur oxidation being much lower than the gold liberation. This relationship appeared to be independent of particle size. A 90% gold liberation was achieved for about 30% sulphur oxidation, after which no more gold was liberated.

8. The higher gold liberation is probably due to preferential bacterial attack along dislocations in the pyrite crystal, where fine discrete gold particles are suspected to be located.

9. The free bacterial population initially inoculated at a concentration of $1,0 \times 10^{6}$ cells/ml, reached its maximum concentration of about $2,8 \times 10^{9}$ cells/ml after about 8 days of active growth. This concentration, approximately the same for all size fractions, did not change significantly during the rest of the leach.

10. Only a portion of the iron leached remained in solution the rest precipitating probably as jarosite. The iron concentration in solution reached a maximum of about 7g/l for all size fractions, after which it remained constant throughout leaching.

6.2 Recommendations

Future research work must take into consideration the following:

1. The kinetic models that were derived in this study need to be applied to a wide range of sulphide ores and particle size fractions, so that the models' validity can be checked and possible alterations made.

2. The propagating-pore model derived is a crude model in so far as its treatment of the pore length distribution and pore deactivation. A more elaborate development of the model is needed.

3. Careful thought needs to be given to the surface area determination method used for the calculation of surface oxidation rates.

4. The sterile tests in this work showed that partial gold liberation occurred due to the particles' breakage caused by the mechanical agitation. Any future workers aiming to quantitatively examine bacterial gold liberation should ensure that an agitation system that causes the least possible particle breakage is employed.

5. A shortcoming of this work was the absence of data on the attached bacteria numbers. The attached bacteria growth needs to be measured together with the free bacteria growth, so that the role of free and attached bacteria in the oxidation of sulphide minerals can be elucidated.

6. The use of the SEM in this work showed that observations of the leach residues at a high magnification can provide very useful information on the leaching behavior of ores. It therefore becomes evident that any fundamental research work on the bacterial leaching of minerals needs to be supplemented by microscopic and mineralogical observations of the ore before and after leaching, so that leaching mechanisms can be elucidated.

REFERENCES

ATKINS, A.S. (1978), Studies on the Oxidation of Sulphide Minerals (Pyrite) in the Presence of Bacteria. In L.E. MURR, A.E. TORMA and J.A. BRIERLEY (Eds) Metallurgical Applications of Bacterial Leaching and Related Microbiological Phenomena. Academic Press, New York, 403-426.

AMELINCKX, S. (1964), The Direct Observations of Dislocations. In F. SEITZ and D. TURNBULL (Eds), Solid State Physics, 6, Academic Press.

BALDENSPERGER, J., L.J. GUARRAIA and W.J. HUMPHREYS (1974), Scanning Electron Microscopy of Thiobacilli Grown on Colloidal Sulphur. Arch. Microbiol., 99, 323-329.

BENNETT, J.C. and H. TRIBUTSCH (1978), Bacterial Leaching Patterns on Pyrite Crystal Surfaces. J. Bacteriol., 134, (1), 310-317.

BERRY, V.K. and L.E. MURR (1978), Direct Observations of Bacteria and Quantitative Studies of their Catalytic Role in the Leaching of Low-Grade, Copper-Bearing Waste. In L.E. MURR, A.E. TORMA and J.A. BRIERLEY (Eds), Metallurgical Applications of Bacterial Leaching and Related Microbiological Phenomena. Academic Press, New York, 103-135.

BLANCARTE-ZURITA, M.A., R.M.R. BRANION and R.W. LAWRENCE (1985), Application of a Shrinking Particle Model to the Kinetics of Microbiological Leaching. Paper presented at the 5th International Symposium on Biohydrometallurgy, Vancouver (August 1985).

BOYLE, R.W. (1979), The Geochemistry of Gold and its Deposits. Geol. Surv. Can. Bull., 280, 584.

BRIERLEY, C.L. (1977), Thermophilic Microorganisms in Extraction of Metals from Ores. Dev. Ind. Microbiol., 18, 273.

BRIERLEY, C.L. (1978), Bacterial Leaching. CRC Crit. Rev. Microbiol., 6, (3), 207-262.

BRIERLEY, C.L. (1982), Microbiological Mining. Sci. Am. 247, 42-51.

BROCK, T.D., K.M. BROCK, R.T. BELLY and R.L. WEISS (1972), Sulpholobus: A New Genus of Sulphur-Oxidising Bacteria Living at Low pH and High Temperature. Arch. Mikrobiol., 84, 54-68.

BRUYNESTEYN, A. (1984), Bioleaching of Refractory Gold-Silver Ores and Concentrates. Paper presented at the 14th Annual CIM Hydrometallurgical Meeting, Ontario (October 1984).

BRUYNESTEYN, A. and D.W. DUNCAN (1971), Microbiological Leaching of Sulphide Concentrates. Can. Metall. Q., 10, 57.

BRUYNESTEYN, A. and D.W. DUNCAN (1974), Effect of Particle Size on the Microbiological Leaching of Chalcopyrite Bearing Ore. In F.F. APLAN, W.A. McKINNEY and A.D. PERNICHELE (Eds), Solution Mining Symposium 1974. The American Institute of Mining, Metallurgical and Petroleum Engineers, New York, 324-337.

BRYNER, L.C. and R. ANDERSON (1957), Microorganisms in Leaching Sulphide Minerals. Ind. Eng. Chemistry, 49, (10), 1721-1724.

BURTON, C., S. COWMAN, J. HEFFERNAN and B. THORNE (1983), In-Situ Bioleaching of Sulphide Ores at Avoca, Ireland. Part 1 - Development, Characterisation and Operation of a Medium Scale (6000 t) Experimental Leach Site. In G. ROSSI and A. E. TORMA (Eds), Recent progress in biohydrometallurgy. Associazione Mineraria Sarda, Italy, 213-241.

CHANG, Y.C. and A.S. MYERSON (1982), Growth Models of the Continuous Bacterial Leaching of Iron Pyrite by Thiobacillus ferrooxidans. Biotechnol. Bioeng., 24, 889-902.

CHANT, K. (1975), Gold Recovery from Refractory Arsenopyrite by Roasting, Bacterial Leaching and Sodium Carbonate Pressure Leaching. Report to Charter Consolidated Limited, (July 1975).

COLMER, A.R. and M.E. HINKLE (1947), The Role of Microorganisms in Acid Mine Drainage: a Preliminary Report. Science, 106, 253-256.

CORRANS, I.J. (1974), Kinetic and Mechanistic Studies on the Biological and Chemical Leaching of Nickel from Sulphide Ores. Ph.D Thesis, University of Natal, South Africa.

CORRANS, I.J., B. HARRIS and B.J. RALPH (1972), Bacterial Leaching: an Introduction to its Application and Theory and a Study on its Mechanism of Operation. J. S. Afr. Inst. Min. Metall., 72, 221-230.

DISPIRITO, A.A. and O.H. TUOVINEN (1982), Kinetics of Uranous Ion and Ferrous Iron Oxidation by Thiobacillus ferrooxidans. Arch. Microbiol. 133, 33-37.

DUGAN, P.R. and W.A. APEL (1978), Microbiological Desulphurisation of Coal. In L.E MURR, A.E. TORMA and J.A. BRIERLEY (Eds), Metallurgical Applications of Bacterial Leaching and Related Microbiological Phenomena. Academic Press, New York, 223-250.

DUNCAN, D.W. and A.D. DRUMMOND (1973), Microbiological Leaching of Porphyry Copper Type Mineralization: Post-Leaching Observations. Can. J. Earth Sci., 10, 476-484.

DUNCAN, D.W., J. LANDESMAN and C.C. WALDEN (1967), Role of Thiobacillus ferrooxidans in the Oxidation of Sulphide Minerals. Can. J. Microbiol., 13, 397-403.

DUNCAN, D.W., C.C. WALDEN and P.C. TRUSSELL (1966), Biological Leaching of Mill Products. Can. Min. Metall. Bull., 59, 1075-1079.

DUTRIZAC, J.E. (1974), Ferric Ion as a Leaching Medium. Miner. Sci. Eng., 6, 69-100.

EHRLICH, H.L. (1963), Bacterial Action on Orpiment. Econ. Geol., 58, 991-994.

EHRLICH, H.L. and S.I. FOX (1967), Environmental Effects on Bacterial Copper Extraction from Low-Grade Copper Sulphide Ores. Biotechnol. Bioeng., 9, 471-485.

ERICKSON, L.E., L.T. FAN, P.S. SHAH and M.S.K. CHEN (1970), Growth Models of Cultures with two Liquid Phases: 4. Cell Adsorption, Drop Size Distribution and Batch Growth. Biotechnol. and Bioeng., 12, 713-746.

FISCHER, J.R. (1966), Bacterial Leaching of Elliot Lake Uranium Ore. Can Min Metall Bull., 59, 588-592.

GORMELLY, L.S. (1973), Continuous Microbiological Leaching of a Zinc Sulphide Concentrate. Ph.D Thesis, University of British Columbia, Vancouver.

GORMELLY, L.S. and D.W. DUNCAN (1974), Estimation of Thiobacillus ferrooxidans Concentrations. Can. J. Microbiol., 20, 1453.

GORMELY, L.S., D.W. DUNCAN, R.M.R. BRANION and K.L. PINDER (1975), Continuous Culture of Thiobacillus ferrooxidans on a Zinc Sulphide Concentrate. Biotechnol. Bioeng., 17, 31-49.

GROUDEV, S.N. (1979), Mechanism of the Bacterial Oxidation of Pyrite. MiKrobioloiia. no.1, 75-87.

GROUDEV, S.N. (1982), Leaching of Nickel from Sulphide Minerals by Pure and Mixed Cultures of Chemolithotrophic Bacteria. Dokl. Bolg. Akad. Nauk., 35, (8), 1113-1116.

GROUDEV, S.N., F.N. GENCHEV and S.S. GAIDARJIEV (1978), Observations on the Microflora in an Industrial Copper Dump Leaching Operation. In L.E. MURR, A.E. TORMA and J.A BRIERLEY (Eds), Metallurgical Applications of Bacterial Leaching and Related Microbiological Phenomena. Academic Press, New York, 253-274.

GUAY, R., M.SILVER and A.E. TORMA (1976), Microbiological Leaching of a Low-Grade Uranium Ore By Thiobacillus ferrooxidans. Eur. J. Appl. Microbiol., 3, 157-167.

HARRISON, V.F., W.A. GOW and M.R. HUGHSON (1966), 1. Factors Influencing the Application of Bacterial Leaching to a Canadian Uranium Ore. J. Met., 18, 1189-1194.

HENLEY, K.J. (1975), Gold-Ore Mineralogy and its Relation to Metallurgical Treatment. Miner. Sci. Eng., 7, (4), 289-312.

HERBERT, D., R. ELSWORTH and R.C. TELLING (1956), The Continuous Culture of Bacteria: a Theoretical and Experimental study. J. Gen. Microbiol., 14, 601-622.

IMAI, K. (1978), On the Mechanism of Bacterial Leaching. In L.E. MURR, A.E. TORMA and J.A. BRIERLEY (Eds), Metallurgical Applications of Bacterial Leaching and Related Microbiological Phenomena. Academic Press, New york, 275-295.

IVARSON, K.C. (1973), Microbiological Formation of Basic Ferric Sulphates. Can. J. Soil Sci., 53, 315-323.

KARAIVKO, G.I., S.I. KUZNETSOV and A.I. GOLONIZIK (1977), (Eds), The Bacterial Leaching of Metals from Ores. Technicopy Ltd, England.

KARGI, F. and J.G. WEISSMAN (1984), A Dynamic Mathematical Model for Microbial Removal of Pyritic Sulphur from Coal. Biotechnol. Bioeng., 26, 604-612.

KELLY, D.P., P.R. NORRIS and C.L. BRIERLEY (1979), Microbiological Methods for the Extraction and Recovery of Metals. In A.T. BULL, D.C. ELLWOOD and C. RUTLEDGE (Eds), Microbial Technology: Current State, Future Prospects. 29th Symposium of the Society of General Microbiology, 263-308.

LAU, C.M., K.S. SHUMATE and E.E. SMITH (1970), The Role of Bacteria in Pyrite Oxidation Kinetics. 3rd Symposium on Coal Mine Drainage Research, Mellon Institute, Pittsburg.

LAWRENCE, R.W. (1974), Bacterial Extraction of Metals from Sulphide Concentrates. Ph.D Thesis, University of Wales, Cardiff.

LAWRENCE, R.W. and A. BRUYNESTEYN (1983), Biological Pre-Oxidation to Enhance Gold and Silver Recovery from Refractory Pyritic Ores and Concentrates. CIM Bull., 76, (857), 107-110.

LAWRENCE, R.W. and J.D. GUNN (1985), Biological Pre-oxidation of Pyritic Gold Concentrate. Paper presented at the A.I.M.E. Annual Meeting, New York (February 1985).

LENISOV, G.V., B.G. KOVROV, I.N. TRUBACHEF, I.V. GRIBOVSKAYA, A.A. STEPEN and O.I. NOVOSELOVA (1980), Composition of a Growth Medium for Continuous Cultivation of Thiobacillus ferrooxidans. Microbiol. 49, 341-345.

LE ROUX, N.W., A.A. NORTH and J.C. WILSON (1973), Bacterial oxidation of Pyrite. Paper presented at the 10th International Mineral Processing Congress, London.

LEVENSPIEL, O. (1972), Chemical Reaction Engineering. John Willey and Sons, USA.

LIVESEY-GOLDBLATT, E., P. NORMAN and D.R. LIVESEY-GOLDBLATT (1983), Gold Recovery from Arsenopyrite/Pyrite Ore by Bacterial Leaching and Cyanidation. In G. ROSSI and A.E. TORMA (Eds), Recent Progress in Biohydrometallurgy. Associazone Mineraria Sarda, Italy, 627-641.

LUNDGREN, D.G. and E.E. MALOUF (1983), Microbial Extraction and Concentration of Metals. Advan. Biotechnol. Processes, 1, 223-249.

MALOUF, E.E. and J.D. PRATER (1961), Role of Bacteria in the Alteration of Sulphide Minerals. J. Met., 13, 353-356.

MARCHANT P.B. (1985), Continuous Vat Biooxidation of a Refractory Arsenical Sulphide Concentrate. Paper presented at the 17th Canadian Mineral Processors Conference, Ottawa (January 1985).

McELROY, R.O. and A. BRUYNESTEYN (1978), Continuous Biological Leaching of Chalcopyrite Concentrates: Demonstration and Economic Analysis. In L.E. MURR, A.E. TORMA and J.A. BRIERLEY (Eds), Metallurgical Applications of Bacterial Leaching and Related Microbiological Phenomena. Academic Press, New York, 441-462.

McGORAN, C.J.M., D.W. DUNCAN and C.C. WALDEN (1969), Growth of Thiobacillus ferrooxidans on Various Substrates. Can. J. Microbiol., 15, 135-138.

MILLER, R.P., E. NAPIER, R.A. WELLS, A. AUDSLEY, G.R. DABORN (1963), Natural Leaching of Uranium Ores. Trans. Inst. Min. Metall., 72, 217-254.

MIRONOV, A.G., S.M. ZHMODIK and E.A. MAKSIMOVA (1981), An Experimental Investigation of the Sorption of Gold by Pyrites with Different Thermoelectric Properties. Geochem. Int., 18, (2), 153-160.

MONOD, J. (1949) The Growth of Bacterial Cultures. Ann. Rev. Microbiol., 3, 371-394.

MURR, L.E. and V.K. BERRY (1976), Direct Observations of Selective Attachment of Bacteria on Low-Grade Sulphide Ores and Other Mineral Surfaces. Hydrometall., 2, 11-24.

MYERSON, A.S. and P.C. KLINE (1984), Continuous Bacterial Coal Desulphurisation employing Thiobacillus ferrooxidans. Biotechnol. Bioeng., 26, 92-99.

NELDER, J.A. and R. MEAD (1965), A Simplex Method for Function Minimisation. Comput. J., 5, 308-313.

NORRIS P.R. and L. PARROTT (1985), High Temperature, Mineral Concentrate Dissolution with Sulpholobus. Paper presented at the 5th International Symposium on Biohydrometallurgy, Vancouver (August 1985).

PENMAN, D.W. (1985), Metallurgical Aspects of the Treatment of Refractory Ores from Barberton. Paper presented at the 5th International Symposium on Biohydrometallyrgy, Vancouver (August 1985).

PINCHES, A. (1972), The Role of Microorganisms for the Recovery of Metals from Mineral Materials. Ph.D Thesis, University of Wales, Cardiff.

PINCHES, A., F.O. AL-JAID and D.J.A. WILLIAMS (1976), Leaching of Chalcopyrite Concentrates with Thiobacillus ferrooxidans in Batch Culture. Hydrometall., 2, 87-103.

POLKIN, S.I., G.I. KARAVAIKO, Z.A. TAUZHNYANSKAYA and V.V. PANIN (1970), Bacterial Selective Extraction of Arsenic and Copper from Oxidised Sulphide Tin Concentrates (Engl. transl.). 9th International Mineral Processing Congress, Prague, 347.

RAWLINGS, D.E. (1981), Nutritional Requirements of the Microorganisms Active in the Oxidation of Ferrous Iron in Acid Mine Leach Liquors. J. Appl. Bacteriol., 51, 267-276.

RANGACHARI, P.N., V.S. KRISHNAMACHAR, S.G. PATIL, M.N. SAINANI and H. BALAKRISHNAN (1978), Bacterial Leaching of Copper Sulphide Ores. In L.E. MURR, A.E. TORMA and J.A. BRIERLEY (Eds), Metallurgical Applications of Bacterial Leaching and Related Microbiological Phenomena. Academic Press, New York, 427-439.

RAZZELL, W.E. and P.C. TRUSSELL (1963), Microbiological Leaching of Metallic Sulphides. Appl. Microbiol., 11, 105-110.

RENNER, C.W., M.T. ERRINGTON and F.D. POOLEY (1984), Economics of Bacterial Lleaching. Paper presented at the 23rd Annual Conference of Metallurgists, Quebec (August 1984).

SAKAGUCHI, H., A.E. TORMA and M. SILVER (1976), Microbiological Oxidation of Synthetic Chalcocite and Covellite by Thiobacillus ferrooxidans. Appl. Environ. Microbiol., 31, 7.

SANMMUGASUNDERAM, V. (1981), Kinetic Studies on the Biological Leaching of a Zinc Sulphide Concentrate in two Stages Continuous Stirred Tank Reactors. Ph.D Thesis, University of British Columbia, Vancouver.

SANMUGASUNDERAM, V., R.M.R. BRANION and D.W. DUNCAN (1985), A Growth Model for the Continuous Microbiological Leaching of a Zinc Sulphide Concentrate by Thiobacillus ferrooxidans. Paper presented at the 5th International Symposium on Biohydrometallurgy, Vancouver (August 1985).

SCHAEFFER, W.I., P.E. HOLBERT and W.W. UMBREIT (1963), Attachment of Thiobacillus thiooxidans to Sulphur Crystals. J. Bacteriol., 85, 137-140.

SCHWARTZ, G.M. (1944), The Host Minerals of Native Gold. Econ. Geol., 39, 371-411.

SILVERMAN, M.P. (1967), Mechanism of Bacterial Pyrite Oxidation. J. Bacteriol., 94, (4), 1046-1051.

SILVERMAN, M.P. and H.L. EHRLICH (1964), Microbial Formation and Degradation of Minerals. Advan. Appl. Microbiol., 6, 153-206.

SILVERMAN, M.P. and D.G. LUNDGREN (1959), Studies on the Chemoautotrophic Iron Bacterium Ferrobacillus ferrooxidans, 1. An Improved Medium and a Harvesting Procedure for Securing High Cell Yields. J. Bacteriol., 77, 642.

SILVERMAN, M.P., M.H. ROGOFF and I. VENDER (1961), Bacterial Oxidation of Pyritic Materials in Coal. Appl. Microbiol. 9, 491-496.

SOROKIN, V.N. and G.V. LOMAKIN (1971), Auriferous Mineral Associations of Mindyak Ore Field (Trans.). Inter. Geol. Rev., 13, (5), 752-759.

SOUTHWOOD, M.J. (1985), The Mode of Occurrence of Gold in Pyrite and Arsenopyrite and its Implications for the Release of Gold during Bacterial Leaching. Technical Memorandum, no. 13255, MINTEK, Randburg, South Africa.

SOUTHWOOD, M.J. (1986), Personal communication.

SOUTHWOOD, M.J. and A.J. SOUTHWOOD (1985), Mineralogical Observations on the Bacterial Leaching of Auriferous Pyrite: A New Mathematical Model and Implications for the Release of Gold. Paper presented at the 5th International Symposium on Biohydrometallurgy, Vancouver (August 1985).

TORMA, A.E. (1977), The Role of Thiobacillus ferrooxidans in Hydrometallurgical Processes. In T.K. GHOSE, A. FIECHTER and

N. BLAKEBROUGH (Eds), Advances in Biochemical Engineering. New substrates. Springer-Verlag, New York, 6, 1-37.

TORMA, A.E. (1978), Complex Lead Sulphide Concentrate Leaching by Microorganisms. In L.E. MURR, A.E. TORMA and J.A BRIERLEY (Eds), Metallurgical Applications of Bacterial Leaching and Related Microbiological Phenomena. Academic Press, New York, 375-387.

TORMA, A.E. and K.N. SUBRAMANIAN (1974), Selective Bacterial Leaching of a Lead Sulphide Concentrate. Int. J. Miner. Process., 1, 125-134.

TORMA, A.E., C.C. WALDEN and R.M.R. BRANION (1970), Microbiological Leaching of a Zinc Sulphide Concentrate. Biotechnol. Bioeng., 12, 501-517.

TORMA, A.E., C.C. WALDEN, D.W. DUNCAN and R.M.R. BRANION (1972), The Effect of Carbon Dioxide and Particle Surface Area on the Microbiological Leaching of a Zinc Sulphide Concentrate. Biotechnol. Bioeng., 14, 777-786.

TUOVINEN, O.H. and D.P. KELLY (1972), Biology of Thiobacillus ferrooxidans in Relation to the Microbiological Leaching of Sulphide Ores. Z. Allg. Mikrobiol., 12, 311-346.

TUOVINEN, O.H., S.I. NIEMELA and H.G. GYLLENBERG (1971), Effect of Mineral Nutrients and Organic Substances on the Development of Thiobacillus ferrooxidans. Biotechnol. Bioeng., 13, 517-527.

VAN WYK, E and K. DIXON (1983), The Recovery of Platinum Group Metals and Gold by the Lead-Collection Step of the Fire-Assay Procedure. Report M88, MINTEK, Randburg, South Africa.

VOGEL A.I. (1961), Quantitative Inorganic Analysis. Longmans, 309

VOGLER, K.G. and W.W. UMBREIT (1941), The Necessity for Direct Contact in Sulphur Oxidation by Thiobacillus Thiooxidans. Soil. Sci., 51, 331-337.

WAKAO, N., M. MISHINA, Y. SAKURAI and H. SHIOTA (1982), Bacterial Pyrite Oxidation. 1. The Effect of Pure and Mixed Cultures of Thiobacillus ferrooxidans on Release of Iron. J. Gen. Appl. Microbiol., 28, (4), 331-343.

WAKAO, N., M. MISHINA, Y. SAKURAI and H. SHIOTA (1984), Bacterial Pyrite Oxidation. 3. Adsorption of Thiobacillus ferrooxidans Cells on Solid Surfaces and its Effect on Iron Release from Pyrite. J. Gen. Appl. Microbiol., 30, (1), 63-77.

WEISS, R.L. (1973), Attachment of Bacteria to Sulphur in Extreme Environments. J. Gen. Microbiol., 77, 501-507.

APPENDIX A

Nickel and Copper Analyses of the Unreacted Solid Residue

Table A1: size fraction +75-106 micron

leach time days	nickel conc. in solid residue g/t	copper conc. in solid residue g/t
0	1380	980
10	1200	1000
17	1300	1100
28	1000	1200
37	1700	1300
42	1700	1400
46	1400	1300

Table A2: size fraction +53-75 micron

leach time days	nickel conc. in solid residue g/t	copper conc. in solid residue g/t
0	1790	1200
4	1300	1000
6	1400	1000
8	1400	1000
10	1200	1100
12	1100	1200
14	1200	1200
19	1100	1200
28	1100	1400
42	1100	1500
46	840	1500

Nickel and Copper Analyses of the Unreacted Solid Residue

Table A3: size fraction +38-53 micron

leach time days	nickel conc. in solid residue g/t	copper conc. in solid residue g/t
first series of batch experiments		
0	2135	1350
4	1500	1100
6	1300	1200
8	1100	1060
10	1300	1380
12	1400	1400
14	1500	1600
second series of batch experiments		
0	2140	1270
14	1500	1456
19	1290	1880
28	1150	2070
37	1100	1700
46	1000	1600

Table A4: size fraction +25-38 micron

leach time days	nickel conc. in solid residue g/t	copper conc. in solid residue g/t
first series of batch experiments		
0	1100	670
1	910	360
3	850	370
5	800	390
7	770	410
9	780	420
11	780	440
13	740	450
second series of batch experiments		
0	1390	479
13	878	536
17	811	658
26	766	693
35	727	737
43	765	855
51	830	830

APPENDIX B

Nelder-Mead Optimisation Program and Known Parameters of the System

The Nelder-Mead optimisation routine was used in a program to estimate the model parameters. The program for each model is given on pages 144 to 149.

In both models the known parameters were:
- the initial particle diameter of the size fraction, d_0, and
- the sulphur density in the concentrate, ρ_s.

The initial particle diameter was taken to be equal to the arithmetic mean particle diameter of each size fraction. Since the size fractions had been narrowly sized the arithmetic mean is expected to give a reasonable approximation to the particle diameter. The arithmetic mean values are given in Table B1:

Table B1: Arithmetic mean particle diameter and inverse mean particle diameter of the four size fractions.

size fraction micron	arithmetic mean particle diameter, d0 m $x10^6$	inverse mean particle diameter, 1/d0 m^{-1}
+75-106	90,5	11049
+53-75	64,0	15625
+38-53	45,5	21978
+25-38	31,5	31746

The sulphur density in the concentrate is defined as the amount of sulphur per unit volume of the concentrate. This

is calculated by multiplying the mass fraction of sulphur in the concentrate by the density of the concentrate. The density of each concentrate calculated as described in Section 4.7 is given in Table B2:

Table B2: Density of the four size fractions.

size fraction micron	density of the concentrate kg m^{-3}
+75-106	4859,0
+53-75	4964,0
+38-53	4940,6
+25-38	4970,2

The sulphur density in the concentrate is given in Table B3. The parameter K INPUTed in the program is the product ρ_s d_o and its value for each size fraction is also given in Table B3.

Table B3: Sulphur density in the concentrate and the product ρ_s d_o.

size fraction micron	sulphur density in the concentrate ρ_s kg m^{-3}	product $\rho_s \times d_o$ kg m^{-2}
+75-106	2439,2	0,221
+53-75	2509,3	0,161
+38-53	2521,9	0,115
+25-38	2584,3	0,081

```
080 GOTO 560
090 FOR J = 1 TO N2
100 X(IW,J) = X(N2+5,J)
110 NEXT J
120 F(IW) = F(N2+5)
130 GOTO 560
140 REM * OUTPUT DATA *
150 CLS : LOCATE 10,1:PRINT STRING$(80," ")
160 LOCATE 2,1 : PRINT "TIME (DAYS)" : LOCATE 2,20: PRINT "FRACTION"
170 FOR I = 1 TO N:P=3+I
180 LOCATE P,1 :PRINT T(I) :PRINT B$ : LOCATE P,20 :PRINT R(I)
190 NEXT I
200 LOCATE 16,10 :PRINT " MIN = ";F(IB)
210 LOCATE 18,10 :PRINT " RATE = ";X(IB,1)
220 LOCATE 16,40 :PRINT " TI = ";X(IB,2)
230 LOCATE 18,40 :PRINT " TE = ";X(IB,3)
240 LOCATE 20,10:PRINT "LAG=";X(IB,4)
250 LOCATE 2,40 :PRINT "PRED. FRACTION "
260 I=IB : GOSUB 1490
270 FOR J = 1 TO N
280 LOCATE 3+J,45 :PRINT RR(J)
290 NEXT J
300 LOCATE 22,1
310 INPUT "TO LINE PRINTER Y/N ",A$
320 IF A$="N" OR A$="n" THEN 1470
330 LPRINT TAB(1) "TIME (DAYS)" ;
340 LPRINT TAB(20) "FRACTION     ";
350 LPRINT TAB(40) "PRED. FRACTION"
360 FOR I = 1 TO N:P=3+I
370 LPRINT TAB(1) T(I) ;
380 LPRINT TAB(20) ;
390 LPRINT USING "##.####" ;R(I);
400 LPRINT TAB(45);
410 LPRINT USING "##.####" ;RR(I)
420 NEXT I
430 LPRINT " " : LPRINT " "
440 LPRINT TAB(18) " MIN = ";F(IB)
450 LPRINT TAB(18) "RATE = ";X(IB,1)
460 LPRINT TAB(18) "LAG  = ";X(IB,2)
470 END
480 REM * CALCULATE PREDICTED FRACTIONS *
490 RATE = X(I,1) : TI = X(I,2) : TE = X(I,3):LAG=X(I,4) :ER=0
500 IF TE < 0 GOTO 1530 : IF TI < 0 GOTO 1530
510 IF TE<1 GOTO 1530
520 GOTO 1540
530 F(I) = 1E+08 : GOTO 1620
540 FOR J = 1 TO N
550 IF T(J) <=TI THEN RR(J) =6*(RATE/K)*(T(J)-LAG)
560 IF TI<T(J) AND T(J)<TE THEN RR(J)=6*(RATE/K)*((T(J)-LAG)-(T(J)-TI)^2/(2*(T
TI)))
570 IF T(J)>=TE THEN RR(J)=6*(RATE/K)*(TI+TE-2*LAG)/2
580 E1(J)=(RR(J)-R(J))^2
590 ER = ER + E1(J)
600 NEXT J
610 F(I) = ER
620 RETURN
```

```
40 NEXT I
50 FOR J = 1 TO N2
60 X(N2+2,J) = 0
70 FOR I = 1 TO N2 +1
80 X(N2+2,J) = X(N2+2,J) + X(I,J)
90 NEXT I
00 X(N2+2,J) = (X(N2+2,J) - X(IW,J)) / FL
10 NEXT J : I = N2+2
20 GOSUB 1380
30 EP = 0
40 FOR I = 1 TO N2 + 1
50 EP = EP + (F(I)-F(N2+2))*(F(I)-F(N2+2))
60 NEXT I
70 EP = SQR((EP-(F(IW)-F(N2+2))*(F(IW)-F(N2+2)))/FL)
80 IF EP < .00001 GOTO 1090
90 FOR J = 1 TO N2
00 X(N2+3,J) = X(N2+2,J) +AL * (X(N2+2,J) - X(IW,J))
10 NEXT J : I = N2 +3
20 GOSUB 1380
30 IF F(N2+3) > F(IW) GOTO 760
40 IF F(N2+3) > F(IB) GOTO 790
50 GOTO 930
60 FOR J = 1 TO N2
70 X(N2+4,J) = X(N2+2,J)-BT*(X(N2+2,J)-X(IW,J))
80 NEXT J :I = N2 + 4 : GOTO 820
90 FOR J = 1 TO N2
00 X(N2+4,J) = X(N2+2,J)- BT*(X(N2+2,J) - X(N2+3,J))
10 NEXT J : I = N2 +4
20 GOSUB 1380
30 IF F(N2+4) > F(IW) GOTO 880
40 FOR J = 1 TO N2
50 X(IW,J) = X(N2+4,J)
60 NEXT J
70 F(IW) = F(N2+4) : GOTO 500
80 FOR I = 1 TO N2+1
90 FOR J = 1 TO N2
00 X(I,J) =( X(I,J) + X(IB,J))/2
10 NEXT J : NEXT I
20 GOTO 470
30 FOR J = 1 TO N2
40 X(N2+5,J) = X(N2+2,J) + GM * (X(N2+3,J)-X(N2+2,J))
50 NEXT J :I = N2+5
60 GOSUB 1380
70 IF F(N2+5) < F(IB) GOTO 1030
80 FOR J = 1 TO N2
90 X(IW,J) = X(N2+3,J)
000 NEXT J
010 F(IW) = F(N2+3)
020 GOTO 500
030 FOR J = 1 TO N
040 X(IW,J) = X(N2+5,J)
050 NEXT J
060 F(IW) = F(N2+5)
070 GOTO 500
```

APPENDIX C

Calculation of Geometrical and BET Surface Area Concentration

The geometrical surface area concentration of each size fraction was calculated using the formula:

$$\text{surface area concentration} = \frac{6\ c_o}{\rho_p\ d_o}$$

where: $c_o = 250/2500\ (g/cm^3) = 100\ kg/m^3$
ρ_p is given in Table B2 and
d_o is given in Table A1

The calculated values of geometrical surface area concentration are given in Table 5.7.

The BET surface area concentration was calculated from the BET surface area measurements given in Table C3. These values are given in Table 5.7.

Table C: BET surface area measurements.

size fraction micron	BET surface area $m^2\ g^{-1}$
+75-106	0,0850
+53-75	0,1500
+38-53	0,2500
+25-38	0,1000

APPENDIX D

Change of the Particle Size Distribution with Time

Table D1: Change of the size distribution with time.
Size fraction +75-106 micron.

leach time days	+106 micron mass %	+75-106 micron mass %	+53-75 micron mass %	+38-53 micron mass %	-38 micron mass %
10	0,4	65,6	30,4	2,0	1,6
17	2,0	63,6	29,2	3,1	2,5
28	0,7	46,6	42,2	5,5	5,0
37	2,3	42,2	45,8	5,4	4,4
42	1,5	43,1	44,8	5,6	5,0
46	1,7	40,0	47,1	5,6	5,6

Table D2: Change of the size distribution with time.
Size fraction +53-75 micron.

leach time days	+106 micron mass %	+75-106 micron mass %	+53-75 micron mass %	+38-53 micron mass %	-38 micron mass %
4	0,0	3,0	91,1	5,2	0,7
6	0,0	1,6	90,9	6,3	1,2
8	0,3	1,9	88,5	7,6	1,6
10	0,3	1,2	86,6	9,4	2,4
12	0,9	0,8	72,3	20,5	3,5
14	0,4	0,7	72,0	23,3	3,6
19	0,4	0,6	68,3	26,4	4,3
28	0,6	0,9	70,0	22,0	6,5
42	0,5	0,5	48,1	43,1	7,8
46	0,4	0,5	56,6	34,5	8,1

Table D3: Change of the size distribution with time.
Size fraction +38-53 micron.

leach time days	+53-75 micron mass %	+38-53 micron mass %	-38 micron mass %
4	23,0	65,0	12,0
6	15,6	65,5	18,9
10	13,5	66,5	20,0
12	9,7	68,2	22,1
14	13,4	65,2	21,4
19	5,5	51,1	43,4
28	4,6	48,3	47,1
37	3,5	47,5	49,0
46	3,1	46,1	50,8

APPENDIX E

Fraction of Gold Liberated in the Sterile Control Residue

Table E1: size fraction +75-106 micron.

leach time days	fraction of gold oxidised
10	0,243
17	0,256
28	0,284

Table E2: size fraction +53-75 micron.

leach time days	fraction of gold oxidised
10	0,112
19	0,157
28	0,247

Table E3: size fraction +38-25 micron

leach time days	fraction of gold oxidised
4	0,115
6	0,122
10	0,258
19	0,332
28	0,352

Table E4: size fraction +25-38 micron.

leach time days	fraction of gold oxidised
1	0,099
3	0,040
5	0,086
9	0,194
17	0,155
26	0,286